Investigating Molecular Size Variations In Thin Film Chemical Vapor Sensors

Thesis by

Anna Barr Folinsky

In Partial Fulfillment of the Requirements

for the Degree of

Doctor of Philosophy

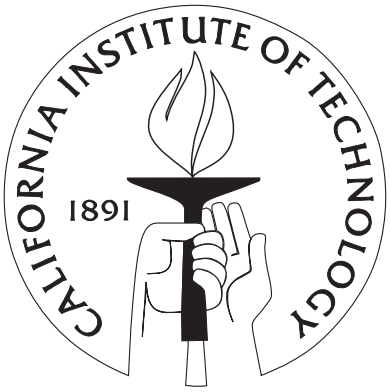

California Institute of Technology

Pasadena, California

2010

(Defended May 12, 2010)

To my mother, who said “Oh, they’ll pay *you*? You should totally do it!”

Acknowledgments

These last couple of months have been tumultuous. My family, and indeed, my entire social network have been there, in strength, and I can never repay that collective debt. Before getting to particular people, I must thank and send all my love to my family. I also must extend thanks to my thesis committee, and finally, to the USFS and NPS for helping me retain my sanity through my graduate career.

Human interaction is fabulously complex. Give and take is rich and varied, and much of the time actual meanings of actions are left unstated, and must be inferred. That said, many people have helped me in a great variety of ways, and I would like to render my heartfelt thanks to the following people, in reverse alphabetical order:

Dr. Ting Gao, Stuart Folinsky, Steven Baldwin, Dr. Sara Klamo, Sandra Mermelstein, Robin Ivester, Robert Folinsky, Richard Tibbetts, Rachel Dillon, Professor Nathan Lewis, Dr. Nathan Eddingsaas, Dr. Michael Walter, Dr. Melanie Yen, Professor Maximilien Riesenhuber, Dr. Matthew Bierman, Marion Sheppard, Dr. Marc Woodka, Madeleine Thompson, Dr. Liana Faye Lareau, Dr. Kimberly Papadantonakis, Kalisa Falzone, 1st Lt. Joseph Sadighi, PhD, Joseph Olivier, Dr. Jennifer Stockdill, Dr. Jennifer Roizen, Jennifer J. Hu, Dr. Jan Streuff, Dr. James Maiolo, Heather McCaig, Professor Harry Gray, Grace Kenney, Gloria Sheppard, Dr. Erin Koos, Erica Folinsky, Dr. Elisa Calimano, Edgardo García-Berríos, Don Walker, Dennis Perepelitsa, Dean Schenker, David Glasser, Dana Joy Gant, Dr. Crystal Shih, Professor Christopher Cummins, Celia Folinsky, Dr. Bruce Brunschwig, Dr. Brian Sisk, Beverly Glassford, Professor Barbara Imperiali, Amittai Axelrod, and Aletta Tibbetts.

Abstract

Vapor sensing arrays composed of broadly responsive, chemically sensitive detectors have been explored for many years. They have been used in fields ranging from good quality control, to environmental monitoring and explosives detection, to disease diagnostics. All of these tasks require high sensitivity and fine discrimination ability. As new challenges arise, the ability to understand the performance and improve the availability of array components becomes paramount.

This work details progress in gaining greater understanding of certain chemical substrates used in sensor arrays. Specifically, arrays using insulator/carbon black composite sensors have been prepared using either polymer or non-volatile small organic molecules as the insulating, chemically sensitive component. The crystallinity of the small molecules as compared to the polymers was determined to cause the differing formulation requirements between the polymers and the small molecules.

Additionally, arrays of sensors composed of varying molecular weights of a given polymer were examined. Very low molecular weights of polystyrene, a high glass transition temperature polymer, exhibited improved behavior and response times compared to higher molecular weights. Finally, arrays composed of varied length carboxylic and dicarboxylic acids were studied. Of these two homologous series, the arrays composed of carboxylic acids provided better discrimination than did those composed of dicarboxylic acids, suggesting the utility of sensor materials containing multiple accessible functional groups.

These studies, taken together, suggest several new ways to increase the number of compounds and chemical functionalities available to use in chemical vapor sensors. Increased sensor choice allows construction of more broadly responsive and finely discriminating sensor arrays, thereby increasing the general utility of composite vapor sensor arrays.

Contents

List of Figures

List of Tables

Chapter 1

Introduction

sensor, n. — A device giving a signal for the detection or measurement of a physical property to which it responds.

Oxford English Dictionary [1]

1.1 Sensors

Throughout human history, people have relied on sensors. Chief among these, never out of vogue, are those comprising our sensory system. Eyes function as light detectors, transducing photons into electrical signals. Our ears do the same for sound waves, and our skin for such things as temperature or mechanical pressure. The brain receives all these electrical signals, and processes the raw data.

As understanding of the physical world grew, so too did our use of sensors in tools. Liquid thermometers detect temperature and transduce it via calibrated thermal expansion. Compasses rely on the magnetic properties of metals to sense the directionality of the planet's magnetic field. Barometers sense changes in air pressure, transduced through changing height of a column of liquid. Sensors are how we know the things we know.

We are surrounded by sensors in our everyday lives, rarely cognizant of their ubiquity. Every system with a remote control contains an infrared sensor. Car and refrigerator doors contain simple mechanical-electrical sensors to determine if a door is open or closed — transduced into a circuit closing, and a light turning on. Elevators sense your presence on their threshold, airplane systems sense the cabin pressure, and gas pumps sense when your tank is full. Sensors are increasingly how our systems know what *they* know, as well.

1.2 Cross Reactive Sensor Arrays

One particular sensor system, studied since the early 1980s, is a vapor-detecting sensor array. Modelled in some ways after the mammalian olfactory system, and because it can be used to "smell" the environment around it, such systems have been colloquially labelled as "electronic noses." In such arrays, each sensor produces a distinct but not deterministic response to an input — exposure to a vapor, such that a given analyte activates multiple sensors, and a given sensor responds to multiple analytes.[2] This is similar to the mammalian olfactory system, in which the olfactory epithelium is studded with odorant receptors (ORs). Each OR is active towards a variety of odorants, and a given odorant likewise activates multiple ORs.[3] However, a mammalian system has hundreds of distinct receptor types (mice have over one thousand different expressed ORs,[4] while humans have around 350[5]), with thousands of copies each. In comparison, array sizes of 10–20 distinct detectors are common in laboratory use, with each additional sensor slightly improving overall discrimination ability, but also adding further noise (Figure 1.1).[6]

In both systems, however, the pattern response from the complete system is passed

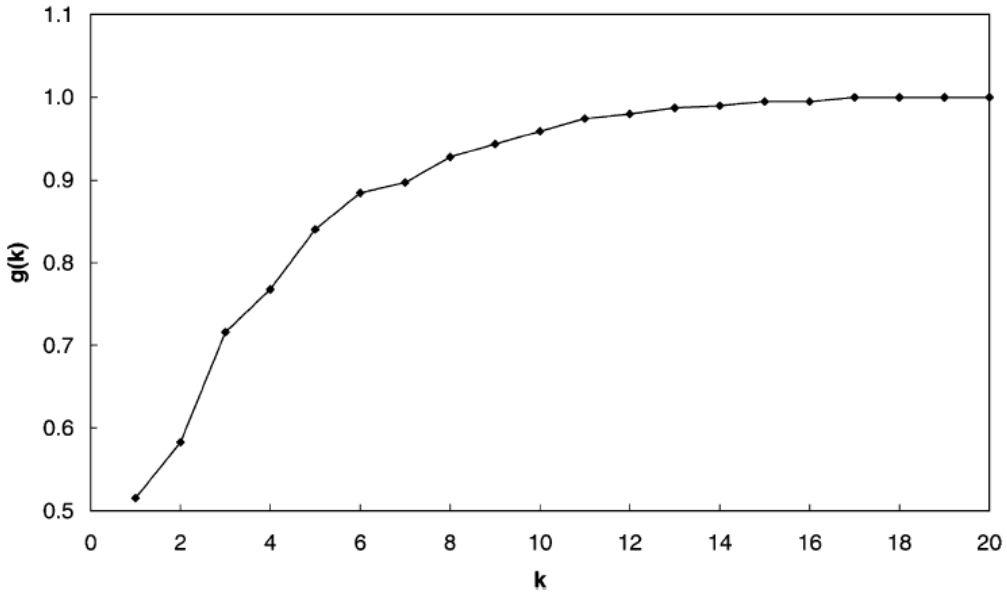

Figure 1.1: Classification performance — g(k) — vs. array size k for a polymer/CB composite sensor array. For each value of k in the range $1 \leq k \leq 20$, an exhaustive search of all possible k-detector combinations from a 20-detector array was performed to identify the array having k detectors that had the best classification performance for each of 21 tasks. For each task, the classification performance for any k-detector array was then compared to that of the full 20-detector array. No combination of k detectors does strictly better than g(k) relative to the full 20-detector array on all 21 tasks.[6]

along to the controlling system (brain or computer) for further processing; analyte determination, discrimination, quantification, or any other tasks. Cross reactive sensor arrays of this type have found use in such fields as food quality control,[7–10] environmental monitoring,[11,12] explosives detection,[13,14] and disease diagnostics.[15–17]

1.3 Sensor Types

A variety of sensor modalities have been used in vapor-detecting sensor arrays, some of the most notable being surface acoustic wave[9,13,18] and bulk acoustic wave detectors,[19,20] semiconducting metal oxide sensors,[10,21] microcantilevers,[22–24] conducting polymers,[7,25–28]

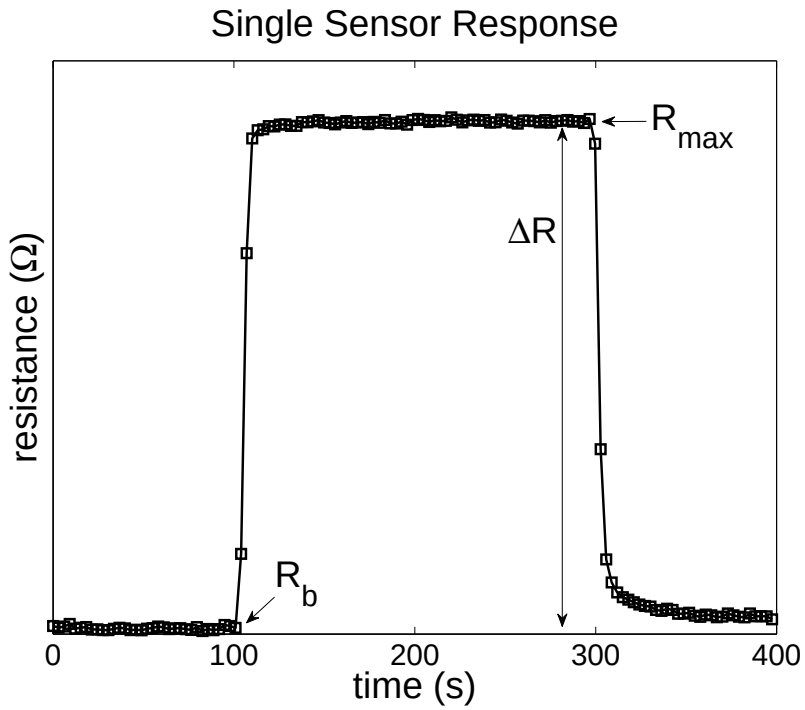

Figure 1.2: Resistance change of a poly(ethylene oxide)/carbon black composite sensor to a 200 second exposure to 2 ppth of chloroform vapor, at an overall flow rate of 2.5 L min^{-1}. R_{b} is the baseline resistance of the sensor, R_{max} the maximum resistance reached during exposure, and ΔR is the difference between the two. Raw data are shown; the absolute change in resistance displayed is around 60 ohms.

and various colorimetric indicators (such as metalloporphyrins).[13,29,30]

One specific approach, and that explored in this thesis, uses sensors comprised of intermixed regions of a conducting material mixed with an insulating organic material. Exposure to an analyte produces detectable changes in the resistance of sensor films cast from these mixtures (Figure 1.2). Conducting materials are often carbon black,[15,31,32] but have also included carbon nanotubes[33] or metal nanoparticles.[34,35] Insulating phases have included polymers,[15,31,32] dendrimers,[36] ligands on metal nanoparticles,[34,35] and non-volatile small organic molecules (SM).[37] All experiments described in this thesis rely on polymer- or SM/carbon black composite films.

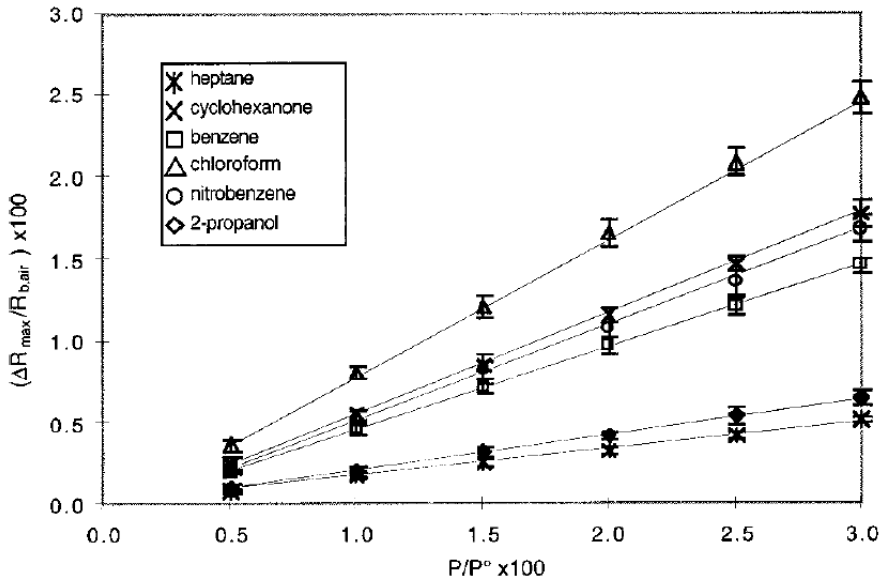

Figure 1.3: Average relative differential resistance responses of a poly(butadiene)/CB composite sensor upon exposure to various analytes, at analyte concentrations ranging from $P/P^0 = 0.005$–0.03, in air, demonstrating linearity of response with respect to analyte concentration.[38]

Polymer/CB composite sensors have been extensively characterized.[6,26,31,32,36–39] Upon exposure to an analyte vapor, some fraction of the vapor sorbs into the film, controlled by the activity coefficient of each particular vapor/solid combination. As the analyte diffuses through the film and comes into equilibrium with the sensor, the volume of the sensor film increases. This swelling increases the average interparticle distance of the carbon black, thereby increasing the overall resistance of the film.[39] Removal of the analyte vapor from the exposure stream allows the sensor to return to its baseline size and resistance. The resistive sensor responses have been shown to be linear with analyte concentration and additive with response to multiple analytes (Figures 1.3 and 1.4).[38] Response times of the films have also been characterized,[40] as have effects of temperature[41] and spatial orientation.[42,43]

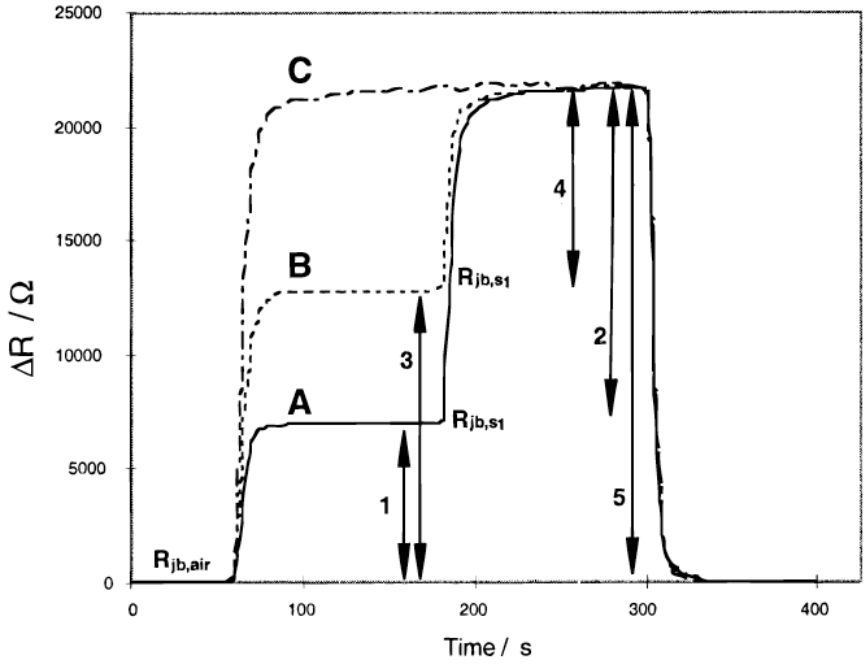

Figure 1.4: Differential resistance response for a poly(ethylene-co-vinyl acetate)/CB composite sensor. A) Exposure to benzene at $P/P^0 = 0.02$, followed by exposure to both benzene and chloroform, each at $P/P^0 = 0.02$. B) Exposure to chloroform at $P/P^0 = 0.02$, followed by exposure to both benzene and chloroform, each at $P/P^0 = 0.02$. C) Simultaneous exposure to benzene and chloroform each at $P/P^0 = 0.02$.[38]

1.4 Sensor Goals

All of this body of work has been aimed towards making better sensor arrays — that is, ones both more broadly responsive, sensitive, and finely discriminating. It has been seen that a given broad polymer/CB sensor array has better discriminatory ability towards gross chemical classes (alcohols, aromatics, etc.) than it has towards physical differences such as molar volume or dipole moment.[44] Similarly, it has been seen that similarities in polarity and functional groups between polymers and analytes creates clear responses.[6,45,46] However, specifically chosen sets of sensors have been shown to perform such difficult discrimination tasks as separating H_2O from D_2O,[6] or distinguishing between an enantiomeric

Analyte	MW (g/mol)	P^0 (kPa, 25 °C)	mp (°C)	bp (°C)	ρ (g/ml, 20 °C)	μ (D)	ε (20 °C)
hexane	86.18	20.2	-95.4	68.7	0.6548[a]	0	1.89
heptane	100.20	6.09	-90.6	98.4	0.6837	0	1.92
toluene	92.14	3.79	-94.9	110.6	0.8669	0.38	2.38[b]
chloroform	119.38	26.2	-63.6	61.1	1.4832	1.04	4.81
ethanol	46.07	7.87	-114.1	78.2	0.7893	1.69	25.30
isopropanol	60.10	6.02	-89.6	82.3	0.7855	1.58	20.18
ethyl acetate	88.11	12.6	-83.6	77.1	0.9003	1.78	6.08

[a] Density at 25 °C
[b] Permittivity at 23 °C

Table 1.1: Listing and physical characteristics of all analytes used in these studies. Values are: molecular weight, melting point, boiling point, density, dipole moment, and the permittivity (dielectric constant).[48]

pair of vapors.[47] As time passes, new challenges in detection continue to arise, notably in cases such as landmine detection, involving very low vapor pressure compounds.

Sensors can often be selected for a particular task, and iterative optimization of a given array can often improve performance. Work has also been done on computationally assisted array selection.[46] Towards all these ends — specific selection of sensors, and the construction of the broadest, most sensitive array possible — we must expand both our set of available sensors and our understanding of how they work. This will yield wider selection, and better comprehension of when and how to select amongst them.

1.5 Outline of This Thesis

This work seeks to address these issues by exploring certain size-related properties of the insulating organic materials used in composite vapor sensors. All the studies presented use one set of analyte vapors; these molecules and some of their physical quantities are pre-

sented in Table 1.1. Previous work has demonstrated the use of small organic molecules in CB composite sensors, and determined them to have notably different formulation requirements than polymer/CB composites. This work compares libraries of polymer/CB and small molecule/CB sensors and determines that the formulation differences stem from the crystallinity of the small molecule materials (Chapter 2). Additionally, varied weight polymers are studied to determine the effects of size and viscosity differences in sensor performance. It is determined that in the case of a high glass transition polymer, sensor response times are greatly improved when using very low weights of that polymer (Chapter 3). Finally, two related homologous series of small molecules, over a range of lengths, are used as sensors. Greater discrimination ability is seen using materials that have increased access to multiple functional groups (Chapter 4). Increased utility of small molecules as sensor substrates, and improved access to many high glass transition temperature polymers, should improve the quality of composite vapor sensor arrays.

1.6 Bibliography

[1] Simpson, J. A.; Weiner, E. S. C. *The Oxford English Dictionary;* Clarendon Press; Oxford University Press: Oxford, New York, 2nd ed., 1989.

[2] Persaud, K.; Dodd, G. *Nature* **1982**, *299*(5881), 352–355.

[3] Breer, H. *Anal. Bioanal. Chem.* **2003**, *377*(3), 427–433.

[4] Zhang, X. M.; Firestein, S. *Nat. Neurosci.* **2002**, *5*(2), 124–133.

[5] Zozulya, S.; Echeverri, F.; Nguyen, T. *Genome Biol.* **2001**, *2*(6), RESEARCH0018.

[6] Burl, M. C.; Sisk, B. C.; Vaid, T. P.; Lewis, N. S. *Sens. Actuators, B* **2002**, *87*(1), 130–149.

[7] Li, C. Y.; Krewer, G. W.; Ji, P. S.; Scherm, H.; Kays, S. J. *Postharvest Biol. Tec.* **2010**, *55*(3), 144–149.

[8] Falchero, L.; Sala, G.; Gorlier, A.; Lombardi, G.; Lonati, M.; Masoero, G. *J. Dairy Res.* **2009**, *76*(3), 365–371.

[9] Barie, N.; Bucking, M.; Rapp, M. *Sens. Actuators, B* **2006**, *114*(1), 482–488.

[10] Musatov, V. Y.; Sysoev, V. V.; Sommer, M.; Kiselev, I. *Sens. Actuators, B* **2010**, *144*(1), 99–103.

[11] Kurup, P. U. *Curr. Sci. India* **2009**, *97*(8), 1212–1219.

[12] Ryan, M. A.; Shevade, A. V.; Zhou, H.; Homer, M. L. *MRS Bull.* **2004**, *29*(10), 714–719.

[13] Toal, S. J.; Trogler, W. C. *J. Mater. Chem.* **2006**, *16*(28), 2871–2883.

[14] Capua, E.; Cao, R.; Sukenik, C. N.; Naamana, R. *Sens. Actuators, B* **2009**, *140*(1), 122–127.

[15] Kateb, B.; Ryan, M. A.; Homer, M. L.; Lara, L. M.; Yin, Y. F.; Higa, K.; Chen, M. Y. *Neuroimage* **2009**, *47*, T5–T9.

[16] Dragonieri, S.; Schot, R.; Mertens, B. J. A.; Le Cessie, S.; Gauw, S. A.; Spanevello, A.; Resta, O.; Willard, N. P.; Vink, T. J.; Rabe, K. F.; Bel, E. H.; Sterk, P. J. *J. Allergy Clin. Immun.* **2007**, *120*(4), 856–862.

[17] D'Amico, A.; Di Natale, C.; Paolesse, R.; Macagnano, A.; Martinelli, E.; Pennazza, G.; Santonico, A.; Bernabei, M.; Roscioni, C.; Galluccio, G.; Bono, R.; Agro, E. F.; Rullo, S. *Sens. Actuators, B* **2008**, *130*(1), 458–465.

[18] Alizadeh, T.; Zeynali, S. *Sens. Actuators, B* **2008**, *129*(1), 412–423.

[19] Ayad, M. M.; El-Hefnawey, G.; Torad, N. L. *J. Hazard. Mater.* **2009**, *168*(1), 85–88.

[20] Si, P.; Mortensen, J.; Kornolov, A.; Denborg, J.; Moller, P. J. *Anal. Chim. Acta* **2007**, *597*(2), 223–230.

[21] Horrillo, M. C.; Getino, J.; Ares, L.; Robla, J. I.; Sayago, I.; Gutierrez, F. J. *J. Electrochem. Soc.* **1998**, *145*(7), 2486–2489.

[22] Senesac, L. R.; Dutta, P.; Datskos, P. G.; Sepaniak, M. J. *Anal. Chim. Acta* **2006**, *558*(1-2), 94–101.

[23] Lang, H. P.; Baller, M. K.; Berger, R.; Gerber, C.; Gimzewski, J. K.; Battiston, F. M.; Fornaro, P.; Ramseyer, J. P.; Meyer, E.; Guntherodt, H. J. *Anal. Chim. Acta* **1999**, *393*(1-3), 59–65.

[24] Bietsch, A.; Zhang, J. Y.; Hegner, M.; Lang, H. P.; Gerber, C. *Nanotechnology* **2004**, *15*(8), 873–880.

[25] Gardner, J. W.; Bartlett, P. N.; Pratt, K. F. E. *IEE P.-Circ. Dev. Syst.* **1995**, *142*(5), 321–333.

[26] Freund, M. S.; Lewis, N. S. *P. Natl. Acad. Sci. USA* **1995**, *92*(7), 2652–2656.

[27] Ramanathan, K.; Bangar, M. A.; Yun, M. H.; Chen, W. F.; Mulchandani, A.; Myung, N. V. *Nano Lett.* **2004**, *4*(7), 1237–1239.

[28] Lange, U.; Roznyatouskaya, N. V.; Mirsky, V. M. *Anal. Chim. Acta* **2008**, *614*(1), 1–26.

[29] Lim, S. H.; Kemling, J. W.; Feng, L.; Suslick, K. S. *Analyst* **2009**, *134*(12), 2453–2457.

[30] Baumes, L. A.; Sogo, M. B.; Montes-Navajas, P.; Corma, A.; Garcia, H. *Tetrahedron Lett.* **2009**, *50*(50), 7001–7004.

[31] Lonergan, M. C.; Severin, E. J.; Doleman, B. J.; Beaber, S. A.; Grubbs, R. H.; Lewis, N. S. *Chem. Mater.* **1996**, *8*(9), 2298–2312.

[32] Doleman, B. J.; Lonergan, M. C.; Severin, E. J.; Vaid, T. P.; Lewis, N. S. *Anal. Chem.* **1998**, *70*(19), 4177–4190.

[33] Philip, B.; Abraham, J. K.; Chandrasekhar, A.; Varadan, V. K. *Smart Mater. Struct.* **2003**, *12*(6), 935–939.

[34] Joseph, Y.; Guse, B.; Yasuda, A.; Vossmeyer, T. *Sens. Actuators, B* **2004**, *98*(2-3), 188–195.

[35] Wohltjen, H.; Snow, A. W. *Anal. Chem.* **1998**, *70*(14), 2856–2859.

[36] Gao, T.; Tillman, E. S.; Lewis, N. S. *Chem. Mater.* **2005**, *17*(11), 2904–2911.

[37] Gao, T.; Woodka, M. D.; Brunschwig, B. S.; Lewis, N. S. *Chem. Mater.* **2006**, *18*(22), 5193–5202.

[38] Severin, E. J.; Doleman, B. J.; Lewis, N. S. *Anal. Chem.* **2000**, *72*(4), 658–668.

[39] Severin, E. J.; Lewis, N. S. *Anal. Chem.* **2000**, *72*(9), 2008–2015.

[40] Briglin, S. M.; Lewis, N. S. *J. Phys. Chem. B* **2003**, *107*(40), 11031–11042.

[41] Homer, M. L.; Lim, J. R.; Manatt, K.; Kisor, A.; Manfreda, A. M.; Lara, L.; Jewell, A. D.; Yen, S. P. S.; Zhou, H.; Shevade, A. V.; Ryan, M. A. *P. IEEE Sens. 2003* **2003**, pages 877–881 1367.

[42] Woodka, M. D.; Brunschwig, B. S.; Lewis, N. S. *Langmuir* **2007**, *23*(26), 13232–13241.

[43] Briglin, S. M.; Freund, M. S.; Tokumaru, P.; Lewis, N. S. *Sens. Actuators, B* **2002**, *82*(1), 54–74.

[44] Sisk, B. C.; Lewis, N. S. *Sens. Actuators, B* **2003**, *96*(1-2), 268–282.

[45] Briglin, S. M.; Gao, T.; Lewis, N. S. *Langmuir* **2004**, *20*(2), 299–305.

[46] Lei, H.; Pitt, W. G. *Sens. Actuators, B* **2007**, *120*(2), 386–391.

[47] Ryan, M. A.; Lewis, N. S. *Enantiomer* **2001**, *6*(2-3), 159–170.

[48] Lide, D., Ed. *CRC Handbook of Chemistry and Physics: A Ready-reference Book of Chemical and Physical Data, 2001–2002;* CRC Press: Boca Raton, 82nd ed., 2001.

Chapter 2

Effects of Film Composition and Structure on the Response of Small Molecule- and Polymer-Based Carbon Black Composite Chemiresistor Vapor Sensors

2.1 Abstract

A series of polymer-based and small molecule (SM)-based carbon black composite vapor sensors has been prepared to understand why the SM-based sensors exhibit higher signal-to-noise ratios at a much higher carbon black loading (75% by weight) than their polymer-based counterparts (40% by weight). Quartz crystal microbalance (QCM), powder X-ray diffraction (XRD), and ellipsometric measurements indicated that the decreased relative differential resistance response of SM-carbon black composite films at low loadings of carbon black is related to the increased rigidity that results from the crystallinity of these films. The SM-based sensors thus require greater carbon black loadings to break the film

Reproduced in part with permission from the *Journal of Physical Chemistry C*, submitted for publication.

crystallinity and hence allow such films to swell by sorption of analyte vapor. In contrast, the polymer/carbon black composite films that were fabricated using low glass transition temperature materials were amorphous, and exhibited good vapor responses over a wide range of carbon black loadings.

2.2 Introduction

Broadly responsive arrays of vapor sensors have attracted significant interest for the detection and quantification of analytes. Systems studied include surface acoustic wave devices,[1–3] metal oxide sensors,[4–6] polymer-coated quartz crystal microbalances (QCMs),[7,8] and polymer-conductor composite chemiresistors[9–11] In such arrays, each sensor displays a distinct but non-selective response towards each analyte. The collective response fingerprint produced by the array provides the information needed to detect and quantify analytes. Chemiresistive sensors made from mixtures of insulating organic polymer with conducting carbon black (CB) sorb vapor into the polymer phase, causing the polymer to swell and thereby changing the overall resistance of the film.[9,12–18] Such sensors are low power,[19,20] can be created using a variety of methods and in a variety of form factors,[21–23] and can be cast onto a variety of substrates.[23–25]

Instead of organic polymers, a variety of low volatility small organic molecules (SM) have recently been used in carbon black composite chemiresistive vapor sensors. In performance tests, such SM-CB chemiresistors exhibited vapor detection performance that was comparable to that of polymer-based CB composites.[26] However the SM-CB composite sensors displayed their highest signal-to-noise ratios (SNR) at 60–75 weight percent of

CB,[26] whereas the polymer-CB (P-CB) sensors yielded best results at 20–40 weight percent of CB.

In the P-CB systems, the resistivity of the film, and the relative differential resistance response of the films to vapors, decreases as the fraction of CB is increased in the mixture.[18] The ability of SM-CB sensors to operate with increased levels of CB allows the use of smaller quantities of potentially expensive materials in the production of such sensors, compared to P-CB sensors. SM-CB sensors also offer potential increases in sensing ability compared to P-CB composites, due to the larger variety of small molecules that are available to broaden the responsive ability of an array of SM-CB sensors.

The SM-CB sensors also have the potential to exhibit increased performance relative to P-CB sensors. The greater density of functional groups in the SM-CB composite films, and the random arrangement of the small molecules within the films, has been suggested to allow high vapor permeability, enhanced vapor-sensor interactions, and potentially increased sensitivity for such materials relative to P-CB films.[26]

In this work, we have investigated and compared the properties of these two different types of sensors, to gain insight into why the SM-CB composite sensor films exhibit optimal performance at higher CB loadings than the P-CB composites. A library of polymers and a library of small molecule analogs that are structurally similar to the polymers were employed to compare and contrast the features of the two types of sensor formulations, and assess if chemical similarity would result in similar behavior. Sets of paired molecules were chosen on the basis of commercial availability (Figure 2.1). Hence, the relative differential resistance responses of these sensors, as well as quartz crystal microbalance (QCM),

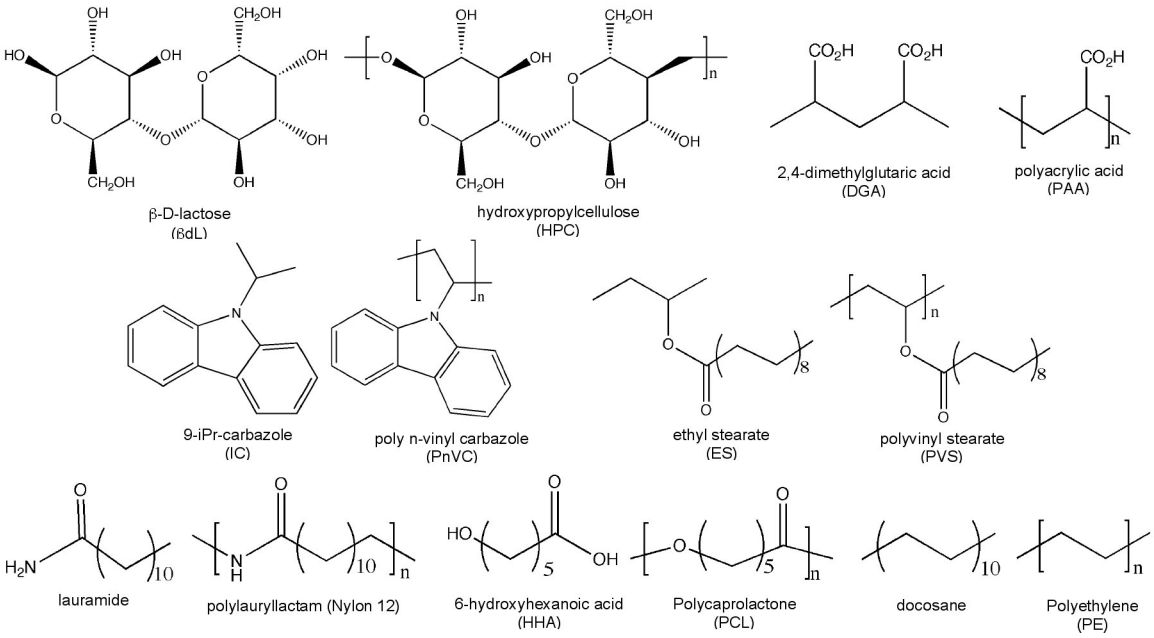

Figure 2.1: All compounds used as sensors in this study. Displayed in matched pairs of small molecule/polymer.

powder X-ray diffraction (XRD), microscopy, and ellipsometric data, were collected for a series of films and analyte vapors.

2.3 Experimental

2.3.1 Materials

Polyethylene (PE, low density), poly(n-vinyl carbazole) (PnVC, molecular weight [M_w] = 1.1 M), poly(caprolactone) (PCL, M_w = 14k), docosane, ethyl stearate (ES), dioctyl phthalate (DOP), gold wire (0.25 mm diam., 99.9+%), 1,1,1,3,3,3-hexafluoroisopropanol (HFIP), and p-xylene were acquired from Aldrich. 2,4-dimethyl glutaric acid (DGA) and 9-isopropyl carbazole (iC) were acquired from Acros Organics, whereas lauramide was obtained from TCI America and Nylon 12 (polylauryllactam) was obtained from Poly-

sciences, Inc. Hydroxypropylcellulose (HPC, M_w = 60k), poly(acrylic acid) (PAA, M_w = 450k), and poly(vinyl stearate) (PVS, M_w = 90k) were purchased from Scientific Polymer Products, and 6-hydroxy hexanoic acid (HHA) and β-d-Lactose (βdL, 80% β, 20% α) were purchased from Alfa Aesar. Reagent grade hexane, heptane, chloroform, ethanol, isopropanol, ethyl acetate, acetone, and tetrahydrofuran were acquired from VWR. Chromium metal was purchased from RD Matthes. Black Pearls 2000, a carbon black (CB) material, was donated by Cabot Co. (Billerica, MA). All materials were used as received.

2.3.2 Sample Preparation

To make sensors, microscope slides (Corning or VWR) were cleaned with methanol and then with hexanes. The long, center axis of each cleaned glass slide was then masked with 1.0 mm wide drafting tape, and two leads were formed on each slide by evaporative deposition of 300 Å of chromium followed by deposition of 600 Å of gold. The tape was then removed and the slide was cut into 0.5 cm x 2.5 cm samples to produce substrates for subsequent deposition of a sensor film.

All sensors were formed from varying ratios of the sensor material, DOP (a plasticizer), and a suspension of CB. Prior to sensor fabrication, the organic material and the plasticizer were dissolved in the solvent, carbon black was added, and the solution was sonicated for $>$30 min to disperse the CB particles. In this process, the materials were added to 20 mL of solvent (Nylon 12 mixtures in HFIP, PAA mixtures in MeOH, PE mixtures in p-xylene, βdL mixtures in 50/50 acetone/water; all of the other materials in THF) in amounts sufficient to produce a total of 200 mg of solid material (Table 2.1). SM-CB mixtures were

Label	Sensor (mg)	Plasticizer (mg)	Carbon Black (mg)	Used
A	90	30	80	ΔR/R, QCM, XRD, SEM, DLS
A/noCB	90	30	0	QCM, XRD, ellipsometry
A/noCB/noDOP	90	0	0	XRD, ellipsometry
B	50	0	150	ΔR/R, QCM, XRD, SEM, DLS
B/noCB	50	0	0	QCM
CB	0	0	80	QCM, SEM
CB/DOP	0	30	80	QCM, SEM

Table 2.1: Composition of all mixtures used to make sensor films. The first column lists the abbreviation used in the manuscript to denote each type of film composition. The last column lists the analyses that were performed on each type of sensor film.

formulated to produce either type A (40 wt% CB) and or type B (75 wt% CB) sensor films, whereas P-CB films were prepared solely in the type A compositional regime (Table 2.1). Dilutions of these mixtures were examined via dynamic light scattering (DLS).

Samples for QCM, XRD, scanning electron microscopy (SEM), and optical microscopy were prepared from these same SM- and P-CB mixtures. QCM, XRD, optical microscopy, and ellipsometric data were also collected on films that were prepared from nominally identical solutions that did not, however, contain carbon black. QCM measurements were additionally performed on films that were made from suspensions of carbon black both with and without plasticizer, but that contained no polymer or small molecule sensor material (Table 2.1).

Using an airbrush (Iwata, Inc), the chemiresistive sensor films were sprayed onto the

sensor substrates until the resistance of the deposited film was between 5 and 1000 kΩ, a level shown to provide consistent responses, with film thicknesses of several hundred nanometers.[26–28] Two sensors were made from each suspension. The substrates for QCM measurements were 10 MHz polished quartz crystals (International Crystal Manufacturing). Each substrate contained a 0.201″ diameter electrode that was formed by deposition of 100 Å of Cr followed by 1000 Å of Au. For QCM measurements, the baseline frequency of the crystal was recorded, and a thin film of sensor material was then sprayed onto the crystal using an airbrush. Each film-coated QCM crystal was placed in a vacuum desiccator for at least 2 h. The frequency shift effected by deposition of the sensor film was then recorded, after which QCM response data were collected.

For XRD measurements, samples were sprayed onto cleaned pieces of a microscope slide. SEM samples were sprayed onto both pieces of silicon wafer and pieces of sensor substrate. Samples for ellipsometry were spin-coated onto pieces of silicon wafers, to obtain the surface smoothness necessary for the laser-based ellipsometric measurements.

2.3.3 Measurements and Data Analysis

2.3.3.1 Chemiresistive Sensors

Automated, LabVIEW-controlled, vapor generation and delivery systems were used to deliver the background and analyte vapors to the chemiresistive detectors.[13,14] The DC resistances of the sensors were monitored using a Keithley 2002 multimeter and a Keithley 7001 multiplexer. All data were recorded to the computer that controlled the analyte exposures.

The sensor array was placed in a chamber made from PTFE and stainless steel that

was connected via Teflon tubing to the vapor delivery system. The sensors were initially exposed to a 2.5 L min^{-1} flow of air for a period of time sufficient to stabilize the baseline resistance of the sensors. A single exposure to an analyte vapor consisted of 100 s of baseline oil-free air with a water content of 12 ppth, followed by 100 s of analyte, followed by a further 100 s purge of air.

The analytes were *n*-hexane, *n*-heptane, chloroform, ethanol, isopropanol, ethyl acetate, and toluene, spanning a range of chemical functionality. The seven analytes were presented in random order 25 times each to the detector array. All exposures were made at an analyte partial pressure in air of $P/P^0 = 0.01$ (where P is the partial pressure and P^0 is the vapor pressure of the analyte at room temperature). All data collection runs were performed at least twice. The first complete run was treated as preconditioning,[29] and data analysis was performed only using the data obtained on later runs.

The resistance of each sensor was measured approximately every 5 s. The sensor response to each analyte exposure was expressed as $\Delta R_{\text{max}}/R_{\text{b}}$, where R_{b} is the steady-state baseline resistance of the sensor and ΔR_{max} is the maximum resistance change observed during exposure to the analyte. ΔR data were calculated by subtracting from all data points a straight line fit to the exposure baseline. From these data, R_{b} was calculated by taking the average of at least five data points recorded immediately before the exposure of analyte was initiated. The value of ΔR_{max} was computed as R_{max}-R_{b}, where R_{max} is the maximum resistance during the exposure. The value of R_{max} was calculated as the average of at least three consecutive resistance measurements that were obtained after the sensor exhibited a steady-state response. The $\Delta R_{\text{max}}/R_{\text{b}}$ value for such chemiresistive sensors has been

shown to be insensitive to the technique used to deliver the analyte vapor, and additionally has been shown to increase linearly with the concentration of the analyte vapor.[27,30] Signal-to-noise ratios (SNR) were also calculated for each exposure, with the SNR value defined as ΔR_{max} divided by the standard deviation of the data points used to calculate R_{b}.

2.3.3.2 QCM Measurements

Crystals for QCM measurements were mounted in a housing made from stainless steel and PTFE, and were exposed to analytes via the same software-controlled vapor delivery and data collection system that was used to collect data on the responses of the chemiresistive vapor sensors. The frequencies of the QCM crystals were measured with an HP53181A frequency counter and were recorded by the controlling computer.

Each QCM crystal was exposed to analytes using a protocol that was similar to that used for the chemiresistors. The time periods for the baseline, analyte exposure, and purge steps for the QCM crystals were 70, 80, and 60 s, respectively. Hexane and ethyl acetate were used as analytes for QCM data collection, and were exposed to the sensors in random order 10 times each. All exposures were performed at a partial pressure of $P/P^0 = 0.01$. Two or more data runs were recorded from each crystal, and the data were analyzed only from the final run.

For small frequency shifts of quartz crystals coated with thin films, the frequency change is primarily determined by the change in mass of the film. Under such conditions, the changes in frequency and mass are related by the Sauerbrey equation, Eq. (2.1):[31]

$$\Delta f = \frac{-2f_0^2}{A\sqrt{\rho_q \mu_q}} \Delta m \tag{2.1}$$

where Δf is the change in resonant frequency (Hz) upon exposure to the analyte of interest, f_0 is the initial resonant frequency of the crystal (Hz), Δm is the change in mass (g), A is the piezoelectrically active area of the crystal (cm^2), ρ_q is the density of quartz (g/cm^3), and μ_q is the shear modulus of quartz (GPa). For a given crystal, all of the values except for Δf and Δm are constants, allowing simplification of Eq. (2.1) to Eq. (2.2):

$$\Delta f = C\Delta m \tag{2.2}$$

Several frequency values were recorded for each crystal. Before film deposition, the baseline frequency (f_0) was recorded. After drying the film, but prior to analyte exposure, a new baseline (f_f) was recorded, yielding $\Delta f_f = f_f$-f_0. The largest frequency shift during exposure, Δf_a, was obtained from f_a-f_f, where f_a is the average of at least three frequency readings collected during the steady-state response portion of the analyte exposure.

The change in frequency, Δf_f, caused by deposition of the film allowed determination of Cm_f, while measurement of the frequency change during analyte exposure, Δf_a, yielded CΔm_a. These two measurements thus allowed determination of a unitless quantity, the mass absorbed per mass of the deposited film, as represented by Eq. (2.3):

$$\frac{\Delta f_a}{\Delta f_f} = \frac{\Delta m_a}{m_f} \tag{2.3}$$

The $\Delta m_a / m_f$ values for all exposures were then calculated and used for further QCM

analysis.

2.3.3.3 DLS

All DLS data was gathered with a Precision Detectors PDExpert multi-angle light scattering platform. Samples in the A regime were examined at a 1:64 dilution, and B regime samples were diluted 1:128. All samples were examined at 90° and 110°.

2.3.3.4 Imaging (SEM and Optical Microscopy)

SEM images were taken on a LEO 1550 VP system, and optical microscopy was performed using a Nikon TE2000S.

2.3.3.5 XRD Data

XRD measurements were performed with a Phillips XPert PRO xray diffractometer (Cu Kα radiation). XRD data were collected from 5–85°, at 10 s step^{-1}, to determine the locations of the peaks. All further exposures were from 5–40° at a rate of 35 s step^{-1}.

2.3.3.6 Ellipsometry

Ellipsometry was performed with a Gaertner L116C system. Samples for ellipsometry were placed in a plastic container that had an opening at each end, which allowed the laser beam to reach the sample and detector in an unobstructed fashion. The baseline thickness readings were collected under a steady stream of air, at 65 mL min^{-1}, with an adjacent ventilation tube used to flush the chamber. Exposures to saturated vapor of ethyl acetate, EtOAc, were performed at a flow rate of 65 mL min^{-1}. During these exposures, the

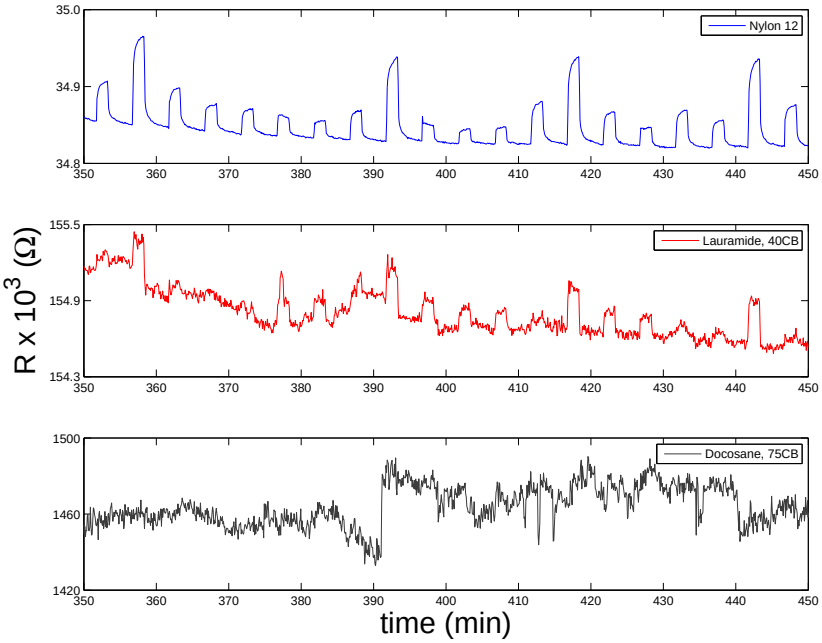

Figure 2.2: Representative responses for different types of sensors. From top to bottom, Nylon 12 A, lauramide A, and docosane B show good, marginal, and no significant response to analyte, respectively. All traces are on the same time scale from the same set of exposures; the y-axes are different on each. Analyte exposure is at $P/P^0 = 0.01$.

ventilation tube was removed, to encourage maximum retention of EtOAc in the chamber. The purge and exposure times were each $\geq$2 min. Each sample was exposed a minimum of five times, and at least five data points were taken during and between each exposure. These data points were averaged to yield the relative thickness change of the film for each analyte exposure.

2.4 Results

2.4.1 Sensor Responses

Table 2.2 presents the SNR values for all of the sensors investigated in this work. (Table 2.3 summarizes this information, Figure 2.2 provides a qualitative overview). The sensors shown in bold (docosane B, DGA A, βdL A, HHA, and PAA) did not produce responses with SNR values above 3, whereas all of other sensors exhibited good SNR values for the analytes of interest. Films of lauramide or iC that contained CB exhibited higher responses in the B regime (75% CB), while ES-containing CB sensors produced higher responses in the A regime. In most cases, the P-CB sensors produced slightly higher SNR values than the SM-CB sensors. No specific correlations in responses between matched pairs were seen.

2.4.2 QCM Data

All of the CB-containing sensor films exhibited clear mass sorption and high SNR values when used as QCM-based sensors (Figure 2.3a). In general, the different SM-CB type B (75% CB) films exhibited higher $\Delta m_{\mathrm{a}}/m_{\mathrm{f}}$ values, but less variation between film materials, than either the P-CB films or the type A films (40% CB) of SM-CB. Films that contained CB exhibited easily differentiable mass uptakes to hexane and ethyl acetate (Figures 2.3, 2.4).

The QCM responses of the films that contained either SM or polymer were also examined in the absence of carbon black (Figure 2.3b). In all cases except one, the $\Delta m_{\mathrm{a}}/m_{\mathrm{f}}$

compounds	CB%	hexane	heptane	toluene	chloroform	EtOH	iPrOH	EtOAc
docosane	40	16 ± 5	14 ± 4	24 ± 7	28 ± 7	6 ± 2	7 ± 2	6 ± 1
docosane	75	1 ± 4	0.8 ± 2	1 ± 2	1 ± 3	0.2 ± 2	0.5 ± 2	0.4 ± 1
ES	40	6 ± 2	5 ± 2	10 ± 3	24 ± 6	4 ± 2	4 ± 2	5 ± 1
ES	75	5 ± 2	4 ± 1	6 ± 2	13 ± 5	2 ± 1	1 ± 1	3 ± 2
lauramide	40	7 ± 3	7 ± 2	10 ± 6	15 ± 6	4 ± 2	4 ± 2	5 ± 2
lauramide	75	29 ± 7	32 ± 9	40 ± 10	80 ± 20	12 ± 3	13 ± 3	14 ± 4
iC	40	11 ± 2	2 ± 1	149 ± 4	12 ± 3	11 ± 3	2 ± 1	2 ± 1
iC	75	22 ± 5	16 ± 3	41 ± 12	21 ± 7	27 ±	14 ± 3	16 ± 4
DGA	40	3 ± 2	1 ± 1	4 ± 2	3 ± 1	3 ± 2	1 ± 1	2 ± 1
DGA	75	94 ± 100	26 ± 9	110 ± 23	70 ± 20	90 ± 23	28 ± 6	40 ± 50
HHA	40	2 ± 1	0.5 ± 1	4 ± 2	2 ± 0.8	2 ± 1	0.7 ± 1	1 ± 1
HHA	75	4 ± 1	1 ± 0.9	3 ± 2	4 ± 2	3 ± 2	2 ± 1	1 ± 1
βdL	40	0.2 ± 1	0.4 ± 1	1 ± 1	0.6 ± 1	0.3 ± 1	0 ± 1	0.2 ± 2
βdL	75	5 ± 2	2 ± 0.9	5 ± 3	6 ± 2	5 ± 2	1 ± 1	2 ± 1
median		9(2.5)	9.2(2.5)	10.5(4.5)	26(6)	4(2)	4(2)	5(1.5)
PE	40	15 ± 6	14 ± 4	17 ± 6	35 ± 13	4 ± 1	5 ± 2	3 ± 2
PVS	40	120 ± 45	110 ± 30	160 ± 50	270 ± 70	38 ± 9	50 ± 17	40 ± 12
Nylon 12	40	32 ± 12	26 ± 10	50 ± 30	120 ± 30	73 ± 30	50 ± 20	70 ± 30
HPC	40	28 ± 8	23 ± 6	50 ± 15	150 ± 60	35 ± 8	50 ± 18	43 ± 9
PnVC	40	36 ± 10	25 ± 8	47 ± 10	96 ± 20	18 ± 5	15 ± 6	19 ± 7
PAA	40	0.3 ± 1	0.3 ± 1	0.8 ± 1	2 ± 1	5 ± 3	0.3 ± 1	2 ± 1
PCL	40	13 ± 3	13 ± 4	23 ± 6	50 ± 9	6 ± 2	7 ± 3	7 ± 4
median		28(8)	23(8)	47(10)	96(20)	18(5)	15(6)	19(7)

Table 2.2: SNR values for all sensors measured in this study. Data are means obtained from 25 exposures to a given analyte. Values above 3 demonstrate an acceptable response. The reported error is one standard deviation.

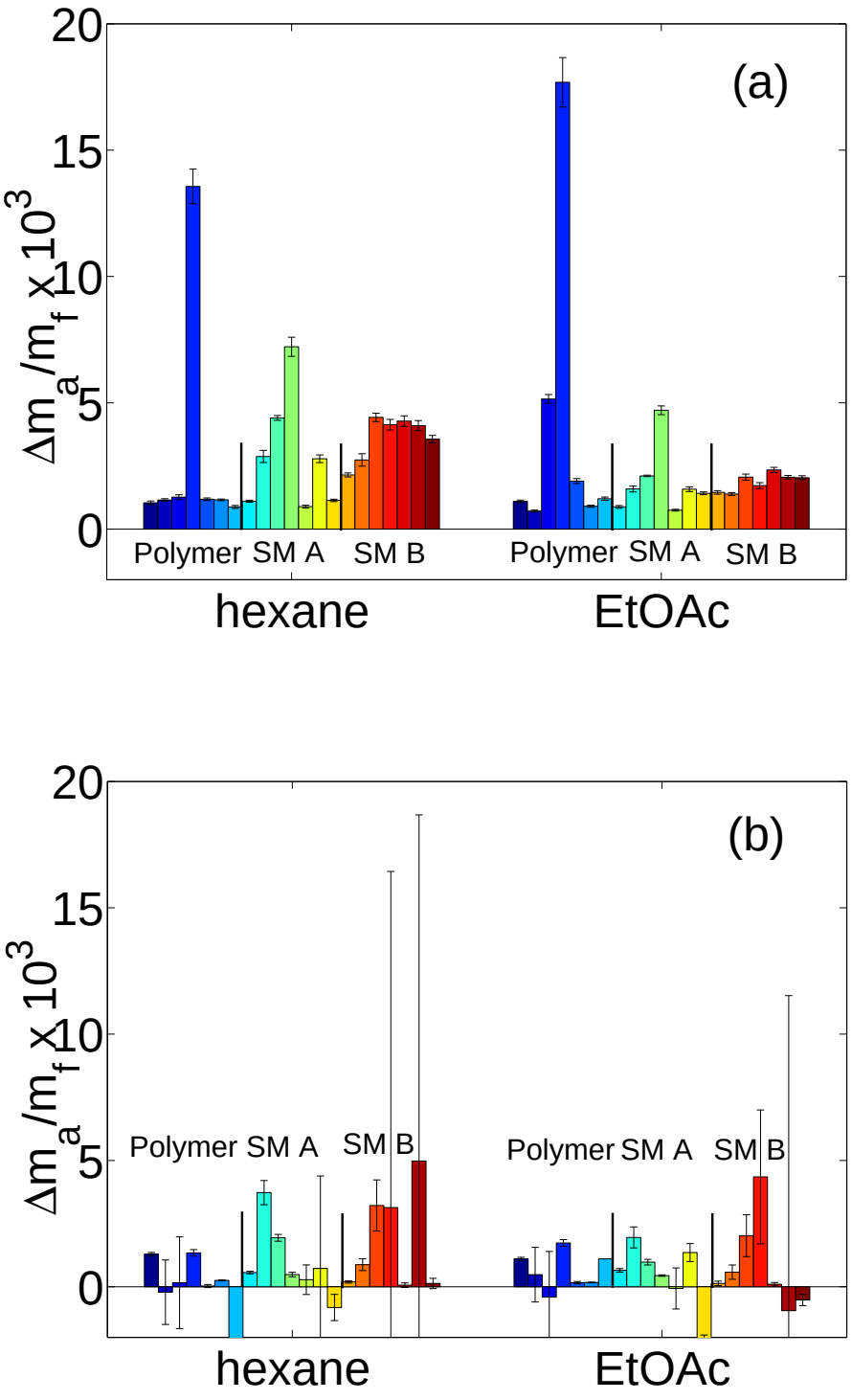

Figure 2.3: QCM responses of a) SM and P films with CB and b) without CB. From left to right: Nylon 12, PE, PAA, PnVC, HPC, PVS, PCL, lauramide A, docosane A, DGA A, iC A, βdL A, ES A, lauramide B, docosane B, DGA B, iC B, βdL B, ES B.

	A/LP (40%)	**B/LP (75%)**	**A/P (40%)**	**B/P (75%)**	**Linear chain atoms**	**MW (g/mol)**
Docosane	>20	<3	6	<3	22	310
ES	8	6	4	<3	22	312
Lauramide	9	>30	4	>10	13	199
iC	>10	>20	<3	>10	-	209
DGA	3	>90	<3	>20	7	160
x HHA	<3	3	<3	<3	8	132
βdL	<3	5	<3	<3	-	342

Table 2.3: Median values of the SNR values for SM A and B type sensors for less polar (LP) analytes (hexane, heptane, toluene, and chloroform) and polar (P) analytes (EtOH, iPrOH, EtOAc)

values of such films were lower than the responses observed for films that contained CB. The films that did not contain CB also exhibited much larger exposure-to-exposure variation (Figure 2.3b). Films made from ES only exhibited high noise values, and the two SMs that failed to yield CB composite chemiresistive sensors (βdL and HHA) did not show significant mass uptake in the QCM measurements.

The QCM response was also investigated for films that were formed from either pure CB or from CB/DOP (Table 2.1, Figure 2.4). The pure CB film showed a high sorbancy, with $\Delta m_{\mathrm{a}}/m_{\mathrm{f}}$ values exceeding by >30% those of almost all of the other films studied. The CB/DOP film showed reduced sorbancy compared to that of pure CB, displaying $\Delta m_{\mathrm{a}}/m_{\mathrm{f}}$ values ∼40% of those of pure CB. Films that contained polymers or small molecules in addition to CB exhibited a variety of QCM responses, with values in some cases larger and in some cases smaller than that of the CB/DOP film. The sorbency of the CB and of the CB/DOP films to hexane was double that to ethyl acetate.

Every SM-CB film that functioned as a sensor sorbed more hexane than EtOAc, in a

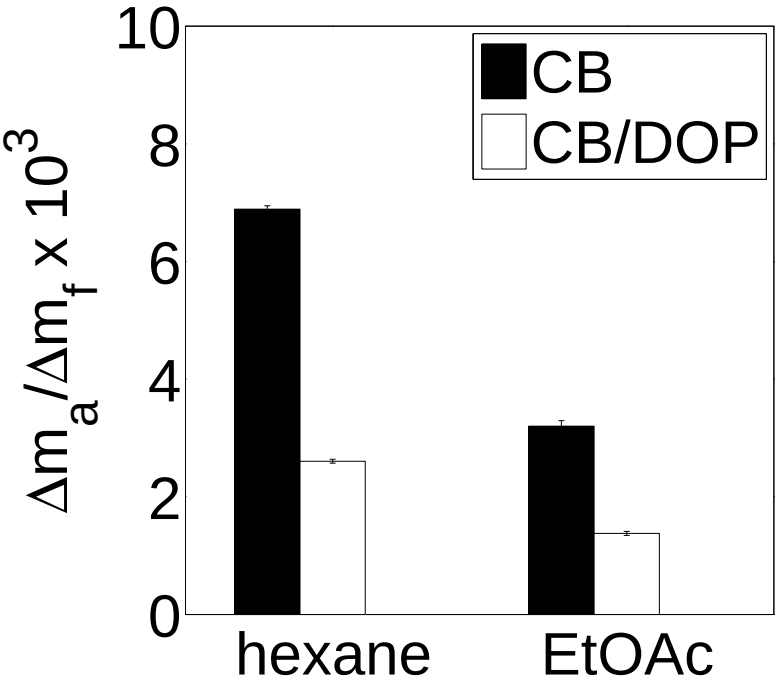

Figure 2.4: QCM responses of CB and CB/DOP films

pattern similar to that observed for the CB and CB/DOP films. This was not the case for the P-CB films (Table 2.4)

2.4.2.1 DLS

At the dilutions necessary to allow the DLS laser to traverse the solution, all CB mixtures were uniformly suspended. No significant CB particle size differences were apparent between all samples tested, except for those clearly explained by solvent variation — βdL in 50/50 acetone/water and PAA in MeOH showed significantly larger particle aggregates (Figure 2.5). PE yielded no information.

Compound		With CB hexane	With CB EtOAc	Without CB hexane	Without CB EtOAc
docosane	A	2.88 ±0.2	1.59 ±0.1	3.73 ±0.5	1.96 ±0.4
docosane	B	2.74 ±0.3	1.39 ±0.06	0.88 ±0.2	0.58 ±0.3
ES	A	2.79 ±0.2	1.58 ±0.09	0.73 ±3.7	1.36 ±0.4
ES	B	4.10 ±0.2	2.06 ±0.07	4.98 ±13.7	−0.94 ±12.5
lauramide	A	1.11 ±0.04	0.88 ±0.05	0.56 ±0.05	0.65 ±0.07
lauramide	B	2.15 ±0.08	1.45 ±0.07	0.19 ±0.04	0.14 ±0.09
βdL	A	0.89 ±0.05	0.75 ±0.04	0.28 ±0.6	−0.07 ±0.8
βdL	B	4.28 ±0.2	2.34 ±0.1	0.07 ±0.09	0.10 ±0.07
iC	A	7.22 ±0.4	4.70 ±0.2	0.49 ±0.09	0.44 ±0.03
iC	B	4.13 ±0.2	1.72 ±0.1	3.14 ±13.3	4.35 ±2.7
DGA	A	4.40 ±0.09	2.11 ±0.03	1.94 ±0.1	0.98 ±0.1
DGA	B	4.42 ±0.2	2.06 ±0.1	3.22 ±1.0	2.02 ±0.8
HHA	A	1.14 ±0.05	1.42 ±0.05	−0.82 ±0.5	−2.37 ±0.5
HHA	B	3.56 ±0.2	2.04 ±0.08	0.13 ±0.2	−0.52 ±0.2
median		3.22(0.16)	1.65(0.07)	0.64(0.36)	0.51(0.32)
PE	A	1.15 ±0.05	0.71 ±0.04	−0.21 ±1.3	0.48 ±1.1
PVS	A	1.16 ±0.03	0.91 ±0.04	0.25 ±0.02	0.17 ±0.01
Nylon 12	A	1.04 ±0.07	1.10 ±0.05	1.29 ±0.07	1.11 ±0.06
HPC	A	1.18 ±0.05	1.90 ±0.1	0.03 ±0.06	0.17 ±0.05
PnVC	A	13.56 ±0.7	17.69 ±1.0	1.35 ±0.1	1.73 ±0.1
PAA	A	1.27 ±0.1	5.15 ±0.2	0.16 ±1.8	−0.41 ±1.8
PCL	A	0.88 ±0.06	1.20 ±0.07	−195.1 ±620.9	1.10 ±0.3
median		1.16(0.06)	1.20(0.07)	0.16(0.13)	0.48(0.13)

Table 2.4: $\Delta m_{\mathrm{a}}/m_{\mathrm{f}}$ x 10^3 values for all compounds, from QCM. Reported error is one standard deviation.

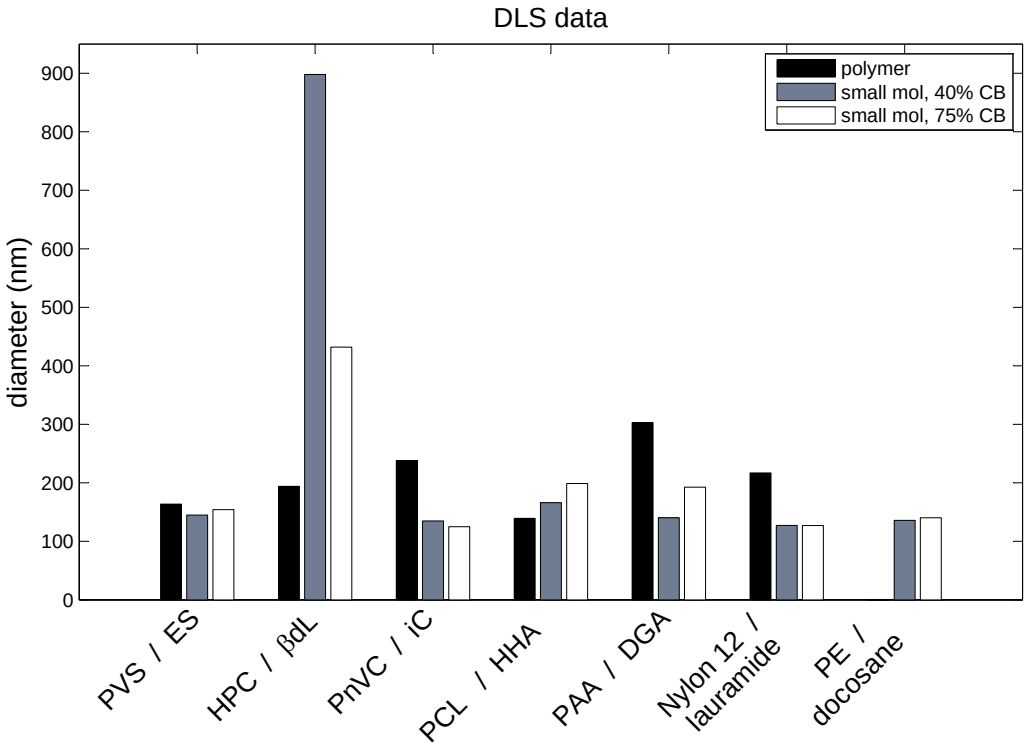

Figure 2.5: DLS CB particle size information. βdL in 50/50 acetone/water, PAA in MeOH, PE in p-xylene, Nylon 12 in HFIP, and all other materials in THF. 40 wt% samples were at 1:64 dilution, and 75 wt% samples were at 1:128 dilution

2.4.3 Imaging

Optical microscopy of the films showed no differences among the films that contained CB. SM films without CB showed highly crystalline growths, whereas the pure polymer films were amorphous (Figure 2.6).

SEM images of SM-CB A or B and P-CB A films showed no clear differences in the structures of the visible CB aggregates. The only difference in the SEM images was that pure carbon black dispersed cleanly, whereas mixtures of CB with SM, polymer, or DOP exhibited droplet formations that were presumably a result of the airbrush deposition process (Figure 2.7). No differences were seen between SEM samples deposited on silicon wafers and samples deposited onto sensor substrates.

2.4.4 XRD

XRD was used to evaluate the crystallinity of the various types of sensor films. Clean microscope slide substrates showed a broad peak at $2\theta \sim 25^{\circ}$ that appeared in all spectra. All pure SM films (A/noCB/noDOP) exhibited sharp peaks indicative of crystallinity, whereas none of the polymer films showed any sharp XRD features. SM films with (SM A/noCB) and without DOP plasticizer (SM A/noCB/noDOP) (Figure 2.8) showed similar XRD patterns, although the count numbers varied for different films, due to a lack of control over the film thickness. The XRD spectra of SM-CB A (40% CB) films exhibited small peaks, but these peaks were undetectable for SM-CB B (75% CB) films (Figure 2.9).

Docosane peaks were assigned according to the literature.[32] The lauramide spectrum does not match the literature pattern precisely.[33] However, such *n*-alkylamides are known

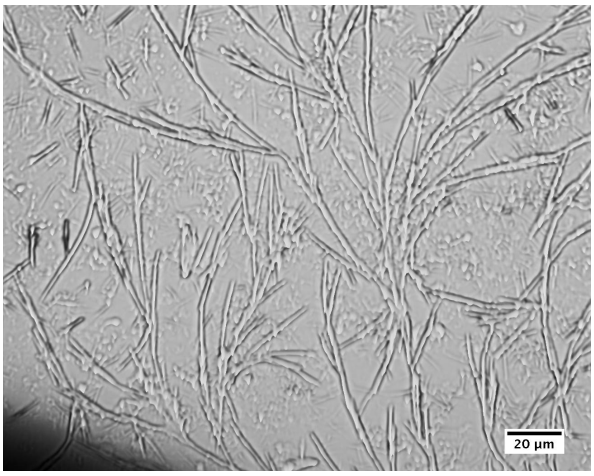

2.6(a) 2,4-dimethyl glutaric acid film, 40x.

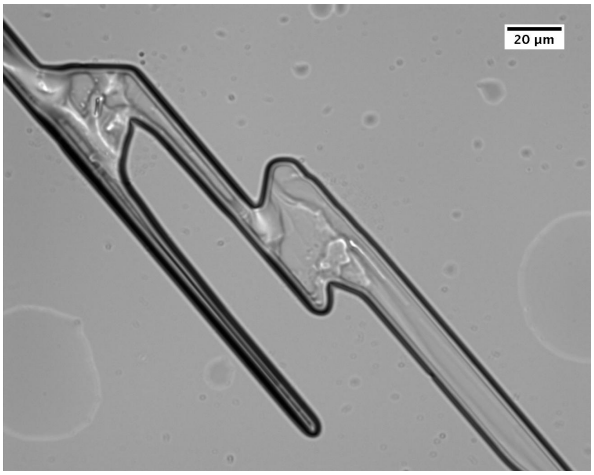

2.6(b) 9-iPr-carbazole/DOP film, 40x.

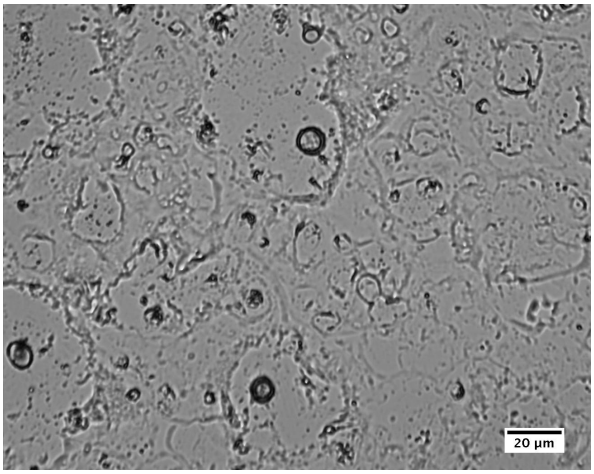

2.6(c) Poly(vinyl stearate)/DOP film, 40x.

Figure 2.6: Optical microscope images of a) 2,4-dimethyl glutaric acid, b) 9-iPr-carbazole/DOP, and c) PVS/DOP films sprayed onto cleaned microscope slides. All images are at 40x and scale bars are 20 μm.

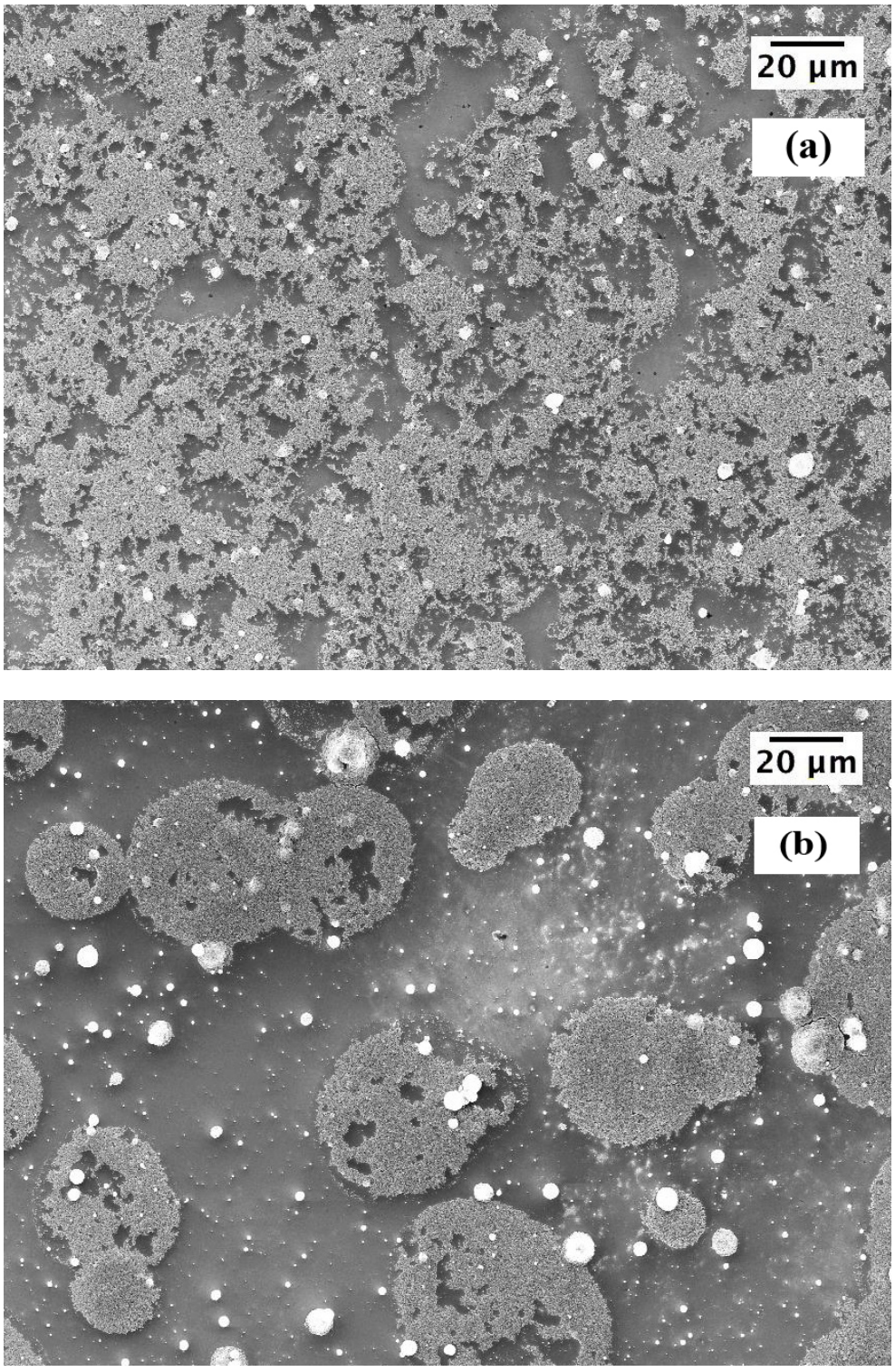

Figure 2.7: SEM images of a) pure carbon black on a silicon substrate and b) lauramide with 75% by mass carbon black on a silicon substrate. Both images are at a magnification of 1,000x.

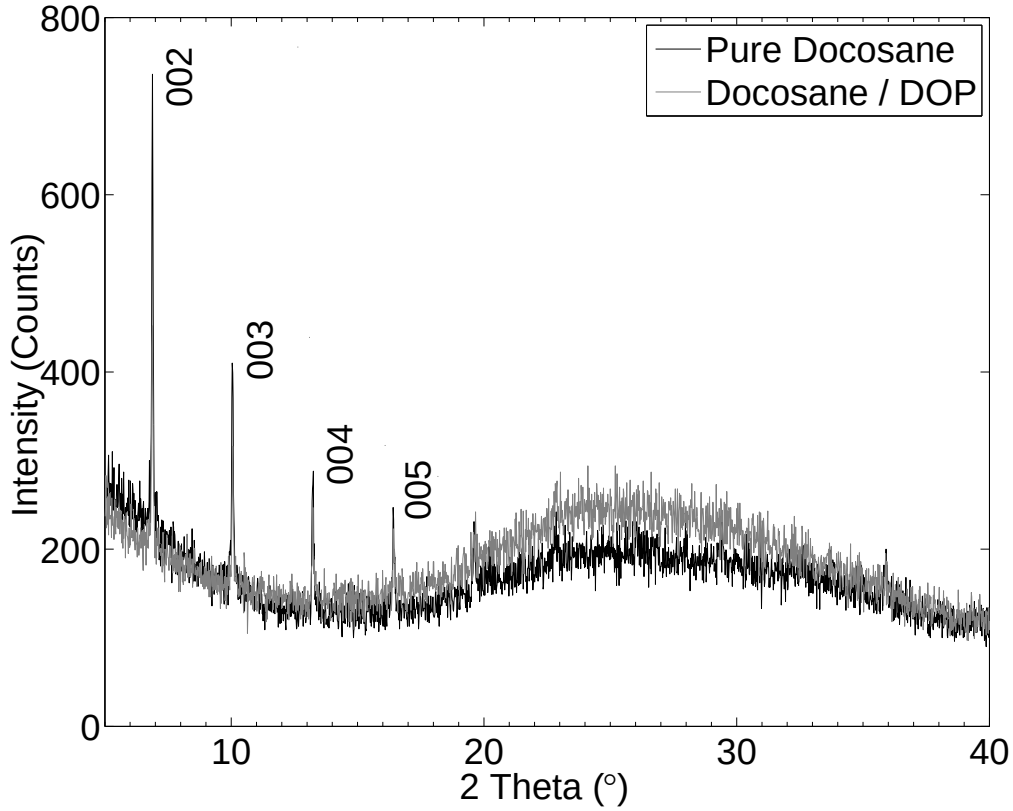

Figure 2.8: XRD spectra of pure docosane (A/noCB/noDOP) and docosane/DOP (A/noCB). The crystalline peaks are in the same locations on each sample. Note the amorphous peak from the glass slide centered around 25°.

to be polymorphic,[34] and the molecular structure of the compound has been confirmed by proton NMR in both *d*-chloroform and *d*-THF. Given the range of long spacings reported for lauramide,[34] the peak in the reported spectrum has been tentatively assigned as the (003) reflection.

2.4.5 Ellipsometry

Ellipsometry was used to probe the thickness changes of the films upon exposure to analyte. Ellipsometric measurements were not performed on films that contained carbon black, because such films were black to the eye and additionally were optically inhomogenous.

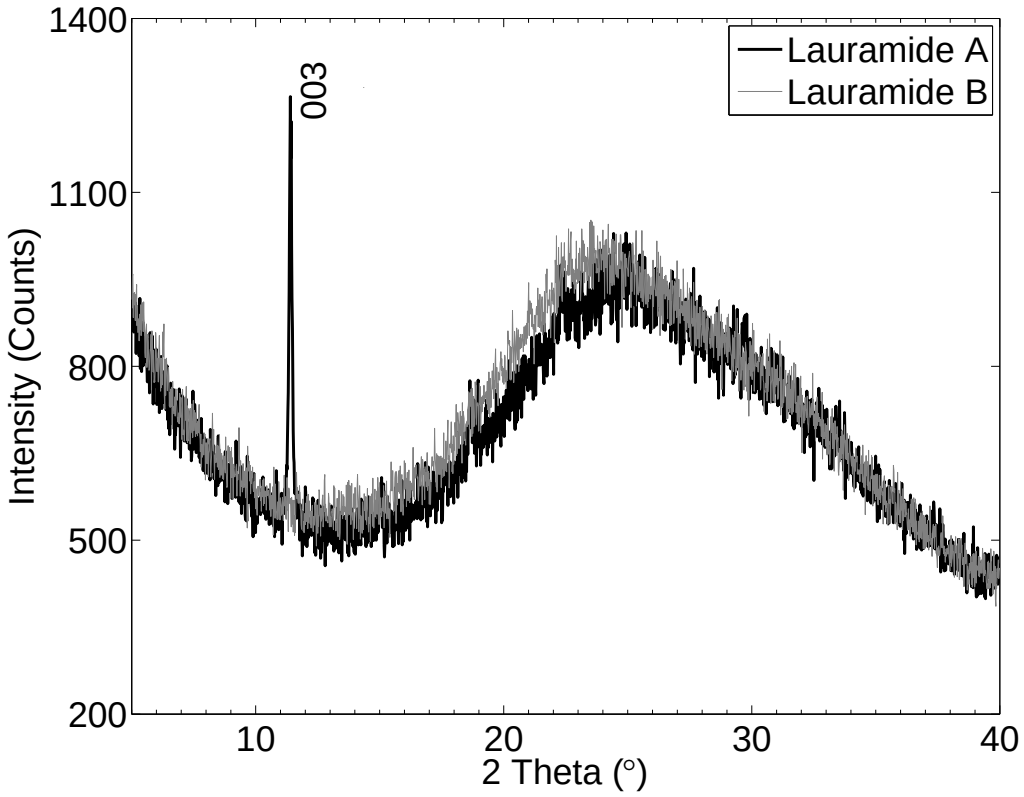

Figure 2.9: XRD of lauramide-CB type A and lauramide-CB type B composite films.

	No DOP Plasticizer		**With Plasticizer**	
	$\Delta h/h$	Δh (Å)	$\Delta h/h$	Δh(Å)
Blank Silicon		4.5		
Docosane	1.2(0.3)	3.8(0.8)	12.9(0.6)	50.9(1.9)
Lauramide	1.4(0.1)	8.5(0.8)	12.8(1.0)	105.1(9.2)
iC	−0.6(0.1)	−0.9(0.2)	n/a	
DGA	2.0(0.3)	4.0(0.5)	16.4(2.6)	16.9(2.9)
PVS	3.0(0.1)	16.6(0.5)	15.9(2.0)	114.3(14.1)
N12	3.7(0.5)	12.3(1.6)	20.2(3.3)	62.6(10.3)
PnVC	12.2(0.6)	37.7(1.8)	7.5(0.8)	39.6(4.3)
HPC	10.0(0.3)	45.6(1.6)	77.3(7.5)	771.8(77.2)

Table 2.5: Ellipsometry data. Averaged percent swelling and thickness change of each film, with and without DOP plasticizer, in response to a saturated flow of ethyl acetate. A blank Si sample showed an ellipsometric signal change equivalent to a film swelling response of $\sim$4 Å. Reported error is one standard deviation

Ellipsometric data were therefore collected only for pure films (A/noCB/noDOP) as well as for films that included plasticizer (A/noCB).

Under a saturated stream of ethyl acetate, the SM films that did not contain added plasticizer swelled $\leq$2% of their original thickness (−1% to +2%), while polymer films swelled $\geq$3% (3–12%). The change in thickness of the SM films was 3–10 Å, while polymer films exhibited thickness changes of 10–45 Å(Table 2.5). Under a saturated stream of EtOAc, a piece of silicon substrate used as a control sample showed a change in ellipsometric signal equivalent to a film swelling response of 4 Å, similar to the change recorded for two of the SM films. Docosane, iC, DGA, and lauramide all showed a decrease in film thickness over the course of the vapor exposures, whereas the polymer films yielded stable responses. The films that contained plasticizer almost uniformly exhibited increased swelling responses, in several cases almost an order of magnitude (Table 2.5) larger than that of unplasticized films.

2.5 Discussion

Small molecule-CB sensors have been determined previously to exhibit the highest SNR values at high carbon black loadings, with concomitantly reduced quantities of organic phase in the sensor film as compared to P-CB sensors. The SM-CB sensors thus form an attractive class of sensor films due to this lowered required mass of organic phase, and also due to the very large number of potential sensing materials that are available as small organic molecules.

Except for docosane, the SM-CB sensors performed better in the 75% CB regime (B) than in the 40% CB regime (A), with all sensors exhibiting higher SNRs for less polar analytes (Table 2.2). Lauramide, ES, and iC performed well in both the A and B regimes, whereas docosane yielded measurable responses only in the A regime, and DGA yielded measurable responses only in the B regime.

2.5.1 Film Composition

SEM images and optical inspection revealed clear crystalline regions in the SM films that did not contain CB. The SM films exhibited a variety of crystalline growths, although docosane exhibited mostly smooth, undifferentiated planes, with occasional small ordered areas. In contrast, all of the polymer films exhibited no long range order visible by microscopy.

No crystalline domains were observed in either SEM or optical microscopy images of the films that contained CB. The P- and SM-CB films showed clear droplet formations that were not observed for the pure CB films. When the airbrush deposition method is used, the

formation of such aggregates has been reported,[30] and their failure to appear in the pure CB films presumably reflects the influence of the mixture composition on the morphology of the films (Figure 2.7).

Carbon black is often understood to simply provide a conductive structure in composite chemiresistive vapor sensors, but its role is more complicated than that simple picture. The QCM data show that CB sorbs solvent vapor and provides a differentiable mass uptake to various analytes. Yet despite the high $\Delta m_{\mathrm{a}}/m_{\mathrm{f}}$ values exhibited by such films, neither pure CB nor CB/DOP function as chemiresistive vapor sensors.[26] Addition of other components almost uniformly effected decreases in the $\Delta m_{\mathrm{a}}/m_{\mathrm{f}}$ values, but such reductions did not follow any clear pattern. Weight averaging the QCM responses of the pure CB film with that of the A/noCB films did not yield the response of the A films (PnVC/CB and iC/CB notably have higher $\Delta m_{\mathrm{a}}/m_{\mathrm{f}}$ values than pure CB). Furthermore, the QCM responses of the SM-CB films exhibited a pattern of responses that was similar to the QCM responses of the pure CB or CB/DOP films, regardless of the QCM responses of their pure films. Thus, from the deposition images and QCM responses of the composite films, certain film features are not the sum of the individual components.

2.5.2 Small Molecule Crystallinity

The pure SM films (including docosane) showed clear, sharp Bragg peaks in the XRD spectra, while pure polymer films showed no such features. The polymer films that contained added plasticizer showed no notable differences from those that did not contain plasticizer. Addition of plasticizer to the SM films did not affect the formation of crystalline structures

in the XRD data, and although the peak amplitudes varied with film thickness, the peak positions did not shift.

Peaks ascribable to residual crystallinity were observed for the SM-CB A films (40% CB), but all such peaks disappeared when the CB content was increased to 75% in the type B films. Hence, 75 wt% CB was sufficient to prevent crystal formation in the SM type B films.

Previous work has explored the nature and effects of crystallinity in selected polymer-CB composites. In one study, at a given level of CB, the more crystalline the polyolefin used, the higher the overall resistivity.[35] In a separate study, triblock polystyrene - poly(ethylene glycol) - polystyrene polymer sensors showed a crystalline region that effectively forced the CB to segregate into the more amorphous region, which was determined to be the region that was primarily responsive to the analyte when such films were used as chemiresistive vapor sensors.[36] Both of these studies dealt strictly with polymers, and used dissimilar methods of sensor preparation from those used in this work, but nevertheless provide evidence consistent with the expectation that the crystallinity of the film can affect the response characteristics of CB composite vapor sensors.

2.5.3 Variations in Swelling Response

Films of the SMs that did not contain DOP showed only very slight swelling responses, both as a percent of the film thickness and on an absolute scale. Some of the small molecules displayed a net decrease in thickness upon exposure to analyte vapor. The crystalline films would not be expected to swell as much as non-crystalline films, in accord with the ob-

served responses.

The presence of plasticizer aids the sensor response of polymer films, decreasing the response time and increasing the magnitude of the relative differential resistance response by increasing the ability of the polymer chains to slide past one another. This behavior suggests that increased rigidity decreases the swelling of the film upon exposure to analyte vapor. However, the addition of plasticizer markedly increased the recorded thickness changes of ellipsometric films that contained either the small molecules or the polymers. For polymers, plasticizer disperses within the polymer film and aids the movement of the polymer chains, thus increasing the swelling response. The XRD data, however, indicated that the addition of the plasticizer (DOP) did not disrupt the crystallinity of the small molecule films. As the SMs retain their crystalline structure, and do not noticeably swell in pure films, the SMs and DOP appear to be segregated in SM-DOP films, with the observed swelling response attributable to the plasticizer portion of the film.

2.5.4 Small Molecule Structure

All of the small molecules are crystalline, and none swell appreciably, yet their formulation requirements varied significantly to produce optimal chemiresistive vapor sensors. If the SMs did not swell when locked into rigid crystalline films, some other aspect of the composite film must break up their crystalline structure.

A distinct trend was observed in the responses of the five functional SMs (Table 2.2). As the molecules became larger and less polar, the resulting sensors switched from working best in the B regime to working best in the A regime. One potential explanation of this

behavior is that the strength of the crystalline interactions in each film is a function of the size and polarity of each small molecule. As the size increases and the polarity decreases the crystalline interactions decrease and less CB is needed to prevent crystal formation.

Docosane, the least polar, and one of the largest, SMs investigated in this work, functioned only with low CB, regime A. No large-scale crystalline features were observed in optical microscopy images of this film. This large, hydrophobic molecule has no structural features to aid crystallization, and less CB should then be needed to disrupt the crystallinity.

The majority of the SMs (ES, lauramide, and iC) exhibited good chemiresistive vapor responses in both regimes of carbon black loading. However, while ES worked about equally well in both regimes, both lauramide and iC yielded significantly better SNR values in the B regime (Table 2.2). ES and lauramide are generally linear in shape, whereas iC is not. These molecules have functional groups that can aid crystallization. ES, which is as large as docosane, contains an ester, but lacks H-bonding protons. Lauramide, half this size, is an amide with H-bonding protons, and iC, much more bulky, has a multi-ring structure that can facilitate π-stacking interactions. Both higher and lower CB regimes break up the crystallinity of such films. ES, the longest of these three and lacking H-bonding protons, was most responsive in the 40% CB regime, containing plasticizer, while the smaller lauramide and iC exhibited better vapor sensor performance at 75% CB, with no plasticizer included.

Finally, DGA, both compact and with excellent H-bonding ability, only functioned well as a vapor sensor at 75% CB, the B regime. The compactness and high self-affinity of DGA made this film harder to disrupt, necessitating a high proportion of CB to make functional

composite sensors.

2.6 Conclusions

Small molecule/carbon black composite sensors have been studied and compared to P-CB composites, to better understand the required composition of this family of sensors. The small molecule sensors had been shown previously to offer an increased density of functional groups, and to have comparable overall performance to their polymeric predecessors. We have shown that the rigid crystalline thin film structure of the small molecule films requires a film composition that can break up the crystallinity to have the film swell and therefore provide a functional relative differential resistance response to analyte vapors. This disruption of the film structure could be produced by either an increased ratio of carbon black to molecule or by the addition of plasticizer/carbon black. A framework for the specific requirements of each film has been proposed, depending on the size and polarity of the small molecule involved.

2.7 Bibliography

[1] Wohltjen, H. *Sens. Actuators* **1984**, *5*(4), 307–325.

[2] Grate, J. W. *Chem. Rev.* **2000**, *100*(7), 2627–2647.

[3] Zellers, E. T.; Park, J.; Hsu, T.; Groves, W. A. *Anal. Chem.* **1998**, *70*(19), 4191–4201.

[4] Getino, J.; Horrillo, M. C.; Gutierrez, J.; Ares, L.; Robla, J. I.; Garcia, C.; Sayago, I. *Sens. Actuators, B* **1997**, *43*(1-3), 200–205.

[5] Romain, A. C.; Nicolas, J.; Wiertz, V.; Maternova, J.; Andre, P. *Sens. Actuators, B* **2000**, *62*(1), 73–79.

[6] Vergara, A.; Llobet, E.; Brezmes, J.; Ivanov, P.; Cane, C.; Gracia, I.; Vilanova, X.; Correig, X. *Sens. Actuators, B* **2007**, *123*(2), 1002–1016.

[7] Abbas, M. N.; Moustafa, G. A.; Mitrovics, J.; Gopel, W. *Anal. Chim. Acta* **1999**, *393*(1-3), 67–76.

[8] Mirmohseni, A.; Oladegaragoze, A. *Sens. Actuators, B* **2004**, *102*(2), 261–270.

[9] Freund, M. S.; Lewis, N. S. *Proc. Natl. Acad. Sci. U.S.A.* **1995**, *92*(7), 2652–2656.

[10] Swann, M. J.; Glidle, A.; Cui, L.; Barker, J. R.; Cooper, J. M. *Chem. Commun.* **1998**, (24), 2753–2754.

[11] Patel, S. V.; Jenkins, M. W.; Hughes, R. C.; Yelton, W. G.; Ricco, A. J. *Anal. Chem.* **2000**, *72*(7), 1532–1542.

[12] Koscho, M. E.; Grubbs, R. H.; Lewis, N. S. *Anal. Chem.* **2002**, *74*(6), 1307–1315.

[13] Doleman, B. J.; Lonergan, M. C.; Severin, E. J.; Vaid, T. P.; Lewis, N. S. *Anal. Chem.* **1998**, *70*(19), 4177–4190.

[14] Sisk, B. C.; Lewis, N. S. *Sens. Actuators, B* **2005**, *104*(2), 249–268.

[15] Burl, M. C.; Sisk, B. C.; Vaid, T. P.; Lewis, N. S. *Sens. Actuators, B* **2002**, *87*(1), 130–149.

[16] Albert, K. J.; Lewis, N. S.; Schauer, C. L.; Sotzing, G. A.; Stitzel, S. E.; Vaid, T. P.; Walt, D. R. *Chem. Rev.* **2000**, *100*(7), 2595–2626.

[17] Sisk, B. C.; Lewis, N. S. *Sens. Actuators, B* **2003**, *96*(1-2), 268–282.

[18] Severin, E. J.; Lewis, N. S. *Anal. Chem.* **2000**, *72*(9), 2008–2015.

[19] Korotchenkov, G.; Brynzari, V.; Dmitriev, S. *Sens. Actuators, B* **1999**, *54*(3), 191–196.

[20] Han, K. R.; Kim, C. S.; Kang, K. T.; Koo, H. J.; Il Kang, D.; He, J. W. *Sens. Actuators, B* **2002**, *81*(2-3), 182–186.

[21] Feller, J. F.; Langevin, D.; Marais, S. *Synth. Met.* **2004**, *144*(1), 81–88.

[22] Chen, J. H.; Tsubokawa, N. *J. Appl. Polym. Sci.* **2000**, *77*(11), 2437–2447.

[23] Briglin, S. M.; Freund, M. S.; Tokumaru, P.; Lewis, N. S. *Sens. Actuators, B* **2002**, *82*(1), 54–74.

[24] Shurmer, H. V.; Corcoran, P.; Gardner, J. W. *Sens. Actuators, B* **1991**, *4*(1-2), 29–33.

[25] Shurmer, H. V.; Gardner, J. W.; Corcoran, P. *Sens. Actuators, B* **1990**, *1*(1-6), 256–260.

[26] Gao, T.; Woodka, M. D.; Brunschwig, B. S.; Lewis, N. S. *Chem. Mater.* **2006**, *18*(22), 5193–5202.

[27] Severin, E. J.; Doleman, B. J.; Lewis, N. S. *Anal. Chem.* **2000**, *72*(4), 658–668.

[28] Sisk, B. C.; Lewis, N. S. *Langmuir* **2006**, *22*(18), 7928–7935.

[29] Maldonado, S.; Garcia-Berrios, E.; Woodka, M. D.; Brunschwig, B. S.; Lewis, N. S. *Sens. Actuators, B* **2008**, *134*(2), 521–531.

[30] Lonergan, M. C.; Severin, E. J.; Doleman, B. J.; Beaber, S. A.; Grubbs, R. H.; Lewis, N. S. *Chem. Mater.* **1996**, *8*(9), 2298–2312.

[31] Sauerbrey, G. *Z. Phys.* **1959**, *155*(2), 206–222.

[32] Gerson, A. R.; Roberts, K. J.; Sherwood, J. N. *Acta Crystallogr. B* **1991**, *47*, 280–284.

[33] Matthews, F. W.; Warren, G. G.; Michell, J. H. *Anal. Chem.* **1950**, *22*(4), 514–519.

[34] Sakurai, T. *J. Phys. Soc. Jpn.* **1955**, *10*(12), 1040–1048.

[35] Lagreve, C.; Feller, J. F.; Linossier, I.; Levesque, G. *Polym. Eng. Sci.* **2001**, *41*(7), 1124–1132.

[36] Li, J. R.; Xu, J. R.; Zhang, M. Q.; Rong, M. Z.; Zheng, Q. *Polymer* **2005**, *46*(24), 11051–11059.

Chapter 3

Polymer Weight Variations in Polymer/Carbon Black Chemiresistor Vapor Sensors

3.1 Abstract

Broad molecular weight ranges of three polymers have been tested in polymer/carbon black composite chemiresistor sensors to determine if varying M_w alters or adds information to sensor response. The polymers studied — poly(ethylene oxide), poly(vinyl acetate), and polystyrene — span a wide range of glass transition temperatures (T_g). Sensor responses revealed that in the case of polystyrene, the high T_g polymer, response times were sharply decreased for the lowest M_w samples, increasing its practical use as a vapor sensor. Quartz crystal microbalance (QCM) measurements demonstrate that this decreased sensor response time is notably faster than the mass uptake response of the pure polymer.

3.2 Introduction

Conductive composites of carbon black mixed with thermoplastic polymers have attracted widespread interest over the last two decades for their uses as chemiresistive vapor sensors.[1–7] Films of such materials swell reversibly when exposed to an analyte vapor, yielding a change in the resistance of the sensor film.[8]

Responses of a given sensor vary with analyte, but are non-selective. Creating an array of such sensors each utilizing a different polymer yields response patterns allowing detection and quantification of a wide variety of analytes.[1,9] The selection of polymers for use in a sensor array depends on the intended use of the array. Similarities in polarity and functional groups between polymer and analyte are known to produce clear responses, and a broadly responsive array would incorporate polymers collectively containing a variety of functional groups.[10–12] Chiral polymers have been employed to differentiate between enantiomeric pairs of analyte vapors,[13]and reactivity between acidic and basic groups has been exploited to increase the overall sensitivity of an array.[14]

Less attention has been paid to the physical nature of the polymers used as the responsive chemical component in such arrays. A given polymer is assumed to have a glass transition temperature (T_g) below which the long-range motions of the polymer chains stop, and it assumes glassy, brittle qualities. Above T_g the polymer chains can slide past each other, and the bulk material becomes more flexible. Addition of plasticizer materials can significantly decrease the T_g of a polymer. The plasticizer molecules interpolate themselves between the polymer chains. This increases the average inter-chain separation and acts as an internal lubricant, allowing the chains to slide past one another more easily.[15]

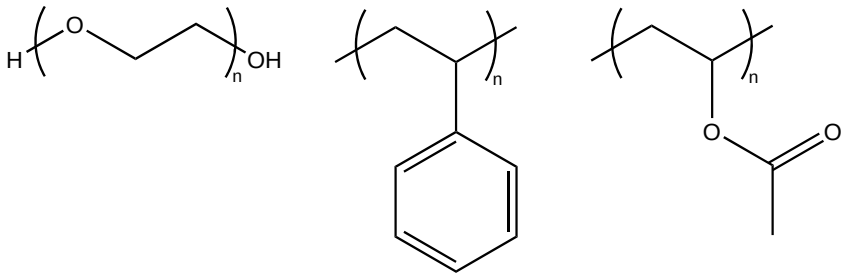

poly(ethylene oxide) polystyrene poly(vinyl acetate)

Figure 3.1: Polymers used in these experiments

Composite chemical vapor sensors as described generally employ polymers with T_g well below the operating temperature of the system, as polymers with high T_g yield extremely slow response times.[3,4] To take advantage of its lubricating properties, a plasticizer material is added to the composite, yielding a tripartate mixture: carbon black, polymer, and plasticizer. Even in materials with low T_g, addition of plasticizer can decrease the sensor response time.

Molecular structure and polarity of a polymer affect T_g.[16] Rigid backbone units or bulky sidegroups all provide barriers to polymer chain motion, which raises T_g. Additionally, increasing polarity increases T_g, as interactions between polymer repeat units increase. As such, even with plasticization, many polymer structures have remained largely unavailable to use in composite chemiresistors, such as many polyamides, or polymers containing many phenylene groups (such as polystyrene).

T_g is not, however, the only attribute that contributes to the polymer response time. The ability of the analyte molecules to penetrate the sensor film also plays a role in this process. Very thick films yield slower response times. It has been proposed that lowered

viscosity of the matrix polymer could aid in the diffusion of organic vapors through the film.[4] Viscosity of a given polymer increases with the molecular weight of the polymer, following the Mark-Houwink-Staudinger-Sakurada (MHSS) relation:

$$[\eta] = K\overline{M}_v^a \tag{3.1}$$

in which K is the MHSS "constant" and a the MHSS exponent. $\overline{M}_v$ is the viscosity average molecular mass. K and a both depend on the exact polymer-solvent pair, as well as the temperature. However, for a linear flexible polymer, a is generally between 0.5 and 0.8. The intrinsic viscosity (or limiting viscosity number) $[\eta]$ is expressed in units of reciprocal density.[16]

Studies have revealed a decrease in the percolation threshold (i.e., the percentage of conducting filler at which the mixture experiences an insulator-to-conductor transition) as the molecular weight of the polymer decreases.[17,18] Another study reports a mix of low and high molecular weight polyethylene (PE) in which the carbon black preferentially disperses into the low molecular weight regions of PE.[19] Polystyrene/CB composite materials prepared by in-situ polymerization showed increased responsivity and decreased response times for lower molecular weight polystyrene.[5] However, none of their sensor responses reached equilibrium status, the polydispersity indices (PDI) of their prepared polymers increased dramatically as molecular weight decreased, and they only covered a single order of magnitude range in the number average molecular weight (M_n) and a twofold variation in the weight average molecular weight (M_w). Most other studies of such sensors have been blind to the molecular weights of the polymers used.

Polymer	T_g (°C)[16]	M_w Used	Reported $[\eta]$ Values (ml/g)
PEO	−67	7.3x10^3–1.2x10^6	152–9330[a]
PVAc	35	1.5x10^4–5.0x10^5	12–189[b]
PS	98	2.5x10^3–2.0x10^6	16–189[c]

[a] Values for PEO M_w = 5k–2.2M, at 25 °C in H_2O.[20]
[b] Values for PVAc M_w = 11k–600k, at 30 °C in acetone.[21]
[c] Values for PS M_w = 38k–3.3M, at 35 °C in cyclohexane.[22]

Table 3.1: Physical characteristics of the polymers used in these experiments. M_w values are the weight average molecular weights of the polymers used. Reported $[\eta]$ (intrinsic viscosity) values are literature values determined for a weight range of each polymer as referenced.

It is clear that molecular weight affects the behaviors of carbon black/polymer composite sensors. In this study, three polymers (Figure 3.1, Table 3.1) spanning a range of T_g values have been explored as sensors, over a range of molecular weights, to determine if varied molecular weight alters or increases sensor responsiveness or sensitivity. The mass sorption and swelling properties of the listed polymers have also been examined via quartz crystal microbalance (QCM) and ellipsometry.

3.3 Experimental

3.3.1 Materials

Poly(ethylene glycol) / poly(ethylene oxide) (PEG/PEO) materials were purchased from Scientific Polymer Products, at the following molecular weights (M_w) and polydispersity indices (PDI, equal to M_w/M_n): M_w = 7290, PDI = 1.08 (PEG 8); M_w = 33,300, PDI = 1.02 (PEG 33); M_w = 100,400, PDI = 1.04 (PEO 100); M_w = 243,200, PDI = 1.04 (PEO 260); M_w = 609,700, PDI = 1.03 (PEO 600); and M_w = 1,020,000, PDI = 1.15 (PEO 1.2M).

Poly(vinyl acetate) (PVAc) was purchased at the approximate M_w of 15k, 100k, and 260k (PVAc 15, PVAc 100, and PVAc 260) from Scientific Polymer Products. PVAc of approximate M_w = 500k (PVAc 500) was purchased from Sigma-Aldrich. GPC determination showed PDI of 2.5–3.5 for all materials.

Polystyrene (PS) GPC powder standards were purchased from Sigma Aldrich, at the following M_w:M_w = 2460, PDI = 1.01 (PS 2k); M_w =13,200, PDI = 1.06 (PS 13); M_w = 44,000, (PS 44, no PDI listed); M_w =280,000, (PS 280, no PDI listed); M_w = 2,043,000, PDI = 1.02 (PS 2M).

Reagent grade hexane, heptane, chloroform, ethanol, isopropanol, ethyl acetate, acetone, and tetrahydrofuran were acquired from VWR. Chromium metal was purchased from RD Matthes and gold wire (0.25 mm diam., 99.9+%) from Sigma-Aldrich. Dioctyl phthalate (DOP) was also acquired from Sigma-Aldrich. Black Pearls 2000, a carbon black (CB) material, was donated by Cabot Co. (Billerica, MA). All materials were used as received.

3.3.2 Sample Preparation

Sensor substrate slides were prepared as previously described (Section 2.3.2). In brief, layers of chromium and gold were thermally evaporated onto cleaned microscope slides, with a masked section down the long center axis of the slide. After deposition, slides were cut into 0.5 cm x 2.5 cm samples to use for later sensor film deposition.

All sensors were deposited from solutions of a given polymer and DOP (a plasticizer), mixed with CB. The polymer and DOP were first dissolved, after which carbon black was added, and the entire mixture then sonicated for $>$30 min to disperse the CB parti-

cles. All materials were added to 20 mL of solvent (PEO in $CHCl_3$, and PVAc and PS in THF) in amounts totalling 200 mg of solid materials. Mixtures for all polymers were prepared at both 20 and 40 weight percent (wt%) of CB, and all had a 3:1 mass ratio of polymer:DOP — i.e., solutions were prepared of 40/120/40 and 80/90/30 mg respectively of CB/polymer/DOP. Solutions containing only 90 mg of polymer or 90/30 mg of polymer/DOP (but no CB) were also prepared.

Resistive sensors and QCM samples were prepared from the CB-containing mixtures. Pure polymer and polymer/DOP films were used for both QCM and ellipsometry measurements. Two mixtures were made of each CB-containing formulation. Two resistive sensors were made from each mixture. QCM films were prepared from both mixtures.

All samples were prepared as previously described (Section 2.3.2). In brief, sensor and QCM samples were deposited via airbrush onto sensor substrates or QCM crystals, respectively, and ellipsometry samples were deposited onto cleaned pieces of silicon wafer using a spin coater, in order to obtain smooth, homogenous films. The baseline frequency of each QCM crystal was noted prior to film deposition, and all QCM samples were placed in a vacuum desiccator for at least 2 h prior to use. The frequency shift effected by deposition of the sensor film was then recorded, prior to QCM response data collection.

3.3.3 Measurements and Data Analysis

3.3.3.1 Chemiresistive Sensors

An automated vapor generation and delivery system was used to deliver background air and analyte vapors to the array of chemiresistive detectors (Section 2.3.3.1). Resistances

of all sensors were continuously monitored by and recorded to the controlling computer.

The sensor array was placed in a chamber made from PTFE and stainless steel that was connected via Teflon tubing to the vapor delivery system. The sensors were initially exposed to a 2.5 L min^{-1} flow of air for a period of time sufficient to stabilize the baseline resistance of the sensors. A single exposure to an analyte vapor consisted of a baseline period of oil-free air with a water content of 12 ppth, followed by exposure to analyte, followed by a further purge of air. For PEO samples, these time periods were 200/100/200 s. PVAc samples were exposed to 100/100/100 s baseline/exposure/purge times. PS samples were initially run with time periods of 100/100/100 s, which were later increased to 200/350/200 s.

Analytes for all sensors were *n*-hexane, *n*-heptane, chloroform, ethanol, isopropanol, ethyl acetate, and toluene. In each sensor run, the seven analytes were presented in random order 25 times each to the detector array. All exposures were made at an analyte partial pressure ratio in air of $P/P^0 = 0.01$ (where P is the partial pressure and P^0 is the vapor pressure of the analyte at room temperature). Every sensor array was exposed to at least three sensor runs.

The resistance of each sensor was measured approximately every 5 s. The sensor response to each analyte is expressed as the relative change in resistance, $\Delta R_{\text{max}}/R_{\text{b}}$, where R_{b} is the steady-state baseline resistance of the sensor and ΔR_{max} is the maximum resistance change observed during exposure to the analyte. Signal-to-noise ratios (SNR) were also calculated for each exposure, with the SNR value defined as ΔR_{max} divided by the standard deviation of the data points used to calculate R_{b}. All values were calculated as

previously reported (Section 2.3.3.1). Principal components analysis (PCA)[23] was performed on all sets of array data to visualize the analyte resolving ability of each array. All data analysis was undertaken in MATLAB.

3.3.3.2 QCM Measurements

Coated QCM crystals were mounted in a chamber and exposed to analytes via a similar system to that used for the chemiresistive sensors (Section 2.3.3.2). Each crystal was exposed to baseline, analyte exposure, and purge steps. For all PEO films, these time periods were 100 s each. Mixed PVAc films were exposed to time periods comprising 60/70/80 s, while pure PVAc films were exposed for periods of 100/100/100 s. All mixed PS films were exposed for time periods of 100/150/100 s, and pure PS films, due to extreme slowness of response and purge time, were sampled with time periods of 300/600/300 s. Hexane and ethyl acetate were the analytes for QCM measurements, and were exposed to the QCM films at a partial pressure of $P/P^0 = 0.01$. The two analytes were presented in random order 10 times each. Two or more data runs were recorded for each crystal.

Deposition of the sensor film on the QCM crystal causes a change in frequency Δf_{f}, and each exposure to an analyte causes a further frequency shift, Δf_{a}. The ratio of the analyte shift to the film shift allows the determination of the mass absorbed per mass of the deposited film ($\Delta m_{\mathrm{a}}/m_{\mathrm{f}}$, a unitless quantity) via the use of the Sauerbrey equation (Section 2.3.3.2), which directly relates changes in mass and frequency of a thin film coated quartz crystal. The $\Delta m_{\mathrm{a}}/m_{\mathrm{f}}$ values for all exposures were then calculated and used for further QCM analysis.

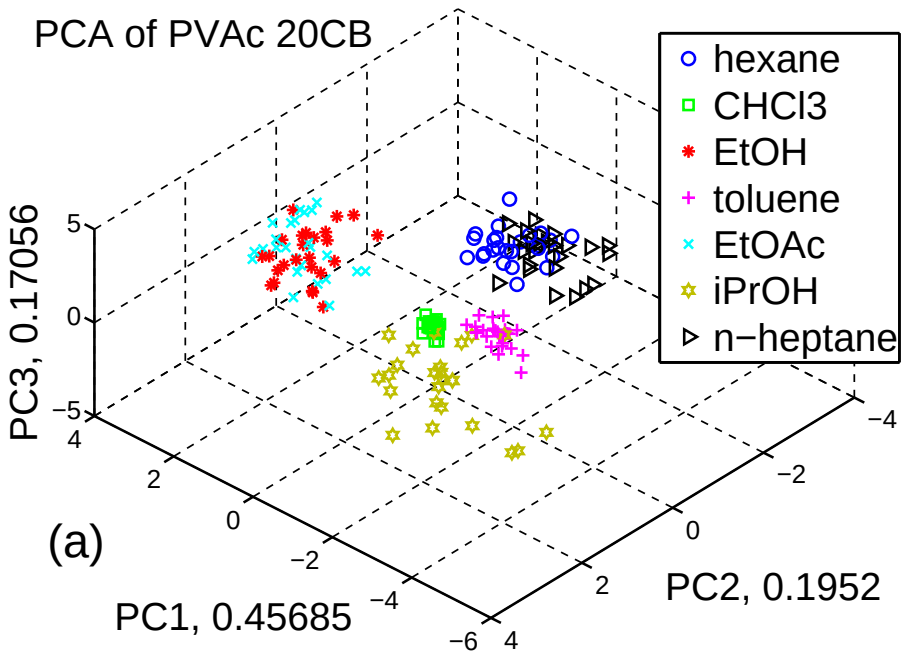

3.2(a) PCA plot PVAc 20 wt%

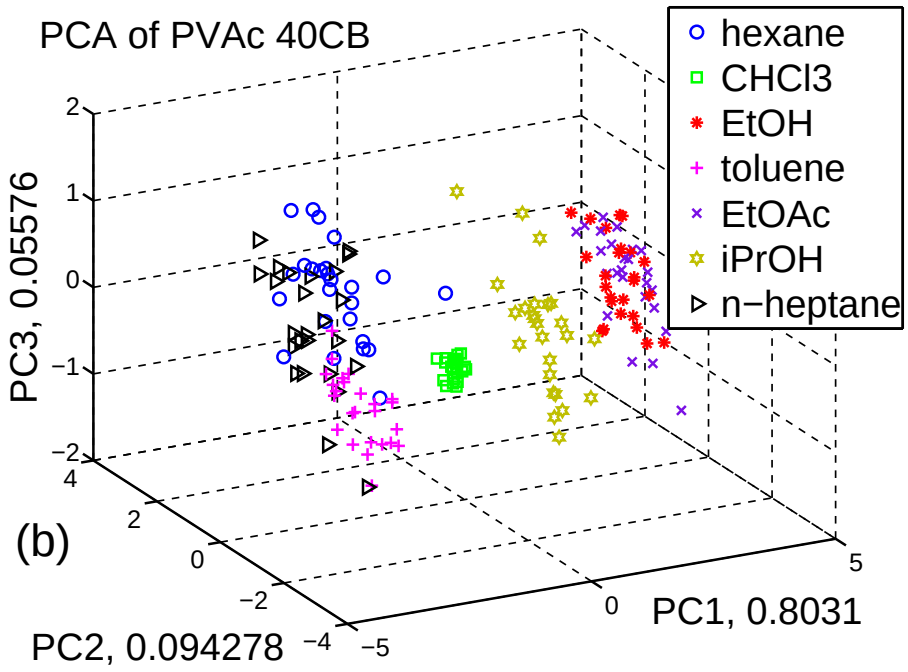

3.2(b) PCA plot PVAc 40 wt%

Figure 3.2: PCA plots of a) PVAc 20 wt%, b) PVAc 40 wt%, and c) both PVAc 20 and 40 wt% sensors. There are 25 exposures to each analyte. Numbers next to each principal component axis reflect the percentage of the total sensor response variance contained in that principal component (continued on next page).

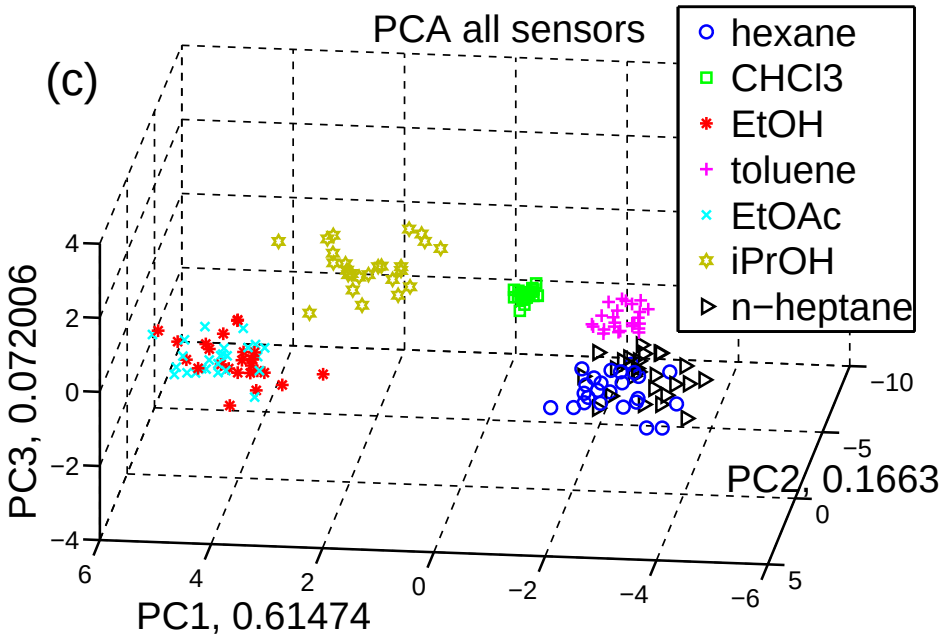

3.2(c) PCA plot PVAc 20 and 40 wt%

Figure 3.2: (cont.) PCA plots of a) PVAc 20 wt%, b) PVAc 40 wt%, and c) both PVAc 20 and 40 wt% sensors. There are 25 exposures to each analyte. Numbers next to each principal component axis reflect the percentage of the total sensor response variance contained in that principal component.

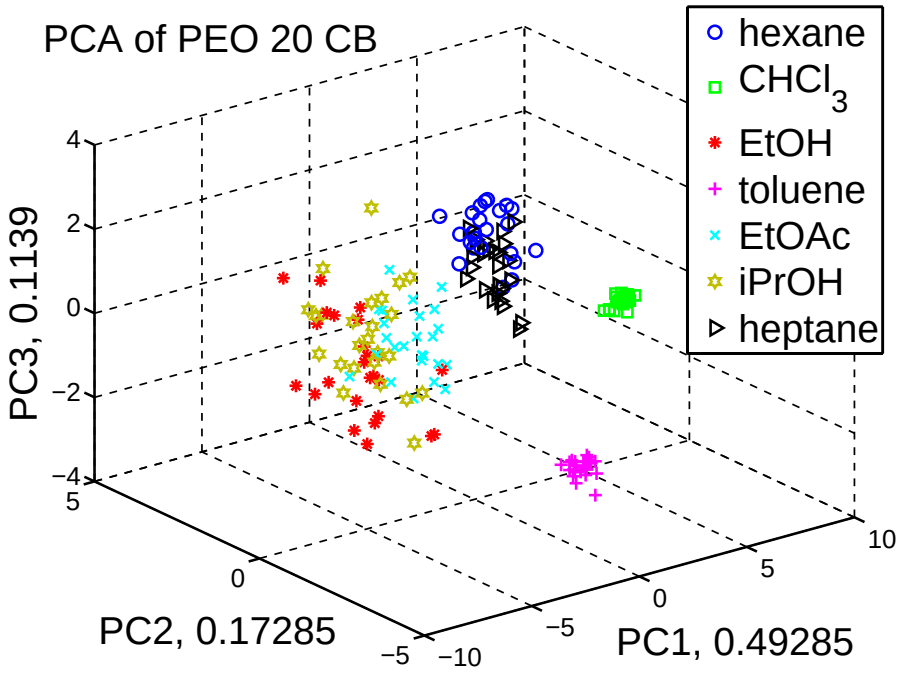

Figure 3.3: PCA plot of PEO 20 wt%. There are 25 exposures to each analyte. Numbers next to each principal component axis reflect the percentage of the total sensor response variance contained in that principal component

3.3.3.3 Ellipsometry

Ellipsometry was performed with a Gaertner L116C system. Samples for ellipsometry were placed in a plastic chamber with a drilled opening at each end to allow the laser beam to reach the sample and detector in an unobstructed fashion. Baseline thickness readings were collected under a steady 65 mL min^{-1} stream of air, with an adjacent ventilation tube used to flush the chamber. Exposures to saturated hexane vapor at 65 mL min^{-1} were initiated by hand. During the exposures, the ventilation tube was removed, to encourage maximum retention of hexane in the chamber. The purge and exposure times were each $\geq$5 min. Each sample was exposed a minimum of five times, and at least five data points were measured during and between each exposure. These data points were averaged to yield the relative thickness change of the film for each analyte exposure.

3.4 Results

3.4.1 Chemiresistive Sensors

All sensors responded to all analytes presented to the arrays. PEO sensors responded in an equilibrium fashion in the time periods investigated. PVAc sensors generally responded within the given time. PS sensors mostly did not achieve equilibrium resistance responses within either the 100 s or 350 s exposure periods. All sensors had highest $\Delta R/R_b$ values in response to $CHCl_3$ and toluene.

PCA plots of both PEO and PVAc sensor responses responses yielded separation between some analytes (non-equilibrium responses of PS are not suitable for PCA). Both

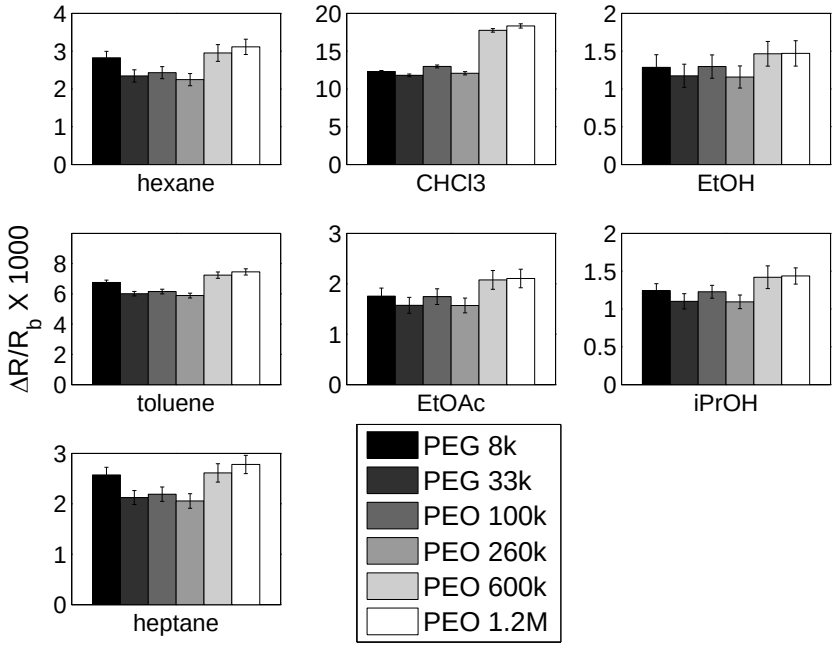

Figure 3.4: PEO (20 wt% CB) $\Delta R/R_b$ values in response to all seven analytes. Values are the average of 25 exposures to each analyte, and the error shown is one standard deviation.

polymers clearly separated chloroform and toluene from all other analytes, and separated the other polar analytes (EtOH, iPrOH, and EtOAc) from the alkanes (hexane and heptane). PEO arrays separated hexane from heptane, and provided partial separation betwen the polar analytes (Figure 3.3). PVAc provided no separation between the alkanes, and did not differentiate between EtOH and EtOAc, but did clearly separate iPrOH from them. PCA using responses from both 20 and 40 wt% PVAc sensors provided clearer separation than either PVAc 20 or PVAc 40 sensors by themselves (Figure 3.2).

All molecular weights of a given polymer displayed the same pattern of responses to the varied analytes. PVAc $\Delta R/R_b$ values were not entirely consistent across the M_w distribution, with $\Delta R/R_b$ values generally highest for PVAc 15. PEO displayed flat responses across all molecular weights to each analyte (Figure 3.4).

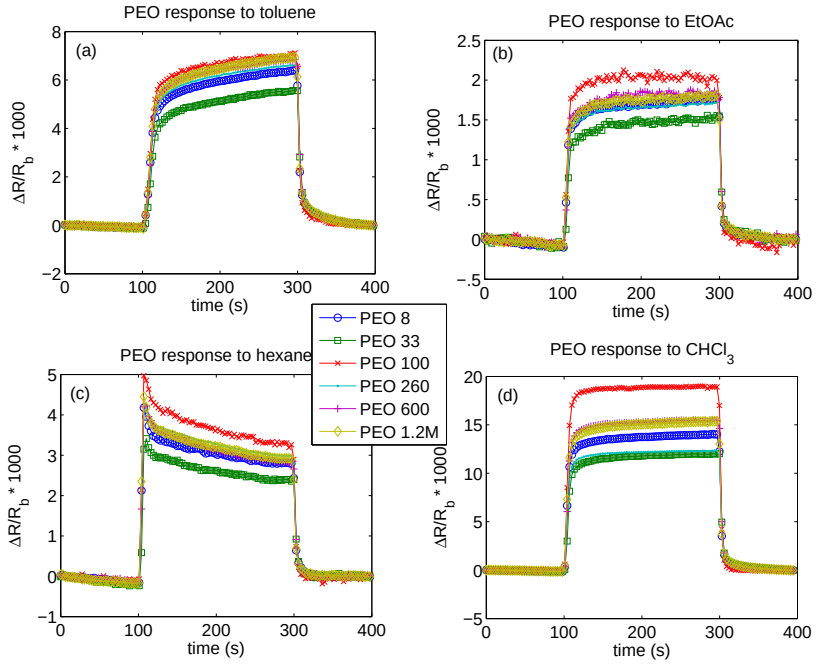

Figure 3.5: $\Delta R/R_b$ values of 200 second single exposures of PEO (20 wt% CB) to a) toluene, b) EtOAc, c) hexane, and d) $CHCl_3$. Each analyte was presented at $P/P^0 = 0.01$, in a total 2.5 L min^{-1} flow of air.

Single response curves of all weights of PEO displayed similar response times and curve shapes to all analytes (Figure 3.5). PS curves at both 100 s (Figure 3.6) and 350 s (Figure 3.7) exposure times showed a change in response as M_w of the polymer increased, showing quick equilibrium responses for PS 2k and PS 13, and much slower rise and fall times for all other molecular weights. At 350 s exposures, larger M_w polymers came to a greater percentage of the $\Delta R/R_b$ of the PS 2k/PS 13 response than during the 100 s exposures. They still did not achieve equilibrium during the longer exposure to any analyte other than chloroform, to which they displayed a stable response after about 200 s.

3.4.2 QCM Responses

All films displayed mass uptake responses. For all three polymers, $\Delta m_{\mathrm{a}}/m_{\mathrm{f}}$ for 40 wt% CB films were larger than for 20 wt% CB films. Responses for each polymer were larger for CB-containing films than for non-CB-containing films. Responses were generally flat across M_w ranges.

All PEO films responded in an equilibrium manner within their 100 s exposure period. PVAc films were generally noisy, with smaller responses than PEO films. PS films at 40 wt% CB came to an equilibrium response within the 150 s exposure time. PS 20 wt% films did not quite achieve equilibrium within this time period, although PS/plasticizer films not containing CB did equilibrate within that length of time. Pure PS films did not achieve equilibrium within a 600 s time period, other than the PS 2k film (Figures 3.8–3.11).

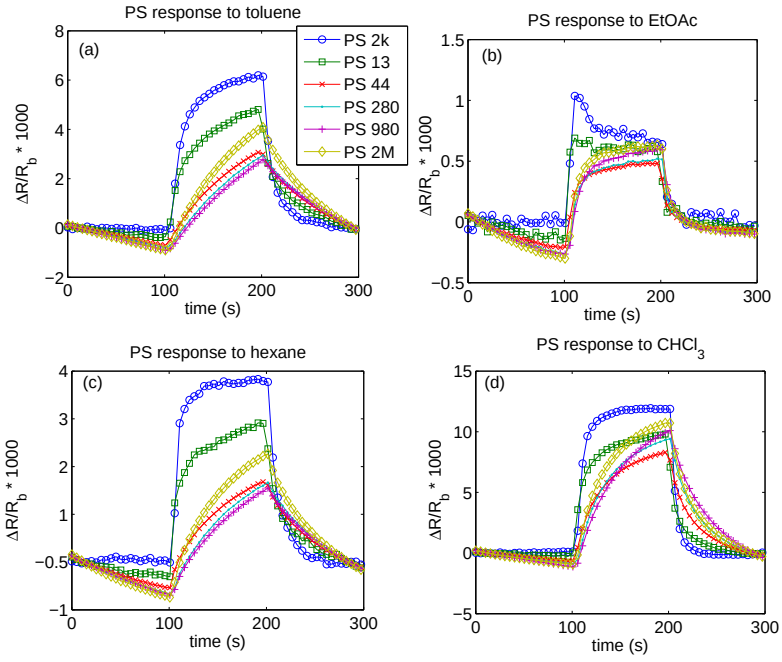

Figure 3.6: $\Delta R/R_b$ values of 100 second single exposures of PS (20 wt% CB) to a) toluene, b) EtOAc, c) hexane, and d) $CHCl_3$. Each analyte was presented at $P/P^0 = 0.01$, in a total 2.5 L min^{-1} flow of air.

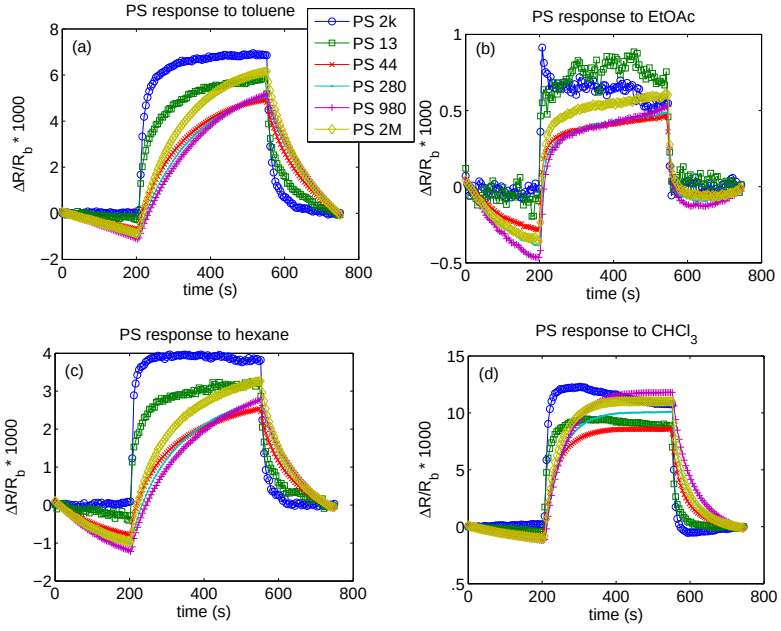

Figure 3.7: $\Delta R/R_b$ values of 350 second single exposures of PS (20 wt% CB) to a) toluene, b) EtOAc, c) hexane, and d) $CHCl_3$. Each analyte was presented at $P/P^0 = 0.01$, in a total 2.5 L min^{-1} flow of air.

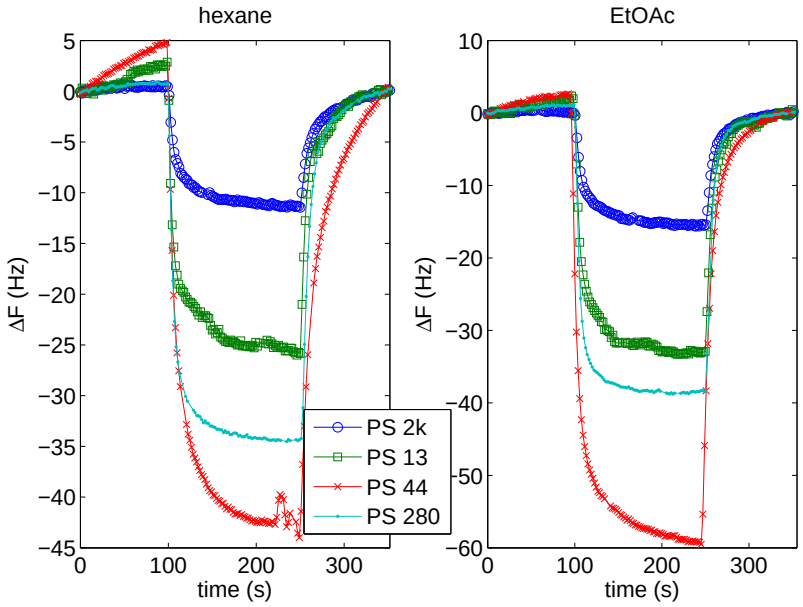

Figure 3.8: Single QCM responses of PS (40 wt% CB) films to hexane and EtOAc. Each analyte was presented at $P/P^0 = 0.01$, in a total flow 2.5 L min^{-1} of air. PS 980 and PS 2M films are not displayed as their absolute responses were very large, due to the thickness of those films.

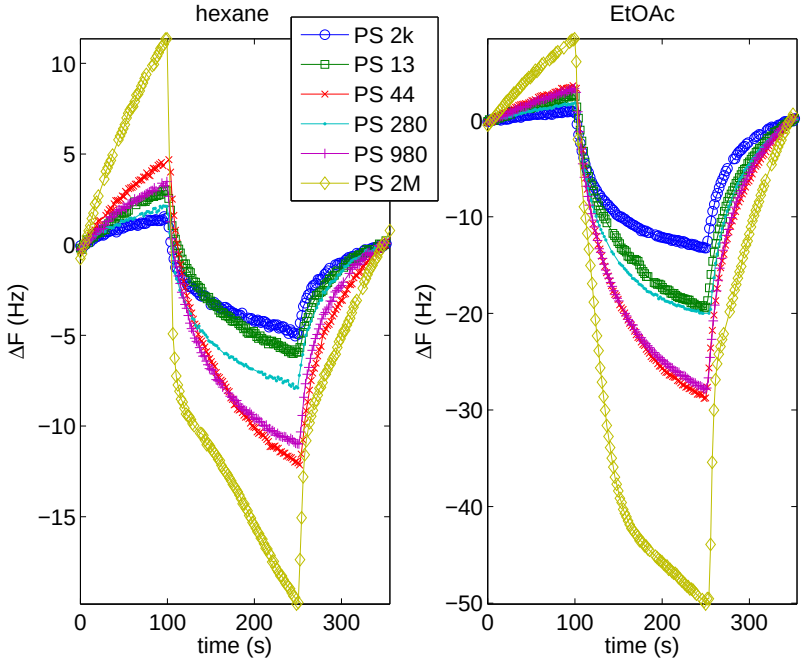

Figure 3.9: Single QCM responses of PS (20 wt% CB) films to hexane and EtOAc. Each analyte was presented at $P/P^0 = 0.01$, in a total flow 2.5 L min^{-1} of air.

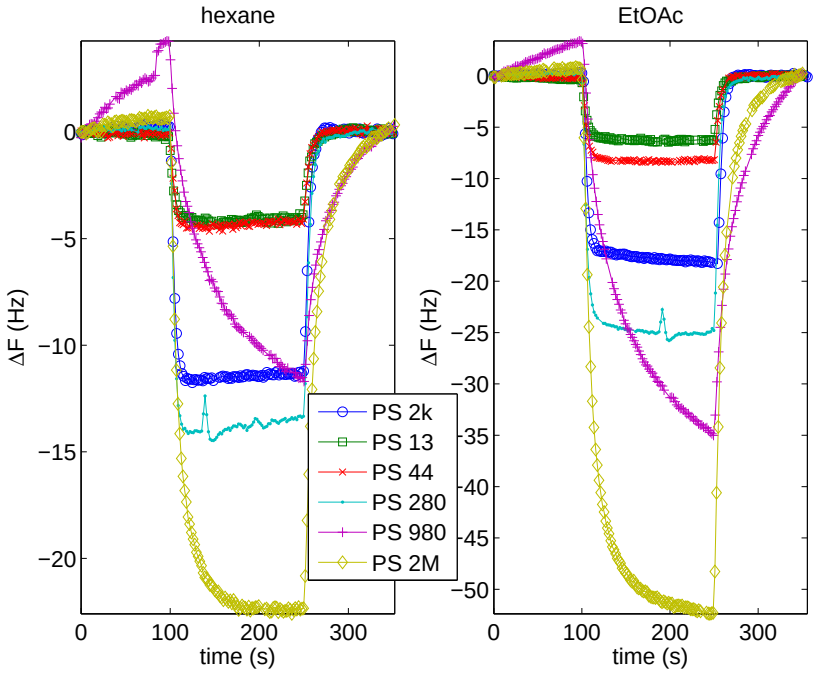

Figure 3.10: Single QCM responses of PS/plasticizer (3:1 ratio) films to hexane and EtOAc. Each analyte was presented at $P/P^0 = 0.01$, in a total flow 2.5 L min^{-1} of air.

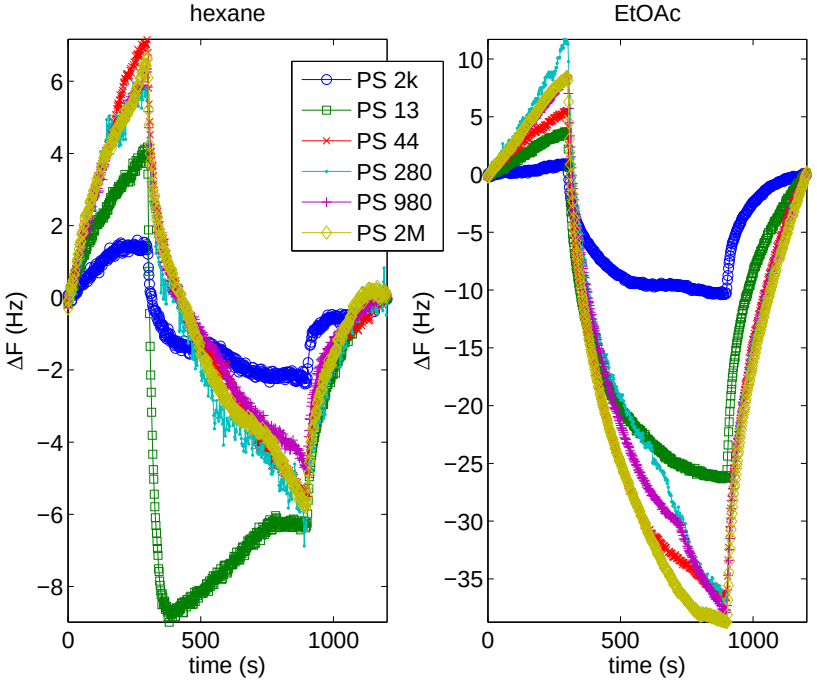

Figure 3.11: Single QCM responses of pure PS films to hexane and EtOAc. Each analyte was presented at $P/P^0 = 0.01$, in a total flow 2.5 L min^{-1} of air.

3.4.3 Ellipsometry

All polymer films responded to hexane vapor, showing stable responses after the 5 minute exposure period. Both pure polymer and polymer/plasticizer films displayed stable baseline thicknesses, with pure polymer films shifting $\leq$1% and polymer/plasticizer films shifting $\leq$2% of their original thicknesses over the course of the exposures.

Pure PEO and PVAc displayed swelling responses of $\sim$1.5–2% of their original thickness. Pure PS films swelled to a greater extent, around 6–7% in most cases (Table 3.2). Mixed polymer/plasticizer films were thicker than their respective pure polymer films, although deposition quantities were not rigorously controlled. Mixed films also swelled to a much greater extent than the pure films, usually from 8–12%. Responses were generally flat across the studied molecular weight ranges.

3.5 Discussion

High T_g polymers have largely been seen as unsuitable for use in polymer/carbon black composite chemiresistor sensors due to their extremely slow response times. These very long response times have been attributed to the swelling mechanism of such sensors being inhibited in their glassy state, below their T_g. Lower viscosity, however, can be seen as affecting both the ability of a polymer to swell, and the ability of an analyte vapor to penetrate a polymer matrix. Here use of arrays of monodisperse molecular weight polymers are seen to provide some discrimination ability. Additionally, very low M_w sensors of polystryene, a high T_g polymer, respond on a much reduced time scale, potentially opening the door to use of other high T_g sensors in composite sensors.

Polymer		No DOP Plasticizer		With Plasticizer	
		t (Å)	$\Delta h/h$ (%)	t (Å)	$\Delta h/h$ (%)
PEO	8	313	1.5(0.3)	381	10.3(0.5)
		330	1.7(0.3)	367	13.4(0.3)
	35	355	1.5(0.1)	402	18.8(0.8)
		363	1.3(0.1)	393	17.7(0.8)
	100	402	1.6(0.1)	461	10.8(1.0)
		399	1.9(0.2)	532	5.1(0.5)
	250	410	1.9(0.2)	627	11.4(0.5)
		428	1.3(0.2)	582	12.5(0.8)
	600	450	2.1(0.6)	698	7.1(0.3)
		446	1.9(0.3)	601	2.9(0.1)
	1.2M	574	1.8(0.3)	911	8.2(0.4)
		606	1.6(0.3)	889	8.3(1.0)
PVAc	15	367	2.1(0.1)	365	10.0(0.7)
		369	2.2(0.2)	380	7.6(1.3)
	100	363	1.6(0.2)	511	10.1(0.7)
		372	0.9(0.1)	497	10.3(0.3)
	260	372	1.4(0.3)	457	8.2(1.0)
		326	1.4(0.1)	434	16.3(1.0)
	500	354	1.7(0.4)	489	7.2(0.5)
		391	1.7(0.1)	428	12.5(0.5)
PS	2k	283	9.1(0.7)	570	10.9(0.5)
		337	8.5(0.7)	460	n/a
	13	285	6.7(0.5)	421	10.2(0.5)
		282	6.6(0.2)	417	9.0(0.3)
	44	303	7.1(0.6)	400	10.4(0.2)
		313	6.2(0.6)	395	9.9(0.6)
	280	377	6.8(0.6)	547	9.7(0.8)
		383	6.6(0.1)	518	10.6(0.4)
	980	339	7.3(0.2)	458	8.1(0.3)
		347	5.9(0.5)	612	11.4(0.4)
	2M	303	7.1(0.3)	704	11.2(1.1)
		349	6.8(0.2)	806	9.5(1.0)

Table 3.2: Averaged ellipsometry responses of PS, PVAc, and PS films to saturated hexane vapor at 65 mL min^{-1}. Reported error is one standard deviation. PS 2k film with no listed response began to break up during exposure.

3.5.1 Sensor Responses

Looking at $\Delta R/R_b$ values and single sensor responses yields valuable information about what does and does not change as the M_w of a given polymer is varied. Differing weight changes nothing about the chemical functionality of a polymer. As such, we see clearly that all tested M_w values show the same pattern of responses to the test suite of analytes. In Figure 3.4, all sensors have notably the largest response to chloroform, followed by their responses to toluene, with all other analytes eliciting smaller responses. The response pattern is presumed to be predicated on the chemical functionality of the polymer, and the pattern retention across M_w values provides further evidence of this.

In PEO, a sensor that achieves equilibrium resistance changes within tens of seconds (Figure 3.5), it is also seen that M_w does not change the $\Delta R/R_b$ values reached (Figure 3.4). This flat response indicated that in systems already reaching rapid equilibrium (e.g., low T_g polymer composites) viscosity variations do not alter the ability to achieve an equilibrium response.

In a high T_g polymer such as polystyrene, however, we can see a substantial decrease in response time attributable to viscosity differences. The lowest weights of PS tested, PS 2k and PS 13, achieved an equilibrium response within a time period similar to that of PEO, tens of seconds. Higher M_w PS polymers generally did not reach stable $\Delta R/R_b$ responses in 100 s for any analyte (Figure 3.6), and not in over five minutes of exposure time for non-polar analytes (Figure 3.7). Time for resistance recovery to baseline also greatly decreased in the low M_w PS sensors, indicating that both adsorption and desorption processes are affected.

In the case of polystyrene, T_g does drop as M_w values get very low. The changes in T_g have been experimentally determined to follow the Kanig-Ueberreiter equation, Eq. (3.2):[24,25]

$$\frac{1}{T_g(M_n)} = \frac{1}{T_g(\infty)} + \frac{K}{M_n} \tag{3.2}$$

with K = 0.78, and the asymptotic value of T_g = 371 K (98 °C). Even at the low weight limit of PS 2k, however, with reported M_n = 2440, the T_g = 61 °C, still well above the operating temperature of the sensors. PS 13, with reported M_n = 12,400, has T_g = 92 °C, very close to the limiting value. While dioctyl phthalate as a plasticizer does lower the T_g values of polystyrene,[26] the difference in baseline T_g between PS 13 and the higher M_w polystyrenes is insufficient to allow plasticization of the molecule to solely explain the disparities in their response curves.

Both of the quickly responsive molecular weights of PS are also below the critical molecular weight (M_c) of polystyrene of around 31,000 (M_c for PVAc is around 24,000 and for PEO is under 5,000. All PEO weights used were above this, and the PVAc samples used were all high PDI).[27] M_c is the weight above which the polymer molecules have sufficient length to intertwine, and the dependence of the zero shear rate viscosity versus log of molecular weight enters a different power regime. This weight directly references a quality of the pure polymer, whereas the intrinsic viscosity relates to the ability of a polymer to affect a mixed solution viscosity. Entanglement molecular weight is often used in discussion of high temperature pure polymer melts and solids, and it is difficult to assess how it reflects on composite sensor materials.

Lowered viscosity due to molecular weight, lack of entanglement, and potential plasticization all allow the lower M_w polystyrene samples to respond much more quickly as composite vapor sensors. Low molecular weight fractions of other high T_g polymers could also display these same improvements.

3.5.2 Array Discrimination

Both PEO and PVAc sensor arrays were able to provide some discriminatory power between analytes (Figures 3.3 and 3.2). A simple examination of the $\Delta R/R_b$ values for PEO (Figure 3.4) shows much larger responses for chloroform and toluene than for the other analytes. However, the simple $\Delta R/R_b$ responses to hexane are not notably different than those in response to EtOH or EtOAc, yet hexane is clearly separated from those in PCA plots, and clustered with heptane.

Enough information is clearly being captured across the sensor responses to make that separation. PVAc had a similar pattern of responses to PEO, and also showed separation along more than one axis of variance. Examination of the PCA plot for the PVAc 40 wt% CB sensors does reveal most separation along the first principal component, capturing 80% of the total variance returned by the sensors (Figure 3.2b). But the plots for PEO 20 wt% CB and PVAc 20 wt% CB have less than 50% of their total variance within the first PC, revealing a broader set of information being captured.

However, each analyte array contained multiple sensors of each molecular weight, thus increasing the overall number of inputs to PCA. We would expect very poor or no discrimination between analytes (and not along more than one dimension) if all sensors in the

array were functionally identical. While this may indicate added resolving power afforded by molecule weight variation, it is not possible to completely disentangle that contribution from the variation added by having multiple copies of each sensor — deposition differences between each film could be a confounding source of added variation. The added clustering provided by the merging of the sensor response from both PVAc 20 and 40 wt% CB indicates how an induced difference of a physical nature can add variation (even as it showcases a simple way to increase sensor variety while including absolutely minimal chemical variation among a set of sensors).

3.5.3 Mass Uptake and Swelling

Pure PS films are very slow to sorb mass during QCM exposures, as PS in its glassy state below T_g is not highly permeable. Only PS 2k comes to an equilibrium response within the full 10 minutes of analyte exposure, although, as with the sensor responses, PS 13 comes close (Figure 3.11). This further supports these M_w levels being beneath some limiting mass that renders them more rapidly responsive, though they are still slow at mass uptake.

Mixed PS/plasticizer films, however, showed an enormous decrease in mass sorption times, with almost all mixed films coming to equilibrium within one minute. While this does not directly address changes in swelling time, it does indicate that plasticizer aids all M_w samples equally in pure mass sorption. It further demonstrates the difference between mass sorption and sensor response, as does the fact that all QCM films showed greater response to EtOAc than to hexane, the reverse of which held true with the chemiresistors.

Addition of carbon black to QCM films slowed down mass uptake compared to the

polymer/plasticizer films. The CB-containing films were still notably faster than the pure polymer films. Unlike the sensor responses, or the pure polymer QCM films, no real response time differences related to M_w were seen, indicating the role of CB in mass sorption, and, again, highlighting the importance of both sorption and swelling in the responsiveness of these composite films.

When examined by ellipsometry, pure films of PS displayed much greater swelling in response to hexane than did films of PEO or PVAc, even with the relatively short exposure times (5 min.) compared to the response time scales seen with sensors and QCM films. As seen in Figures 3.4–3.7, the $\Delta R/R_b$ responses to hexane of the plasticized 20 wt% CB films of PEO and PS are similar in scale. However, the notable swelling of the PS film emphasizes the potential use of PS, a material not previously considered a good sensor candidate, due to its high T_g.

3.6 Conclusions

Polymer/CB sensor arrays comprised of only a single polymer substrate, but encompassing several molecular weights of that polymer, have been studied to examine the effect of M_w on sensor and array response. There is some evidence that the M_w variations are sufficient to provide analyte separation. Also, examination of low M_w polystyrene samples showed much improved sensor response times. As polystyrene and other high T_g polymers have generally been considered unsuitable for use in composite chemical vapor sensors, these data provide a path toward incorporating many other high T_g polymers previously considered inaccessible.

3.7 Bibliography

[1] Freund, M. S.; Lewis, N. S. *P. Natl. Acad. Sci. USA* **1995**, *92*(7), 2652–2656.

[2] James, D.; Scott, S. M.; Ali, Z.; O'Hare, W. T. *Microchim. Acta* **2005**, *149*(1–2), 1–17.

[3] Koscho, M. E.; Grubbs, R. H.; Lewis, N. S. *Anal. Chem.* **2002**, *74*(6), 1307–1315.

[4] Dong, X. M.; Luo, Y.; Xie, L. N.; Fu, R. W.; Zhang, M. Q. *Thin Solid Films* **2008**, *516*(21), 7886–7890.

[5] Li, J. R.; Xu, J. R.; Zhang, M. Q.; Rong, M. Z. *Carbon* **2003**, *41*(12), 2353–2360.

[6] Brudzewski, K.; Osowski, S.; Markiewicz, T. *Sens. Actuators, B* **2004**, *98*(2-3), 291–298.

[7] Thaler, E. R.; Kennedy, D. W.; Hanson, C. W. *Am. J. Rhinol.* **2001**, *15*(5), 291–5.

[8] Severin, E. J.; Lewis, N. S. *Anal. Chem.* **2000**, *72*(9), 2008–2015.

[9] Lonergan, M. C.; Severin, E. J.; Doleman, B. J.; Beaber, S. A.; Grubbs, R. H.; Lewis, N. S. *Chem. Mater.* **1996**, *8*(9), 2298–2312.

[10] Briglin, S. M.; Gao, T.; Lewis, N. S. *Langmuir* **2004**, *20*(2), 299–305.

[11] Burl, M. C.; Sisk, B. C.; Vaid, T. P.; Lewis, N. S. *Sens. Actuators, B* **2002**, *87*(1), 130–149.

[12] Lei, H.; Pitt, W. G. *Sens. Actuators, B* **2007**, *120*(2), 386–391.

[13] Ryan, M. A.; Lewis, N. S. *Enantiomer* **2001**, *6*(2-3), 159–170.

[14] Tillman, E. S.; Lewis, N. S. *Sens. Actuators, B* **2003**, *96*(1-2), 329–342.

[15] Odian, G. G. *Principles of Polymerization;* Wiley: New York, 3rd ed., 1991.

[16] Mark, J. E. *Physical Properties of Polymer Handbook;* Springer: New York, 2nd ed., 2006.

[17] Homer, M. L.; Lim, J. R.; Manatt, K.; Kisor, A.; Manfreda, A. M.; Lara, L.; Jewell, A. D.; Yen, S. P. S.; Zhou, H.; Shevade, A. V.; Ryan, M. A. *P. IEEE Sens. 2003* **2003**, pages 877–881.

[18] Rwei, S. P.; Ku, F. H.; Cheng, K. C. *Colloid. Polym. Sci.* **2002**, *280*(12), 1110–1115.

[19] Bin, Y.; Xu, C.; Agari, Y.; Matsuo, M. *Colloid. Polym. Sci.* **1999**, *277*(5), 452–461.

[20] Kawaguchi, S.; Imai, G.; Suzuki, J.; Miyahara, A.; Kitano, T. *Polymer* **1997**, *38*(12), 2885–2891.

[21] Ueda, M.; Kajitani, K. *Makromolekul. Chem.* **1967**, *108*(Oct), 138–152.

[22] Sun, S. F.; Fan, J. R. *Polymer* **1997**, *38*(3), 563–570.

[23] Duda, R. O.; Hart, P. E.; Stork, D. G. *Pattern Classification;* Wiley: New York, 2nd ed., 2001.

[24] Ueberreiter, K.; Kanig, G. *J. Colloid. Sci.* **1952**, *7*(6), 569–583.

[25] Santangelo, P. G.; Roland, C. M. *Macromolecules* **1998**, *31*(14), 4581–4585.

[26] Zhang, J.; Wang, C. H. *Macromolecules* **1988**, *21*(6), 1811–1813.

[27] Ferry, J. *Viscoelastic Properties of Polymers;* Wiley: New York, 3d ed., 1980.

Chapter 4

Varied Weight Linear Carboxylic and Dicarboxylic Acids in Carbon Black Composite Vapor Sensors

4.1 Abstract

Varied length carboxylic (C10–C24) and dicarboxylic (C2–C14) acids have been tested in small molecule/carbon black composite chemiresistor sensors. Minor chain length effects were noted in the dicarboxylic acid series, and the smallest molecule in each series provided unpredictable responses. Carboxylic acid arrays provided greater discriminatory ability than dicarboxylic arrays. This benefit possibly accrues from the greater availability of both carboxyl and alkyl groups in the carboxylic acids, suggesting future use of different multi-functional group small molecules in thin film vapor sensors.

4.2 Introduction

Arrays of resistive thin film vapor sensors have found use in fields as diverse as environmental monitoring,[1,2] disease diagnostics,[3,4] food quality control,[5,6] and explosives detec-

tion.[7,8] Systems such as intrinsically conducting polymers,[9,10] ligand-capped metal nanoparticles,[11–13] and organic insulators mixed with a conductor such as carbon nanotubes[14,15] or carbon black[16–18] have all been explored. Varying the chemical functionality present among the detectors in the array ensures a widely responding and finely discriminating system. Each sensor in such an array provides a varying set of responses to different classes of analyte vapors, thus creating distinct patterns of response when the array response is taken as a whole.

Composite sensor films of insulating polymers mixed with carbon black have been broadly investigated in our lab,[16,19–21] and more recently, the use of a variety of non-volatile small organic compounds instead of polymers has been examined.[18] Sensors made of these composite films work by a swelling mechanism. Adsorption of an analyte vapor into the film causes the insulating phase to expand, increasing the average distance between the conductive carbon black (CB) particles, and causing a rapid, reversible change in the film resistance.[19]

As compared to the polymer composite films, increased functional group density and disordered arrangement in small molecule composite films has been proposed to allow greater vapor permeability and increased analyte-sensor interactions, making these materials engaging sensor candidates. Small molecule composite films have generally exhibited highest signal-to-noise (SNR) ratios in mixtures containing 60–75 wt% of CB, whereas polymer composites perform best at the much lower levels of 20–40 wt% of CB. Investigations have suggested (Chapter 2) that the inherent crystallinity of the small molecule films impedes their ability to swell. In turn, the larger quantities of CB relative to the polymer

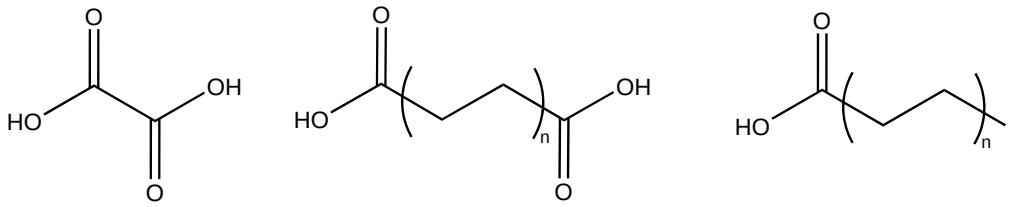

oxalic acid dicarboxylic acids carboxylic acids

Figure 4.1: Images of the basic structures of the carboxylic and dicarboxylic acids used.

films are necessary to to break up the large scale crystalline features in small molecule films. Differences in the size and polarity of the small molecules has been proposed to affect the requirements and responses of each small molecule.

In this study, two related homologous series of molecules have been used to prepare composite vapor sensors. Incorporating *n*-alkyl carboxylic and α, ω-dicarboxylic acids of varied length into vapor sensor arrays (referred to hereinafter as carboxylic and dicarboxylic acids, Figure 4.1, Table 4.1) allows investigation of the effects of controllably varied length differences — in each series, the ratio of alkyl to carboxylic groups steadily changes as the overall chain length increases. Additionally, the effects of mono- versus di-terminal strongly H-bonding groups are explored. Use of only the C_{2n} acids avoids any confounding effects from the even-odd variations seen in such molecules.[22,23]

Single sensor responses and overall array discrimination will be explored for these organic acid/CB composite sensor films. Additionally, their mass sorption and swelling behaviors will be examined through the use of quartz crystal microbalance (QCM) measurements and ellipsometry.

Acid Compound	C_n (n)	MW (g/mol)	mp (°C)	ρ (g/cm^3)
oxalic	2	90.04	190	1.90
succinic	4	118.09	186	1.56
adipic	6	146.14	153	1.36
suberic	8	174.20	140	1.27
sebacic	10	202.25	131	1.21
dodecanedioic	12	230.31	128	1.15
tetradecanedioic	24	258.36	127	1.08
decanoic	10	172.27	32	0.9
myristic	14	228.38	54	0.86
palmitic	16	256.43	62	0.85
stearic	18	284.48	69	0.85
tetracosanoic	24	368.65	80	0.85

Table 4.1: Listing and physical characteristics of all small molecules used in this study. Values are number of carbon atoms in molecule backbone, molecular weight, melting point, and density.

4.3 Experimental

4.3.1 Materials

All carboxylic and dicarboxylic acids, as well as dioctyl phthalate (DOP) were acquired from Sigma-Aldrich (Figure 4.1, Table 4.1). Except for stearic acid (95%), all compounds purchased were of 98% purity or greater. Gold wire (0.25 mm diam., 99.9+%) was also purchased from Sigma-Aldrich. Reagent grade hexane, heptane, chloroform, isopropanol, ethanol, ethyl acetate, and tetrahydrofuran were acquired from VWR. Chromium metal was purchased from RD Matthes. Black Pearls 2000, a carbon black (CB) material, was donated by Cabot Co. (Billerica, MA). All materials were used as received.

4.3.2 Sample Preparation

Sensor substrates were prepared by thermal evaporation of layered Cr (30 nm) and Au leads (60 nm) onto glass slides, after which the slide was cut into 0.5 cm x 2.5 cm pieces, as previously described (Section 2.3.2). The substrates for QCM measurements were 10 MHz polished quartz crystals (International Crystal Manufacturing). Each crystal contained a 0.201″ diameter electrode of 100 nm of Au on top of 10 nm of Cr. Ellipsometry samples were deposited onto cleaned pieces of polished silicon wafer.

All sensor solutions and mixtures were prepared in 20 mL of THF. In all cases, the organic acid and DOP, if used, were first dissolved in the solvent. The appropriate mass of carbon black was then added, and the mixture sonicated for at least 30 minutes to adequately disperse the CB particles. Mixtures with CB contained a total of 200 mg of solid materials, in three different ratios — one at 75 weight percent (wt %) CB, and two at 40 wt% CB (Table 4.2). Additionally, solutions were prepared from the pure acid, or the acid mixed in a 3:1 mass ratio with the plasticizer material.

Sensors and QCM films were prepared from each CB-containing mixture, while pure acid and acid/DOP solutions were used to prepare QCM and ellipsometry films. Two mixtures were made of each CB-containing formulation. Two sensors were deposited from each mixture, and QCM films were also prepared from both mixtures.

Sensor and QCM films were deposited via airbrush onto sensor slides or QCM crystals (Section 2.3.2). Ellipsometry samples were deposited via spin coater onto pieces of silicon wafer, yielding homogenous, optically smooth surfaces. The baseline frequency of each QCM crystal was noted prior to film deposition. All QCM samples were placed in a vacuum

Label	Acid (mg)	Plasticizer (mg)	Carbon Black (mg)
75	50	0	150
40	120	0	80
40/p	90	30	80

Table 4.2: Composition of all CB-containing mixtures used. The first column lists the abbreviation used in the manuscript to denote each type of film composition.

desiccator for at least 2 h prior to use. The frequency shift caused by deposition of the film was recorded immediately prior to data acquisition.

4.3.3 Measurements and Data Analysis

4.3.3.1 Chemiresistive Sensors

The sensors in an array were placed in an airtight PTFE and stainless steel flow chamber, and connected via Teflon tubing to a computer controlled vapor generation and delivery system (Section 2.3.3.1). The sensors were initially exposed to 2.5 L min^{-1} flow of air for a time period sufficient to stabilize their baseline resistances.

Seven analytes (hexane, heptane, chloroform, ethanol, isopropanol, ethyl acetate, and toluene) were used to test the sensors. All analytes were presented at a fraction saturation of $P/P^0 = 0.01$ (where P is the partial pressure and P^0 is the vapor pressure of the analyte at room temperature). Analytes were presented 25 times each to the sensor array, with the exposure order of the analytes randomized to minimize potential effects of sensor hysteresis. Each analyte exposure consisted of 100 seconds of laboratory air, 200 seconds of analyte, and a final 100 second purge of laboratory air. Data collection runs were performed at least four times on each sensor array. Reported data is from the final set of exposures.

The resistance of each sensor was measured approximately every 5 s. For each analyte exposure to each sensor, the data were first baseline corrected, and a single value, $\Delta R_{\text{max}}/R_{\text{b}}$ (the relative change in resistance) was extracted. R_{b} is the steady-state baseline resistance of the sensor and ΔR_{max} is the maximum resistance change observed during exposure to the analyte. A signal-to-noise ratio (SNR) was also determined for each exposure, with the SNR value defined as ΔR_{max} divided by the standard deviation of the data points used to calculate R_{b}. SNR and $\Delta R_{\text{max}}/R_{\text{b}}$ were calculated as previously reported (Section 2.3.3.1). This work uses principal components analysis (PCA) to visualize how well the sensor arrays distinguish between different analytes.[24] PCA rotates the data such that the first few dimensions contain as much as possible of the variance contained in the entirety of the array response. All data analysis was performed in MATLAB.

4.3.4 QCM Measurements

Coated QCM crystals were mounted in a sealed chamber and exposed to analytes using a setup very similar to that of the chemiresistive sensors (Section 2.3.3.2). The QCM chamber holds only one crystal, and as such, the QCM films were examined consecutively, not in arrays. Each crystal was first exposed to a baseline period of background air, followed by the analyte exposures. Each analyte exposure consisted of a 200 s period of air, followed by 100 s of analyte, followed by another 200 s of air.

Hexane, chloroform, and toluene were the analytes used for QCM experiments. Each crystal was exposed to a random ordering of 10 exposures of each analyte. All analytes were presented at an analyte partial pressure of $P/P^0 = 0.01$. At least two complete sets

of exposures were presented to each film.

The mass of the deposited sensor film causes a shift in the frequency of the QCM crystal Δf_{f}, and each exposure to an analyte causes a further frequency shift, Δf_{a}. Changes of resonant frequency of a coated crystal can be referenced to changes in mass through the Sauerbrey equation (Section 2.3.3.2), which directly relates the two. This allows determination of the analyte mass absorbed per unit mass of the deposited film, $\Delta m_{\mathrm{a}}/m_{\mathrm{f}}$. This value was calculated for each exposure to analyte for each film.

4.3.5 Ellipsometry

Ellipsometry was performed with a Gaertner L116C system. Samples for ellipsometry were placed in a plastic chamber with a drilled opening at each end to allow the laser beam to reach the sample and detector unimpeded. Baseline thickness readings were collected under a steady 65 mL min^{-1} stream of air, with an adjacent ventilation tube used to flush the chamber. Exposures to saturated hexane vapor at 65 mL min^{-1} were initiated by hand. During the exposures the ventilation tube was removed, to encourage maximum retention of hexane in the chamber. The purge and exposure times were each $\geq$5 min. Each sample was exposed a minimum of five times, and at least five data points were measured during and between each exposure. These data points were averaged to yield the relative thickness change of the film for each analyte exposure.

4.4 Results

4.4.1 Chemiresistive Sensors

4.4.1.1 Dicarboxylic Acids

All length dicarboxylic acid sensors responded at all formulations. $\Delta R/R_b$ and SNR values are summarized in Tables 4.3 and 4.4. $\Delta R/R_b$ were generally higher at 75 CB than the other two formulations, and SNR levels were lower at 40/p than in either of the other formulations. $\Delta R/R_b$ responses were highest to toluene at both 40 and 75 CB, while at 40/p responses to $CHCl_3$ notably increased. Responses of C4–C8 acids to the hydrocarbon analytes (toluene, hexane, heptane) were larger than those of the longer chains by 40% or more at all formulations, and 10–20% higher to oxygen containing analytes at 75 CB. Oxalic (C2) acid had widely variable responses, with response profiles of a given sensor changing over time. At 75 CB, responses changed from negative to positive over 6 days for several analytes (Figures 4.2). A similar but smaller effect for $CHCl_3$ and EtOAc was seen at 40 CB, and not seen at 40/p.

Single response curves (Figures 4.3–4.5) of dicarboxylic acids at all three formulations show the overall rapidity of response of all sensors. Curve shapes are similar at 75 and 40 CB, becoming slightly less rapid for chloroform at 40/p. These also display the variegated C2 responses.

PCA plots of dicarboxylic acid sensor arrays (Figures 4.9–4.11) show that the arrays successfully discriminate chloroform, clearly separate the hydrocarbons from the oxygen-containing analytes, and separate hexane from heptane (although they remain close). For-

mulations at 75 and 40 wt% of CB also clearly separate toluene from all other analytes, while at 40/p toluene is much less well separated from hexane/heptane. In no cases are the oxygen-containing analytes differentiated from each other. Both dicarboxylic 40 and 75 CB captured over 90% of the total variance in the first three principal components, whereas 40/p captured only 70% in the first three PCs.

4.4.1.2 Carboxylic Acids

All carboxylic acids responded at all formulations. $\Delta R/R_b$ and SNR values are summarized in Tables 4.5 and 4.6. $\Delta R/R_b$ values at 75 CB for C14–C24 are notably higher than at 40 CB and 40/p. All compounds show an improvement in response to $CHCl_3$ at 40/p compared to 40 CB, and C14–C18 also show an improvement to the hydrocarbon analytes. Except to chloroform, the responses of C24 remain the same or drop upon the switch from 40 CB to 40/p. In all three formulations, the responses of C10 are notably higher than all other weights at that formulation. The responses of C14 carboxylic acid are lower than that of C14 dicarboxylic acid to all oxygen-containing compounds, at all formulations, and lower to $CHCl_3$ at both 40 CB formulations. C14 carboxylic acid returns higher $\Delta R/R_b$ values to the hydrocarbon analytes at 75 CB than C14 dicarboxylic acid, and they produced comparable responses at both 40 CB formulations.

Single response curves for carboxylic acids at all formulations (Figures 4.6–4.8) show the overall speed of the sensor responses. They also highlight the greatly increased response of C10 carboxylic acid compared to the other lengths, and the overall similarity of the responses of the other carboxylic acids.

PCA plots of carboxylic acid sensor arrays (Figures 4.12–4.14) are more divergent than

those of the dicarboxylic acid arrays. The 75 CB plot is similar, clearly separating toluene and $CHCl_3$ from the hexane/heptane and oxygen containing clusters. The 40 CB plot has all analytes more closely together, but starts to show some separation between the oxygen-containing analytes. At 40/p, toluene, $CHCl_3$, hexane and heptane are all clearly separated from all other analytes. The three remaining analytes (EtOAc, EtOH, and iPrOH) all show some remaining overlap, but are loosely separated into three broad bands. All plots have from 80–90% of the total variance in the first three PCs.

4.4.2 QCM Responses

All films containing carbon black displayed rapid, clean mass uptake responses. 75 CB films generally displayed the largest $\Delta m_{\mathrm{a}}/m_{\mathrm{f}}$ of all CB-containing films. Responses of acid/plasticizer films were smaller than those of the CB-containing films, although $\Delta m_{\mathrm{a}}/m_{\mathrm{f}}$ values in response to $CHCl_3$ approached those of 40 CB and 40/p films. Responses of pure acid films were extremely small, with many displaying absolute frequency shifts of $\leq$2 Hz — in comparison, bare crystals show shifts of 0.5–1.5 Hz upon exposure to the same analytes. All film responses were rapid, and complete within the 100 s exposure period.

4.4.3 Ellipsometry

All films displayed responses to saturated hexane vapor. Pure films, however, displayed apparent thickness changes of 4–6 Å, similar to the nominal thickness change indicated by the change in signal displayed by a blank silicon sample wafer upon exposure to analyte. Film deposition volumes were generally equal, but not rigorously controlled. However,

mixed acid/plasticizer films were generally thicker than the pure acid films. (Table 4.7).

Mixed acid/plasticizer films swelled in the range of 4–8%, for overall shifts of 20–35 Å. Pure plasticizer films swelled $\sim$20% of their original thickness, a change of 30–40 Å. Film baselines were stable, shifting $\leq$2% of their total value over all exposures, in most cases.

Oxalic acid films were thinner than all other films, and oxalic acid/plasticizer films displayed larger percent changes than did the other mixed films, although absolute changes were similar. Pure decanoic acid and decanoic acid/plasticizer films cast via spin coater were too unstable to perform ellipsometry measurements.

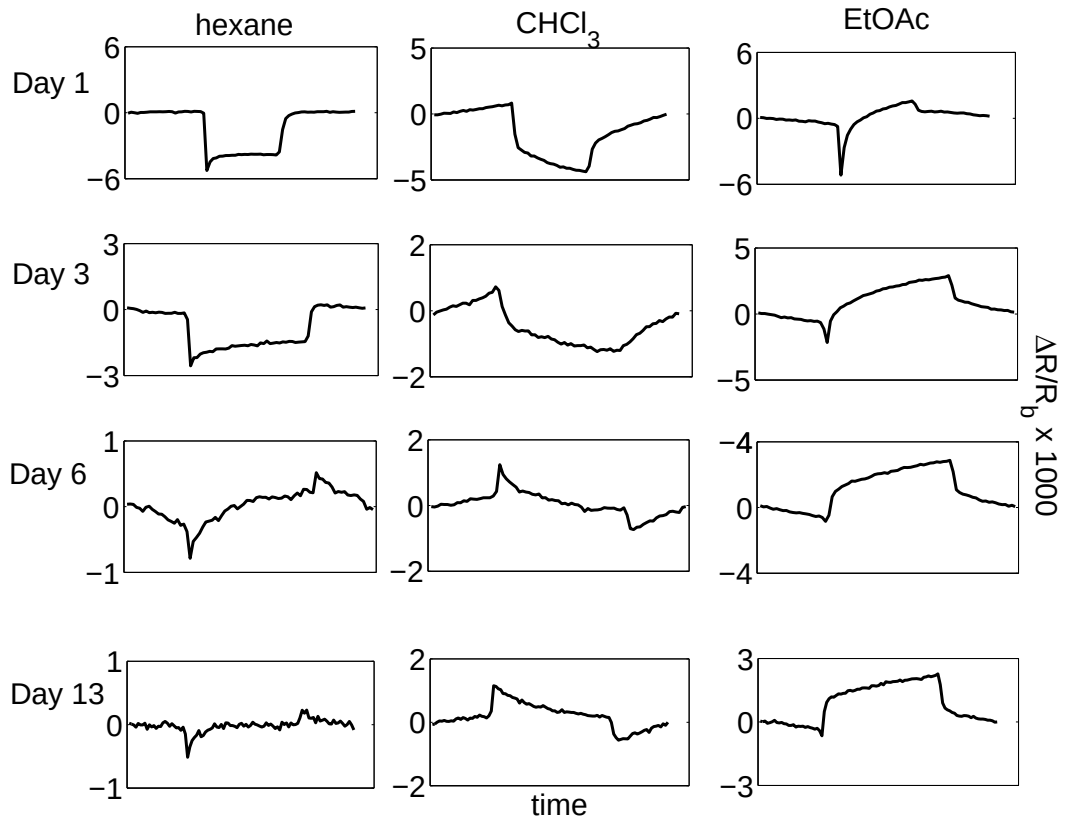

Figure 4.2: Single sensor responses of oxalic acid 75 CB to hexane, chloroform, and ethyl acetate on day 1, 3, 6 and 13 after creation. Day 1 exposure is for 100 s, all others are for 200 s. All exposures are at $P/P^0 = 0.01$, in a total 2.5 L min^{-1} flow of air.

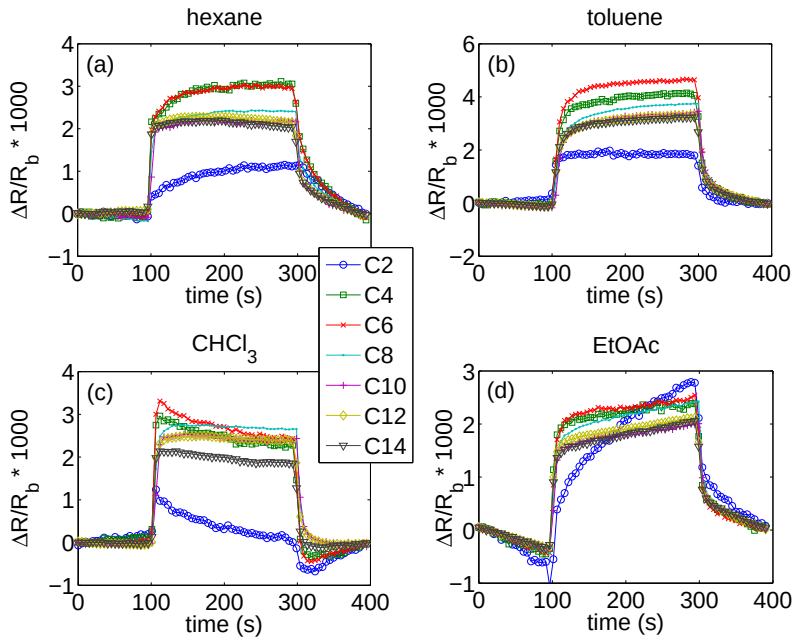

Figure 4.3: $\Delta R/R_b$ values of 200 second single exposures of dicarboxylic acid 75 CB to a) hexane, b) toluene, c) $CHCl_3$, and d) ethyl acetate. Each analyte was presented at $P/P^0 = 0.01$, in a total 2.5 L min^{-1} flow of air.

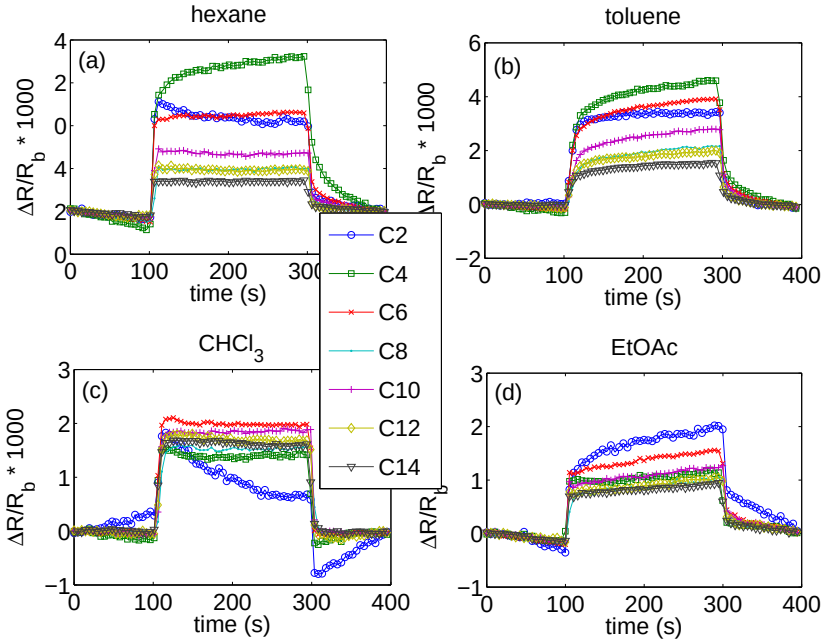

Figure 4.4: $\Delta R/R_b$ values of 200 second single exposures of dicarboxylic acid 40 CB to a) hexane, b) toluene, c) $CHCl_3$,and d) ethyl acetate. Each analyte was presented at $P/P^0 = 0.01$, in a total 2.5 L min^{-1} flow of air.

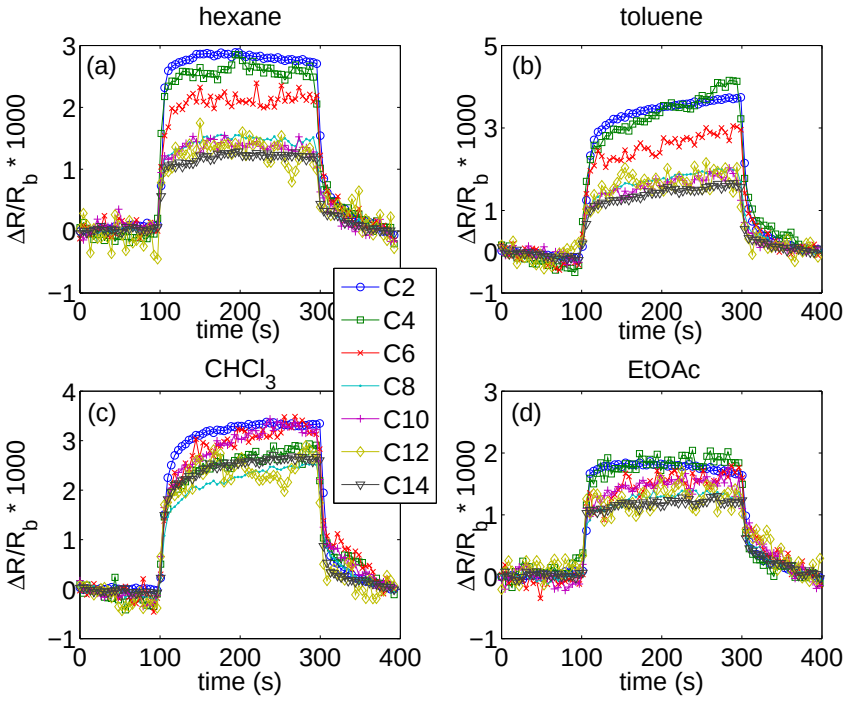

Figure 4.5: $\Delta R/R_b$ values of 200 second single exposures of dicarboxylic acid 40/p to a) hexane, b) toluene, c) $CHCl_3$, and d) ethyl acetate. Each analyte was presented at $P/P^0 = 0.01$, in a total 2.5 L min^{-1} flow of air.

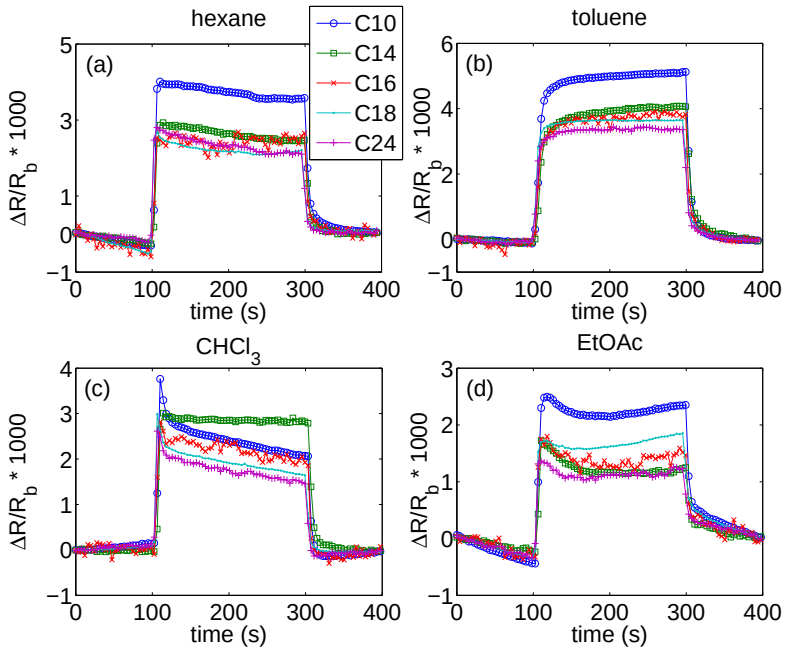

Figure 4.6: $\Delta R/R_b$ values of 200 second single exposures of carboxylic acid 75 CB to a) hexane, b) toluene, c) $CHCl_3$, and d) ethyl acetate. Each analyte was presented at $P/P^0 = 0.01$, in a total 2.5 L min^{-1} flow of air.

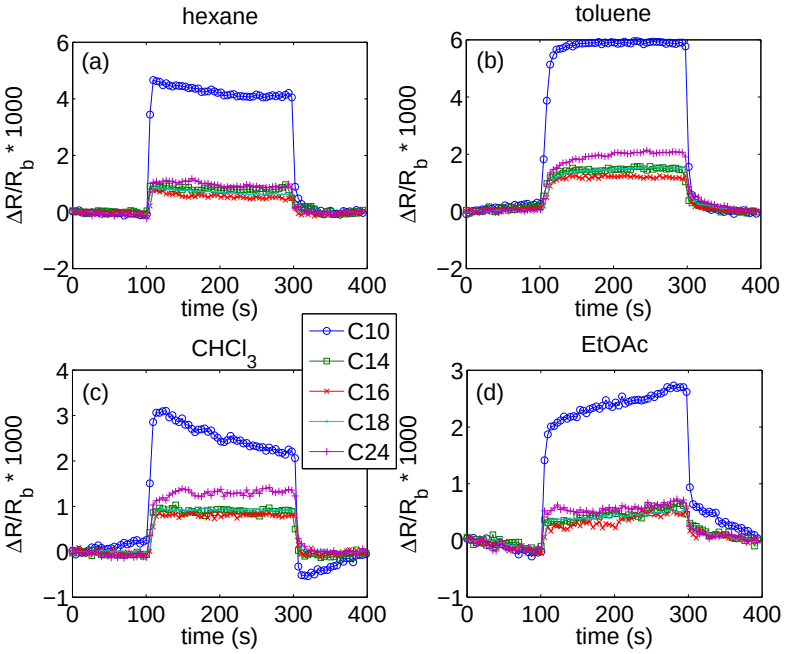

Figure 4.7: $\Delta R/R_b$ values of 200 second single exposures of carboxylic acid 40 CB to a) hexane, b) toluene, c) $CHCl_3$, and d) ethyl acetate. Each analyte was presented at $P/P^0 = 0.01$, in a total 2.5 L min^{-1} flow of air.

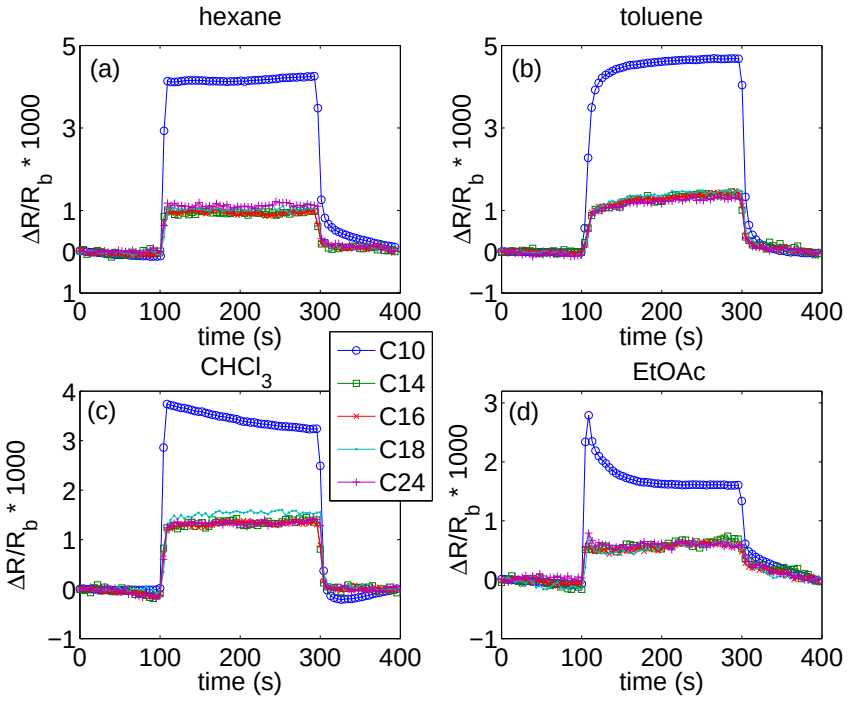

Figure 4.8: $\Delta R/R_b$ values of 200 second single exposures of carboxylic acid 40/p to a) hexane, b) toluene, c) $CHCl_3$, and d) ethyl acetate. Each analyte was presented at $P/P^0 = 0.01$, in a total 2.5 L min^{-1} flow of air.

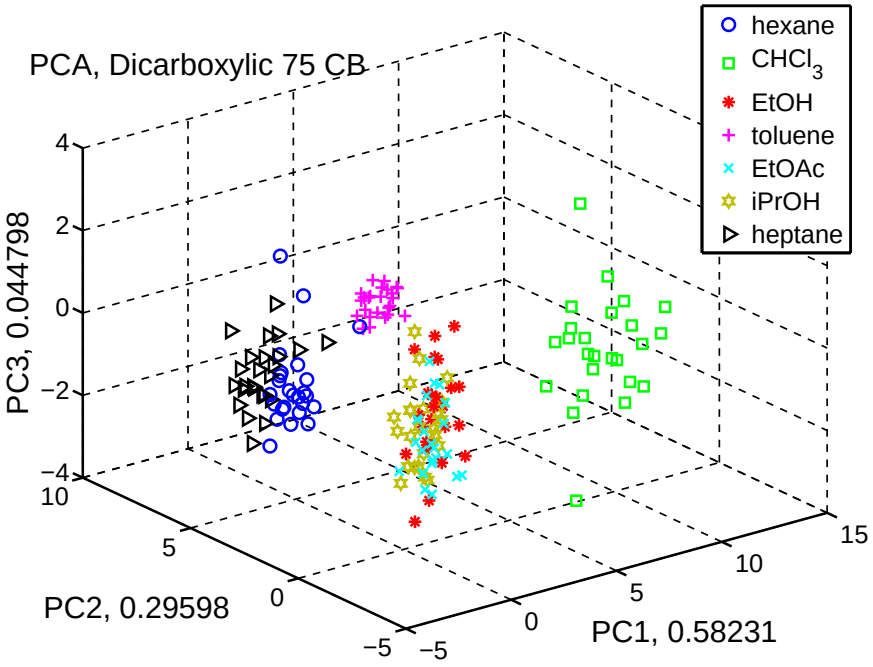

Figure 4.9: PCA plot of dicarboxylic acid 75 CB sensors. There are 25 exposures to each analyte. Numbers next to each principal component axis reflect the percentage of the total sensor response variance contained in that principal component

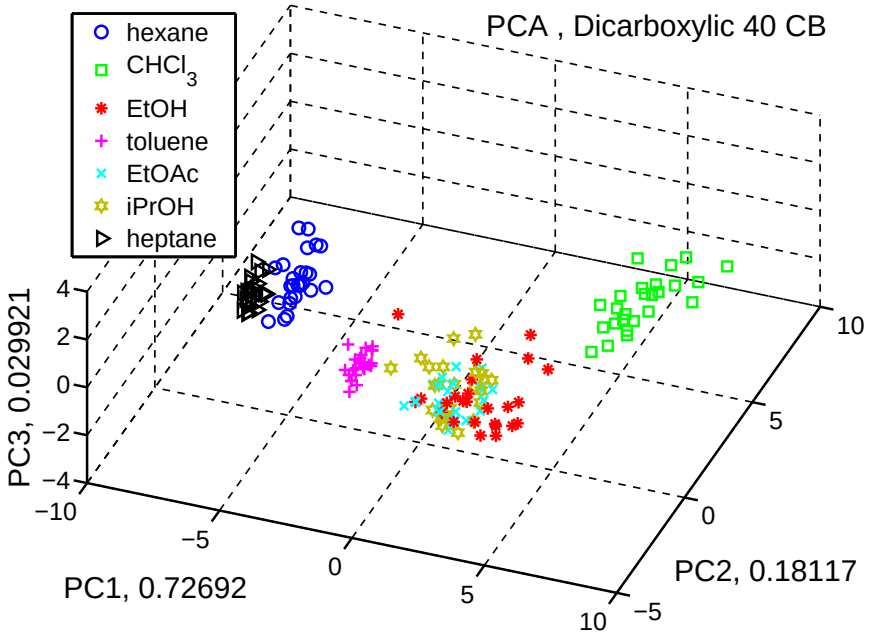

Figure 4.10: PCA plot of dicarboxylic acid 40 CB sensors. There are 25 exposures to each analyte. Numbers next to each principal component axis reflect the percentage of the total sensor response variance contained in that principal component

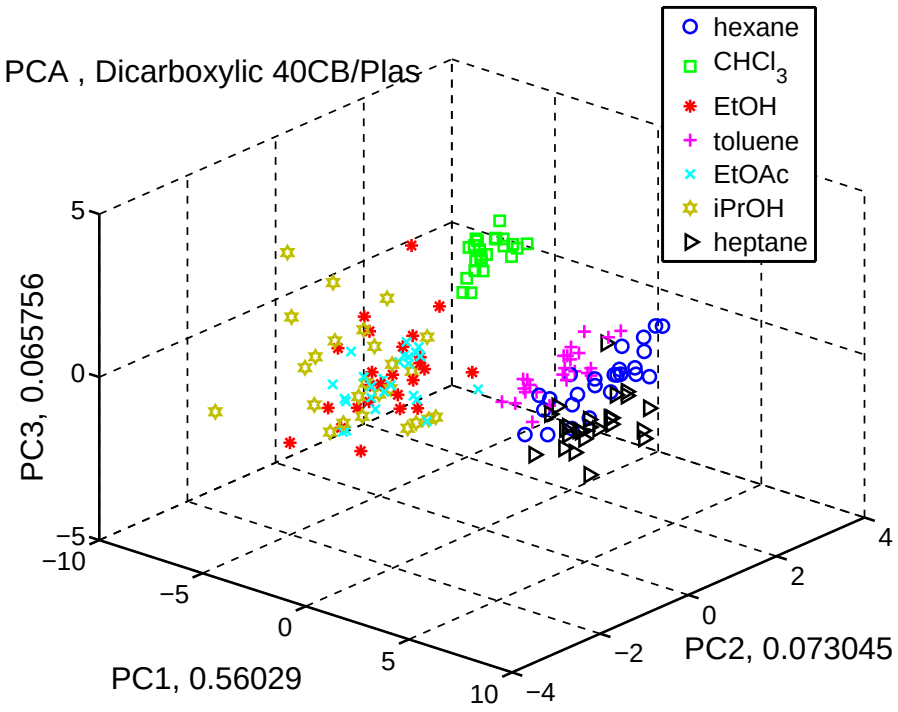

Figure 4.11: PCA plot of dicarboxylic acid 40/p sensors. There are 25 exposures to each analyte. Numbers next to each principal component axis reflect the percentage of the total sensor response variance contained in that principal component

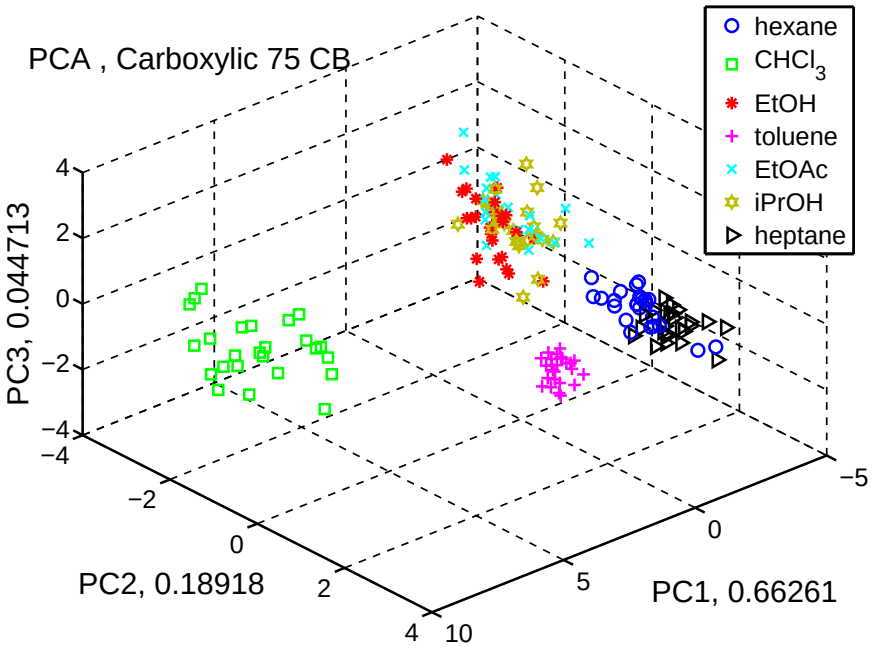

Figure 4.12: PCA plot of carboxylic acid 75 CB sensors. There are 25 exposures to each analyte. Numbers next to each principal component axis reflect the percentage of the total sensor response variance contained in that principal component

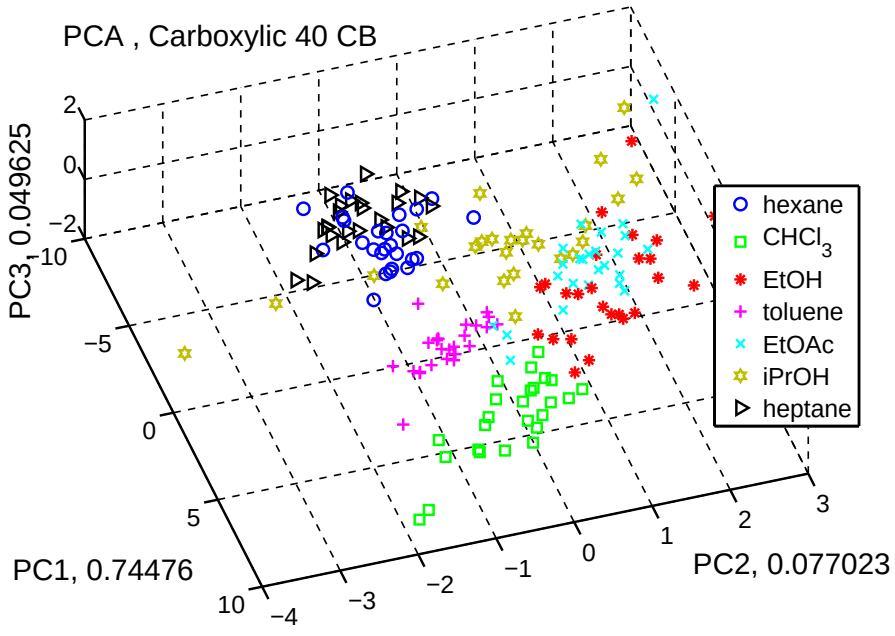

Figure 4.13: PCA plot of carboxylic acid 40 CB sensors. There are 25 exposures to each analyte. Numbers next to each principal component axis reflect the percentage of the total sensor response variance contained in that principal component

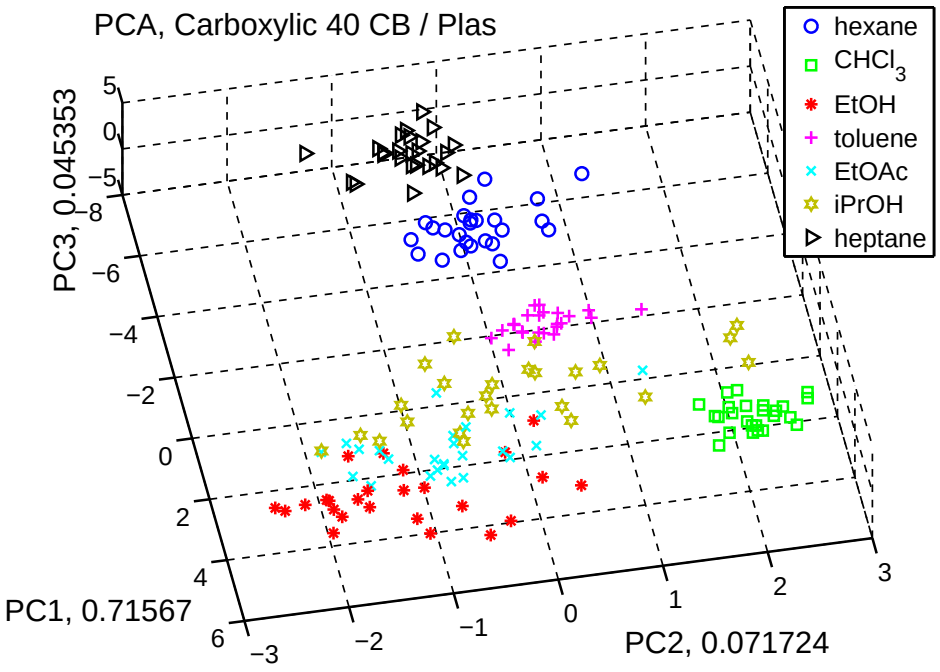

Figure 4.14: PCA plot of carboxylic acid 40/p sensors. There are 25 exposures to each analyte. Numbers next to each principal component axis reflect the percentage of the total sensor response variance contained in that principal component

CB%	Dicarb. acid	hexane	heptane	toluene	chloroform	EtOH	iPrOH	EtOAc
75	C2	0.52 ± 0.30	0.59 ± 0.28	1.59 ± 0.27	0.09 ± 0.22	1.69 ± 0.17	2.00 ± 0.19	2.86 ± 0.22
	C4	2.32 ± 0.03	3.11 ± 0.31	4.00 ± 0.27	2.02 ± 0.13	1.50 ± 0.21	1.85 ± 0.17	2.22 ± 0.24
	C6	2.36 ± 0.30	3.12 ± 0.26	4.27 ± 0.26	2.14 ± 0.14	1.67 ± 0.23	2.06 ± 0.18	2.46 ± 0.26
	C8	1.87 ± 0.24	2.28 ± 0.21	3.73 ± 0.23	2.66 ± 0.11	1.67 ± 0.19	1.91 ± 0.16	2.45 ± 0.16
	C10	1.71 ± 0.20	2.01 ± 0.18	3.36 ± 0.19	2.39 ± 0.10	1.36 ± 0.15	1.62 ± 0.12	1.97 ± 0.12
	C12	1.59 ± 0.23	1.91 ± 0.24	3.30 ± 0.28	2.34 ± 0.12	1.40 ± 0.18	1.65 ± 0.15	2.04 ± 0.18
	C14	1.49 ± 0.21	1.81 ± 0.23	3.20 ± 0.27	1.79 ± 0.13	1.36 ± 0.17	1.62 ± 0.14	1.96 ± 0.17
40	C2	1.80 ± 0.25	2.47 ± 0.20	3.67 ± 0.26	1.10 ± 0.25	1.13 ± 0.25	1.24 ± 0.10	1.65 ± 0.15
	C4	3.56 ± 0.20	4.74 ± 0.31	4.36 ± 0.20	1.42 ± 0.11	0.73 ± 0.16	0.80 ± 0.10	1.04 ± 0.14
	C6	2.12 ± 0.10	2.75 ± 0.11	3.86 ± 0.09	1.96 ± 0.08	1.12 ± 0.12	1.18 ± 0.08	1.49 ± 0.10
	C8	0.94 ± 0.07	1.09 ± 0.06	2.17 ± 0.07	1.55 ± 0.04	0.79 ± 0.07	0.79 ± 0.07	1.04 ± 0.08
	C10	1.22 ± 0.08	1.46 ± 0.08	2.84 ± 0.08	1.85 ± 0.06	0.91 ± 0.10	0.93 ± 0.07	1.22 ± 0.08
	C12	0.90 ± 0.05	1.02 ± 0.06	1.98 ± 0.06	1.69 ± 0.04	0.78 ± 0.08	0.79 ± 0.06	1.01 ± 0.06
	C14	0.64 ± 0.05	0.69 ± 0.06	1.43 ± 0.05	1.50 ± 0.09	0.71 ± 0.06	0.72 ± 0.06	0.90 ± 0.06
40/p	C2	2.42 ± 0.20	2.78 ± 0.22	3.48 ± 0.21	3.21 ± 0.19	1.11 ± 0.21	1.03 ± 0.15	1.49 ± 0.18
	C4	2.37 ± 0.27	2.93 ± 0.30	3.44 ± 0.29	2.28 ± 0.25	1.20 ± 0.27	1.24 ± 0.21	1.69 ± 0.23
	C6	1.78 ± 0.22	2.02 ± 0.25	2.69 ± 0.23	2.75 ± 0.22	0.99 ± 0.17	0.93 ± 0.15	1.30 ± 0.21
	C8	1.23 ± 0.16	1.28 ± 0.19	1.90 ± 0.17	2.25 ± 0.19	0.87 ± 0.17	0.69 ± 0.14	1.13 ± 0.16
	C10	1.01 ± 0.21	0.92 ± 0.27	1.72 ± 0.25	2.97 ± 0.27	0.98 ± 0.21	0.74 ± 0.20	1.21 ± 0.24
	C12	1.17 ± 0.23	1.19 ± 0.27	1.73 ± 0.23	2.58 ± 0.27	0.89 ± 0.21	0.71 ± 0.20	1.11 ± 0.26
	C14	0.99 ± 0.15	0.95 ± 0.16	1.53 ± 0.15	2.55 ± 0.22	0.81 ± 0.14	0.75 ± 0.14	1.05 ± 0.15

Table 4.3: $\Delta R_{\max}/R_{\mathrm{b}}$ values x 1,000 for all dicarboxylic acids measured in this study. Data are means obtained from 25 exposures to a given analyte. The reported error is one standard deviation.

CB%	Dicarb. acid	hexane	heptane	toluene	chloroform	EtOH	iPrOH	EtOAc
75	C2	17 ± 12	23 ± 17	35 ± 24	1 ± 13	48 ± 29	62 ± 54	68 ± 53
	C4	60 ± 28	83 ± 41	100 ± 63	48 ± 35	44 ± 28	52 ± 20	62 ± 37
	C6	59 ± 22	82 ± 35	148 ± 80	74 ± 47	58 ± 28	82 ± 59	72 ± 41
	C8	93 ± 38	92 ± 47	160 ± 49	257 ± 106	72 ± 29	131 ± 144	81 ± 22
	C10	83 ± 37	102 ± 44	122 ± 56	128 ± 62	57 ± 20	71 ± 29	68 ± 22
	C12	77 ± 34	98 ± 46	215 ± 282	220 ± 173	62 ± 31	105 ± 81	113 ± 219
	C14	58 ± 31	75 ± 38	169 ± 136	91 ± 53	58 ± 42	81 ± 57	62 ± 18
40	C2	63 ± 30	86 ± 49	112 ± 45	22 ± 17	35 ± 18	40 ± 15	59 ± 28
	C4	110 ± 65	132 ± 52	91 ± 47	50 ± 30	24 ± 18	34 ± 13	39 ± 19
	C6	140 ± 49	177 ± 93	212 ± 85	155 ± 90	50 ± 13	104 ± 91	85 ± 34
	C8	50 ± 32	47 ± 16	98 ± 25	74 ± 24	41 ± 14	49 ± 20	51 ± 24
	C10	89 ± 82	96 ± 37	133 ± 78	121 ± 51	59 ± 28	68 ± 42	67 ± 23
	C12	51 ± 19	62 ± 36	118 ± 94	84 ± 30	53 ± 30	41 ± 19	47 ± 15
	C14	36 ± 11	47 ± 18	77 ± 25	76 ± 35	54 ± 25	55 ± 26	58 ± 27
40/p	C2	118 ± 35	146 ± 88	161 ± 51	163 ± 64	54 ± 26	55 ± 20	76 ± 21
	C4	27 ± 9	36 ± 14	45 ± 40	28 ± 13	15 ± 8	18 ± 6	20 ± 10
	C6	21 ± 8	22 ± 7	26 ± 12	27 ± 10	15 ± 9	12 ± 8	16 ± 10
	C8	39 ± 17	39 ± 19	59 ± 24	78 ± 33	30 ± 14	25 ± 14	33 ± 15
	C10	18 ± 16	15 ± 8	25 ± 11	47 ± 37	15 ± 4	11 ± 5	17 ± 5
	C12	9 ± 4	9 ± 5	13 ± 4	23 ± 10	8 ± 3	5 ± 2	10 ± 6
	C14	28 ± 13	36 ± 15	52 ± 29	98 ± 65	34 ± 18	24 ± 13	31 ± 9

Table 4.4: SNR for all dicarboxylic acids measured in this study. Data are means obtained from 25 exposures to a given analyte. The reported error is one standard deviation.

CB%	Carb. acid	hexane	heptane	toluene	chloroform	EtOH	iPrOH	EtOAc
75	C10	3.42 ± 0.22	4.49 ± 0.23	5.25 ± 0.18	1.76 ± 0.24	1.67 ± 0.29	1.76 ± 0.20	2.29 ± 0.14
	C14	2.46 ± 0.16	3.06 ± 0.15	4.19 ± 0.11	2.65 ± 0.18	0.89 ± 0.22	0.95 ± 0.14	1.18 ± 0.11
	C16	2.36 ± 0.20	3.12 ± 0.22	3.98 ± 0.25	1.90 ± 0.22	1.06 ± 0.24	1.12 ± 0.18	1.35 ± 0.14
	C18	1.99 ± 0.22	2.66 ± 0.25	3.69 ± 0.21	1.36 ± 0.27	1.35 ± 0.28	1.44 ± 0.24	1.72 ± 0.18
	C24	1.88 ± 0.18	2.60 ± 0.25	3.43 ± 0.22	1.20 ± 0.25	0.90 ± 0.21	0.99 ± 0.17	1.16 ± 0.15
40	C10	4.07 ± 0.23	5.11 ± 0.19	5.46 ± 0.20	2.29 ± 0.23	1.19 ± 0.26	2.14 ± 0.16	2.55 ± 0.18
	C14	0.66 ± 0.12	0.68 ± 0.09	1.34 ± 0.08	0.96 ± 0.07	0.44 ± 0.11	0.37 ± 0.09	0.55 ± 0.08
	C16	0.52 ± 0.08	0.57 ± 0.06	1.17 ± 0.05	0.82 ± 0.06	0.39 ± 0.09	0.31 ± 0.07	0.47 ± 0.07
	C18	0.62 ± 0.07	0.66 ± 0.07	1.42 ± 0.05	0.91 ± 0.04	0.44 ± 0.07	0.38 ± 0.06	0.52 ± 0.06
	C24	0.89 ± 0.10	0.97 ± 0.09	2.01 ± 0.07	1.34 ± 0.08	0.56 ± 0.11	0.53 ± 0.09	0.69 ± 0.08
40/p	C10	3.50 ± 0.32	4.53 ± 0.30	4.81 ± 0.35	3.31 ± 0.30	1.07 ± 0.16	1.11 ± 0.21	1.40 ± 0.16
	C14	0.77 ± 0.12	0.79 ± 0.08	1.35 ± 0.11	1.37 ± 0.13	0.50 ± 0.07	0.40 ± 0.10	0.58 ± 0.08
	C16	0.77 ± 0.09	0.79 ± 0.07	1.43 ± 0.09	1.37 ± 0.09	0.46 ± 0.05	0.37 ± 0.07	0.53 ± 0.06
	C18	0.87 ± 0.09	0.90 ± 0.07	1.51 ± 0.10	1.63 ± 0.09	0.45 ± 0.08	0.38 ± 0.07	0.54 ± 0.08
	C24	0.85 ± 0.12	0.93 ± 0.12	1.41 ± 0.11	1.43 ± 0.13	0.42 ± 0.08	0.39 ± 0.11	0.51 ± 0.07

Table 4.5: $\Delta R_{\max}/R_{\mathrm{b}}$ values x 1,000 for all carboxylic acids measured in this study. Data are means obtained from 25 exposures to a given analyte. The reported error is one standard deviation.

CB%	Carb. acid	hexane	heptane	toluene	chloroform	EtOH	iPrOH	EtOAc
75	C10	275 ± 116	421 ± 337	645 ± 562	128 ± 56	93 ± 39	146 ± 77	109 ± 34
	C14	125 ± 44	187 ± 130	206 ± 83	165 ± 107	55 ± 28	66 ± 38	76 ± 31
	C16	36 ± 17	45 ± 20	62 ± 21	29 ± 11	21 ± 11	22 ± 9	26 ± 19
	C18	181 ± 149	144 ± 110	292 ± 318	65 ± 46	69 ± 29	89 ± 46	108 ± 115
	C24	62 ± 32	86 ± 56	104 ± 45	31 ± 22	33 ± 19	35 ± 22	40 ± 23
40	C10	137 ± 74	126 ± 41	157 ± 71	52 ± 24	52 ± 16	66 ± 30	70 ± 29
	C14	19 ± 8	18 ± 12	38 ± 12	26 ± 12	15 ± 10	11 ± 7	17 ± 8
	C16	21 ± 12	20 ± 6	44 ± 22	33 ± 21	17 ± 9	13 ± 6	16 ± 7
	C18	50 ± 17	51 ± 20	133 ± 69	81 ± 39	39 ± 24	34 ± 14	52 ± 29
	C24	28 ± 16	34 ± 16	62 ± 41	42 ± 17	19 ± 8	18 ± 9	21 ± 8
40/p	C10	508 ± 286	841 ± 629	651 ± 350	495 ± 374	116 ± 73	162 ± 78	135 ± 98
	C14	20 ± 9	21 ± 7	40 ± 15	35 ± 14	16 ± 7	13 ± 6	17 ± 7
	C16	37 ± 17	37 ± 14	70 ± 30	73 ± 33	24 ± 8	19 ± 8	19 ± 7
	C18	31 ± 13	36 ± 21	55 ± 32	51 ± 18	17 ± 5	20 ± 11	19 ± 7
	C24	56 ± 137	29 ± 15	42 ± 17	43 ± 21	15 ± 6	14 ± 6	19 ± 8

Table 4.6: SNR for all carboxylic acids measured in this study. Data are means obtained from 25 exposures to a given analyte. The reported error is one standard deviation.

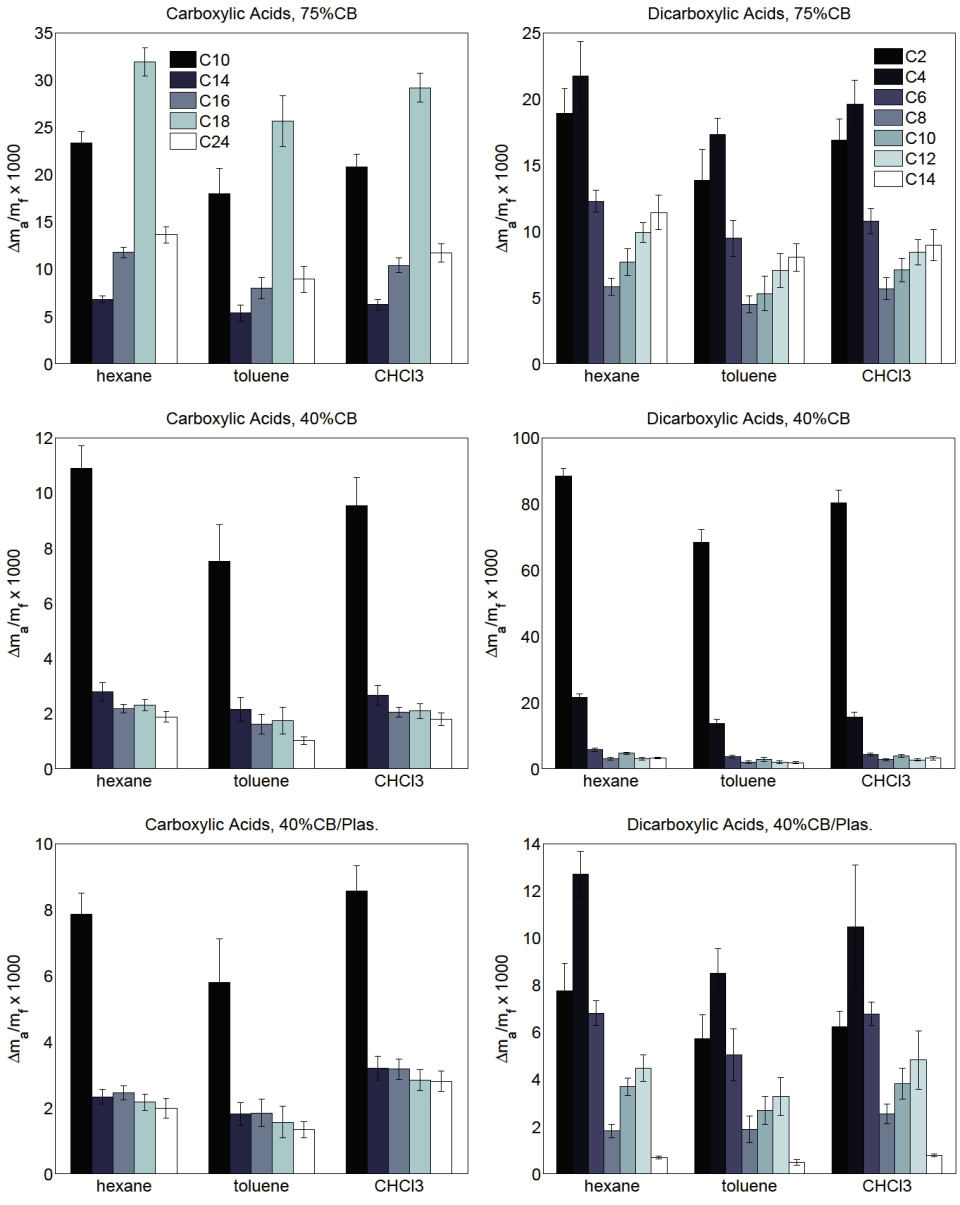

Figure 4.15: $\Delta m_{\mathrm{a}}/m_{\mathrm{f}}$ QCM values for all CB-containing films. Values are from the final run of each film, and are the average of 10 exposures to each analyte. Error is one standard deviation.

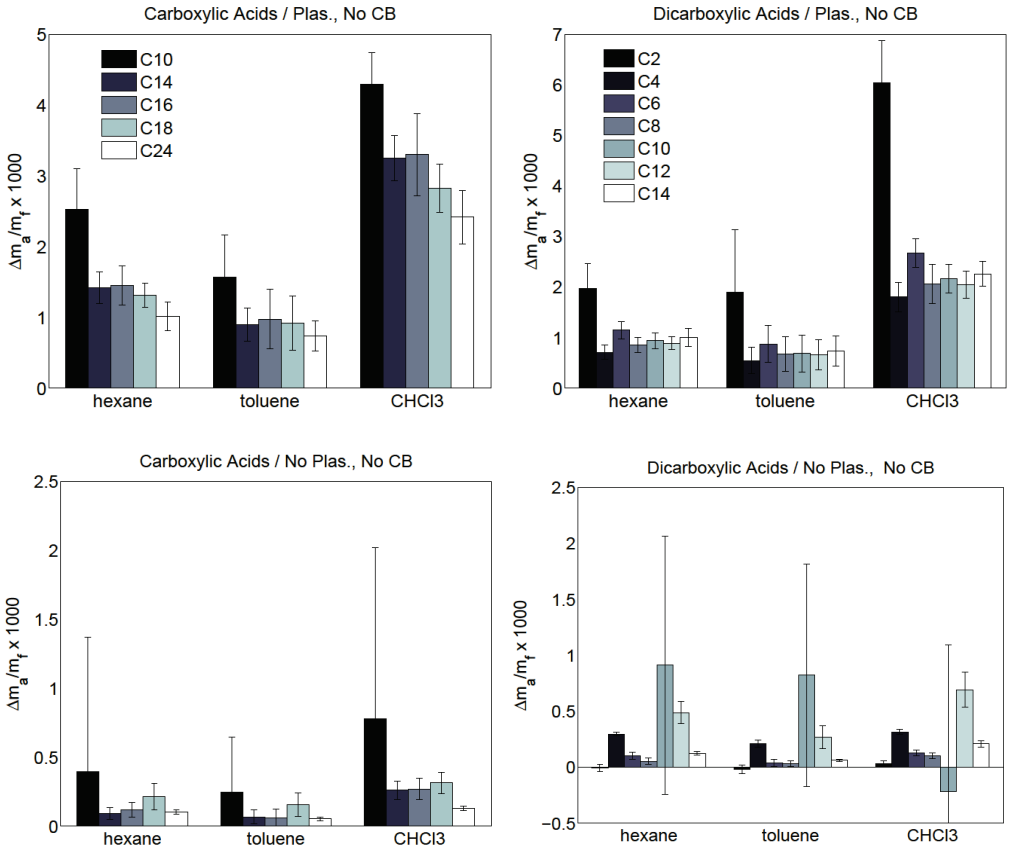

Figure 4.16: $\Delta m_{\mathrm{a}}/m_{\mathrm{f}}$ QCM values for all non-CB-containing films. Values are from the final run of each film, and are the average of 10 exposures to each analyte. Error is one standard deviation.

Acid Compound	No DOP Plasticizer			With Plasticizer		
	t (Å)	$\Delta h/h$ (%)	Δh (Å)	t (Å)	$\Delta h/h$ (%)	Δh (Å)
decanoic	-	-	-	-	-	-
myristic	361	2.4(0.7)	8.2(1.5)	388	5.5(0.3)	21.3(1.3)
	315	1.3(0.4)	4.0(1.2)	456	6.0(0.7)	27.5(3.4)
stearic	262	1.8(0.1)	5.3(1.1)	501	4.2(0.5)	21.0(2.8)
	252	2.0(0.4)	5.1(1.2)	295	8.1(0.3)	24.0(1.0)
palmitic	370	1.6(0.4)	6.0(1.6)	398	5.2(0.4)	19.8(1.5)
	311	1.4(0.1)	4.2(0.4)	474	7.4(0.3)	35.4(1.3)
tetracosanoic	275	2.4(0.4)	6.4(1.4)	440	8.1(0.3)	36.6(1.2)
	340	1.3(0.2)	4.3(0.6)	413	6.5(0.5)	30.3(2.0)
oxalic	204	1.7(0.3)	3.6(0.7)	208	16.9(1.9)	34.5(3.8)
	261	2.2(0.7)	5.7(2.0)	172	14.1(1.1)	23.7(1.5)
succinic	341	1.2(0.2)	3.9(0.6)	272	7.0(0.5)	18.9(1.4)
	204	4.2(0.2)	8.6(0.3)	383	9.2(0.3)	35.3(1.1)
adipic	330	1.7(0.2)	5.6(0.8)	456	5.6(0.2)	25.4(1.2)
	226	3.0(0.6)	7.5(0.3)	527	6.3(0.2)	33.1(1.3)
suberic	298	1.5(0.2)	4.4(0.6)	483	4.7(0.3)	22.7(1.5)
	337	1.6(0.1)	5.2(0.3)	504	6.1(0.4)	30.8(2.3)
sebacic	327	1.3(0.1)	4.1(0.4)	510	4.6(0.3)	23.3(1.8)
	387	1.3(0.2)	5.2(0.4)	553	4.0(0.3)	22.2(1.9)
dodecanedioic	334	1.4(0.2)	4.6(0.8)	426	6.1(0.6)	26.2(2.7)
	349	2.0(0.2)	6.9(0.6)	586	4.7(0.1)	27.6(0.9)
tetradecanedioic	332	0.7(0.1)	2.5(0.3)	465	5.7(0.3)	26.3(1.3)
	322	1.1(0.0)	3.6(0.1)	445	5.5(0.4)	25.5(2.1)
blank			5.1(0.4)			
			4.4(0.1)			
plasticizer				167	19.1(0.9)	31.7(1.6)
				162	23.4(0.6)	38.6(1.6)

Table 4.7: Averaged ellipsometry responses of carboxylic and dicarboxylic acid films. Reported error is one standard deviation. Decanoic acid films deposited by spin coating were not stable.

4.5 Discussion

Composite vapor sensors using small molecule substrates have several potential advantages over their polymer composite forebears. Unlike polymer composites, small molecule sensors almost uniformly function at very high carbon black loadings, both allowing decreased use of potentially expensive sensor materials and also hinting at an extremely high relative level of sensitivity. Greater disorder in small molecule films compared to polymer films and potentially higher functional group density have been theorized as causes for the high level of sensitivity. Additionally, use of small molecules allows access to a greater range of functional groups than can be achieved with polymers.

Here we see further confirmation of the sensitivity of the small molecule sensors. Sensor arrays composed of fixed terminal group, but varied chain length di- and monocarboxylic acids show good analyte discrimination. Moreover, accessibility of the small molecule functional groups is seen to aid discrimination, suggesting further use of multifunctional group small molecules to maximize overall discriminatory ability. However, we also see that volatility (both materially and behaviorally) of certain small molecules can lead to unpredictable results.

4.5.1 Small Molecule Responses — Size Variation

All small molecule sensors that produced reliable responses continued the trend of returning largest responses at the highest ratios of CB — i.e., using the smallest amount of responsive sensing material. This is directly counter to findings with polymer composite sensors in which addition of carbon black linearly decreases $\Delta R_{\max}/R_{\mathrm{b}}$ responses.[16] These

materials falling into this pattern provides further support to the theory (Chapter 2) that higher quantities of carbon black more effectively break up the small molecule crystalline structure, better allowing the composite material to swell.

However, very few effects were seen correlated to chain length differences. In the case of the carboxylic acids, the net effect of the increasing chain length from C14–C24 can be expected to be minimal, as there is still a singular carboxylic acid group, and a single alkyl tail, and the overall character of the molecules are similar (C10, however, exhibits distinct behavior, as discussed later). However, the increase in the length alkyl spacer in the dicarboxylic acids was expected to demonstrate a greater effect. Instead, the only clear trend is the increase in $\Delta R_{\text{max}}/R_{\text{b}}$ values of the C4–C8 dicarboxylic acids as compared to the longer chain molecules (oxalic acid, C2, also produced anomalous behavior, discussed later with decanoic acid). Above C8, the sensor responses were essentially flat.

Rather than increasing sensitivity to, e.g., the alkane analytes, an alternative idea is that the alkyl spacer instead provides a larger, flexible region where an analyte vapor can penetrate without displacing the molecule. In contrast, the shorter chain dicarboxylic acids can only accommodate the analyte vapors by physically separating, thus causing a greater physical shift in the CB particle network, and a concomitant increase in resistance. As all the carboxylic acids contain a large alkyl region, they would be less affected by this effect.

The shorter dicarboxylic acids also show somewhat increased mass uptake in QCM measurements (Figure 4.15) compared to the longer chain materials, but only in CB-containing films. While the reported $\Delta m_{\text{a}}/m_{\text{f}}$ values control for relative mass, the differing densities of the small molecules (Table 4.1) could cause volumetric sorption differences. How-

ever, the non-CB-containing QCM films (Figure 4.16), and ellipsometric measurement (Table 4.7), showed no trends correlated to chain length, suggesting that the response increases arises with the interplay between the acids and the carbon black, a set of interactions not yet well understood.

4.5.2 Functional Group Accessibility

While few intra-series differences were noted, clear differences were seen between the discriminating abilities of the carboxylic and dicarboxylic acid sensor arrays. The differences between the intermolecular hydrogen bonding abilities of the two series is clearly reflected in their relative melting points of the two sets of molecules (Table 4.1). As might be predicted from this difference, the dicarboxylic acids have a higher sensitivity to the oxygen-containing analytes than do the carboxylic acids, at all sensor formulations (Tables 4.3 and 4.5).

Despite this, however, only the carboxylic acid arrays demonstrated any ability to discriminate between the more polar analytes. Despite their overall increased density of carboxylic acid groups, PCA plots of all dicarboxylic acid array responses show no separation between EtOH/iPrOH/EtOAC (Figures 4.9 to 4.11). PCA plots of carboxylic accid arrays, however, display separation between these analytes, as well as showing increased separation between hexane and heptane (Figures 4.13 and 4.14). This is all the more remarkable given that there were only five chemically distinct sensors in the carboxylic acid arrays (although four copies of each sensor were present), and that four of those five sensors presented extremely similar sets of responses to each other (Figure 4.7, Table 4.5).

With both lowered overall responsiveness, and greater sensor similarity, carboxylic acids are still better able to discriminate between analytes than is a much more diverse set of dicarboxylic acids. One notable difference between the two sets of molecules is the greater accessibility of the alkyl group in the carboxylic acids. Analytes can interact with the carboxylic acid moiety, but also have free access to the alkyl tail. Compared to the dicarboxylic acids (or most polymeric materials) the analyte can interact with the sensor material in a more stereospecific fashion, allowing finer variations in response, as captured in PCA analysis.

Compared to a polymeric material, a linear small molecule offers greater access to at least two potentially distinct regions — the two ends. While the dicarboxylic acid responses suggest that the interior of a molecule may be blocked from exerting a significant influence, the potential to use a small molecule material with two (or more) distinct functional groups greatly increases the breadth of response available to a given size sensor array.

4.5.3 Unusual Responsiveness — Oxalic and Decanoic Acids

Responses of oxalic and decanoic acids highlight potential features and pitfalls of small molecules used in composite vapor sensors. Both materials — the smallest in each homologous series — displayed behaviors widely diverging from those of the rest of their series.

Decanoic acid reproducibly produced much higher $\Delta R_{\text{max}}/R_{\text{b}}$ values than did all other carboxylic acids, and also sorbed a greater quantity of analyte. However, this molecule is the shortest chain carboxylic acid that is solid at room temperature, and has a melting

point of 32 °C — only 10 °C above the normal laboratory operating conditions. The high responsiveness is thus partnered with a relatively large instability of the pure material, noted especially in the inability to cast ellipsometry films from this material.

Oxalic acid, while more stable in material properties than decanoic acid (with a melting point of 190 °C) proved, however, far more erratic in its responses. Response times and curve shapes of oxalic sensors differed widely from those of the other dicarboxylic acid sensors (Figure 4.3), even after their responses had stabilized over time (Figure 4.2). Oxalic acid, upon surface examination, would appear to have excellent potential to respond to polar analytes, but instead some combination of its own polarity, hydrogen bonding, hygroscopic nature, and other unusual properties leave it with untrustworthy responses.

The instability seen with these two molecules makes clear that the physical characteristics of potential small molecule sensor materials must be taken into consideration, beyond just the identity of their functional groups. The unusual response patterns evidenced by these two materials also shows, however, how very small apparent differences between two small molecules can yield highly varied sensor responses, further pointing out how small molecule composite sensors can aid in fine discrimination tasks in future sensor arrays.

4.6 Conclusions

Small molecule/CB composite vapor sensor arrays of two homologous series of small molecules (linear carboxylic and dicarboxylic acids) have been explored to better understand the effects of chain length and functional group presence in the performance of such sensors. Only minimal chain length effects were noted, although the smallest member of

each chain provided unexpected responses. Arrays comprised of carboxylic acids provided better analyte discrimination than did arrays of dicarboxylic acids, despite fewer distinct sensors in the carboxylic acid arrays. This greater availability of the alkyl group in the carboxylic acids as compared to the dicarboxylic acids could cause this effect. This points the way to new generations of highly sensitive small molecule sensors via selection of materials containing two or more accessible distinct functional groups.

4.7 Bibliography

[1] Young, R. C.; Buttner, W. J.; Linnell, B. R.; Ramesham, R. *Sens. Actuators, B* **2003**, *93*(1-3), 7–16.

[2] Ryan, M. A.; Shevade, A. V.; Zhou, H.; Homer, M. L. *MRS Bull.* **2004**, *29*(10), 714–719.

[3] Kateb, B.; Ryan, M. A.; Homer, M. L.; Lara, L. M.; Yin, Y. F.; Higa, K.; Chen, M. Y. *Neuroimage* **2009**, *47*, T5–T9.

[4] Dragonieri, S.; Schot, R.; Mertens, B. J. A.; Le Cessie, S.; Gauw, S. A.; Spanevello, A.; Resta, O.; Willard, N. P.; Vink, T. J.; Rabe, K. F.; Bel, E. H.; Sterk, P. J. *J. Allergy Clin. Immun.* **2007**, *120*(4), 856–862.

[5] Balasubramanian, S.; Panigrahi, S.; Kottapalli, B.; Wolf-Hall, C. E. *Lwt - Food Sci. Technol.* **2007**, *40*(10), 1815–1825.

[6] Ampuero, S.; Bosset, J. O. *Sens. Actuators, B* **2003**, *94*(1), 1–12.

[7] Toal, S. J.; Trogler, W. C. *J. Mater. Chem.* **2006**, *16*(28), 2871–2883.

[8] Senesac, L.; Thundat, T. G. *Mater. Today* **2008**, *11*(3), 28–36.

[9] Freund, M. S.; Lewis, N. S. *P. Natl. Acad. Sci. USA* **1995**, *92*(7), 2652–2656.

[10] Gardner, J. W.; Bartlett, P. N. *Synthetic Met.* **1993**, *57*(1), 3665–3670.

[11] Briglin, S. M.; Gao, T.; Lewis, N. S. *Langmuir* **2004**, *20*(2), 299–305.

[12] Kim, Y. J.; Yang, Y. S.; Ha, S. C.; Cho, S. M.; Kim, Y. S.; Kim, H. Y.; Yang, H.; Kim, Y. T. *Sens. Actuators, B* **2005**, *106*(1), 189–198.

[13] Wohltjen, H.; Snow, A. W. *Anal. Chem.* **1998**, *70*(14), 2856–2859.

[14] Philip, B.; Abraham, J. K.; Chandrasekhar, A.; Varadan, V. K. *Smart Mater. Struct.* **2003**, *12*(6), 935–939.

[15] Zhang, T.; Mubeen, S.; Myung, N. V.; Deshusses, M. A. *Nanotechnology* **2008**, *19*(33).

[16] Lonergan, M. C.; Severin, E. J.; Doleman, B. J.; Beaber, S. A.; Grubbs, R. H.; Lewis, N. S. *Chem. Mater.* **1996**, *8*(9), 2298–2312.

[17] Sisk, B. C.; Lewis, N. S. *Sens. Actuators, B* **2005**, *104*(2), 249–268.

[18] Gao, T.; Woodka, M. D.; Brunschwig, B. S.; Lewis, N. S. *Chem. Mater.* **2006**, *18*(22), 5193–5202.

[19] Severin, E. J.; Doleman, B. J.; Lewis, N. S. *Anal. Chem.* **2000**, *72*(4), 658–668.

[20] Burl, M. C.; Sisk, B. C.; Vaid, T. P.; Lewis, N. S. *Sens. Actuators, B* **2002**, *87*(1), 130–149.

[21] Briglin, S. M.; Lewis, N. S. *J. Phys. Chem. B* **2003**, *107*(40), 11031–11042.

[22] Bond, A. D. *Crystengcomm* **2006**, *8*(4), 333–337.

[23] Thalladi, V. R.; Nusse, M.; Boese, R. *J. Am. Chem. Soc.* **2000**, *122*(38), 9227–9236.

[24] Duda, R. O.; Hart, P. E.; Stork, D. G. *Pattern Classification;* Wiley: New York, 2nd ed., 2001.

Appendix — Principal Components Analysis

The data initially taken from the experimental setup in this thesis are a long stream of resistances read from each sensor over time. From this data, for each exposure to an analyte from each sensor, we extract a single descriptor:

$$\frac{\Delta R_{\text{max}}}{R_{\text{b}}} \tag{5.1}$$

where R_{b} is the baseline resistance of the sensor prior to exposure, and ΔR_{max} is the maximum change in steady-state resistance (Figure 5.1). This $\Delta R_{\text{max}}/R_{\text{b}}$ value is the partial differential resistance response of one sensor to one exposure of an analyte.

This yields $\mathbf{R} = \{r_{ij}\}$, an $m \times n$ matrix of sensor values, where n is the number of sensors, m is the number of exposures, and r_{ij} represents the response of the jth sensor to the ith exposure of analyte, as shown in Equation 5.1. This leaves the problem of having data in n-space, which is difficult to interpret and visualize. Principal components analysis (PCA) is a multivariate statistical technique employed to reduce the dimensionality of the data, and make it more amenable to interpretation.[1] This is a common method used in pattern analysis, and has been extensively used and reviewed in the sensor array literature.[2] This is the primary method for analyte discrimination used in this thesis.

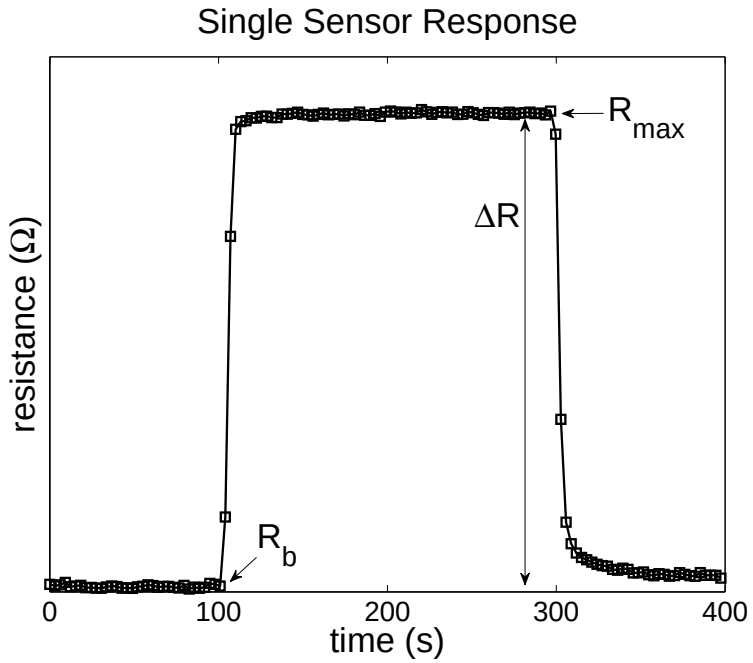

Figure 5.1: Response of a poly(ethylene oxide)/carbon black composite sensor to a 200 second exposure to 2 ppth of chloroform vapor, at an overall flow rate of 2.5 L min^{-1}.

The matrix $\mathbf{R}$ is first preprocessed such that each column in the matrix is normalized and autoscaled (i.e., centered about the mean and defined to have unit standard deviation, resulting in a final matrix $\mathbf{D} = \{d_{ij}\}$. First the r_{ij} values are normalized, creating the matrix $\mathbf{Q} = \{q_{ij}\}$ which helps correct for differences in solvent vapor pressure.

$$q_{ij} = \frac{r_{ij}}{\sum_j r_{ij}} \tag{5.2}$$

These normalized values are then autoscaled, such that they are both mean-centered and set to have a standard deviation of unity.

$$d_{ij} = \frac{q_{ij} - \overline{q}_j}{\sigma_j} \tag{5.3}$$

Here, $\overline{q}_j$ and σ_j represent the mean and standard deviation of each sensor j to all analytes presented to it. This matrix $\mathbf{D} = \{d_{ij}\}$ is then diagonalized (i.e., multiplied by its transpose) to obtain a correlation matrix $\mathbf{M}$.

$$\mathbf{M} = \mathbf{D^T} \cdot \mathbf{D} \tag{5.4}$$

The eigenvalues and eigenvector matrix of $\mathbf{M}$ are then obtained. The n eigenvectors of the eigenvector matrix $\mathbf{V}$ are mutually orthogonal. We multiply this $n \times n$ matrix $\mathbf{V}$ by the data matrix $\mathbf{D}$ to obtain our matrix of principal components, $\mathbf{P}$, an $m \times n$ matrix, in which each row is still associated with a particular analyte exposure, and each column is now a principal component of the data, in which the maximal variance between the members of the original data set is found in the first principal component, the maximal remaining variance found in the second component, and so on. The corresponding eigenvalues of $\mathbf{M}$ tell us how much of the total variance is to be found in each principal component.

$$\mathbf{P} = \mathbf{DV} \tag{5.5}$$

The maximal amount of variance is now front loaded into the first few principal components, allowing us to much more easily visualize the information in the data in just two or three dimensions, rather than the full n-dimensionality of the original sensor set.

5.1 Bibliography

[1] Duda, R.; Hart, P.; Stork, D. *Pattern Classification;* Wiley: New York, 2nd ed., 2001.

[2] Jurs, P.; Bakken, G.; McClelland, H. *Chem. Rev.* **2000**, *100*(7), 2649–2678.